EVALUATING THE HYDROLOGICAL IMPACT OF REMOVING WOODY BIOMASS FOR BIOFUEL PRODUCTION THROUGH UNSATURATED ZONE MODELING

by

Constance Taylor Smith

A thesis submitted to the faculty of
The University of Utah
in partial fulfillment of the requirements for the degree of

Master of Science

Department of Civil and Environmental Engineering

The University of Utah

August 2017

The University of Utah Graduate School

STATEMENT OF THESIS APPROVAL

The thesis of **Constance Taylor Smith**

has been approved by the following supervisory committee members:

Michael Ernest Barber	, Chair	**03/17/17** Date Approved
Jennifer Lee Weidhaas	, Member	**03/17/17** Date Approved
Steven John Burian	, Member	**03/20/17** Date Approved

and by **Michael Ernest Barber** , Chair/Dean of

the Department/College/School of **Civil and Environmental Engineering**

and by David B. Kieda, Dean of The Graduate School.

ABSTRACT

Due to climate change concerns, governments and consumers are demanding higher environmental accountability for transportation fuels, particularly as related to carbon emissions. Wood-based energy markets have been proposed as a means to ensure sustainable forests, enhance energy security, promote environmental quality, and realize social benefits. Biomass crops may offset fossil fuels and reduce CO_2 contributions to greenhouse gases while improving soil and water quality. Key issues among stakeholders include soil and water quality and loss of biodiversity as collecting small-diameter woody biomass may significantly alter post-timber harvesting landscapes. Little is known about how land use changes impact the entire ecological function of the watershed. The objectives of this study were to explore the potential of differences between land use changes and see if the water balance of the watershed would also change. This will help us understand the environmental impacts of different forms of biomass removal in the production of jet fuel. The start of holistic land management strategies focused on hydrologic implications of the entire food web has begun.

Hydrologic measurements were collected from 28 one acre plots subject to different land treatments, analyzed, and compared to a site-specific water balance model UNSAT-H to evaluate if changes in biomass removal influence the subsurface hydrology. Results showed a correlation between compacted soils exhibiting more evaporation when compared to noncompacted sites. A correlation of less drainage to the water table correlates

to a higher clay content value; this correlation did not exist, and was therefore not statistically significant. Since the soils had such unique characteristics at each plot, parameterization and extrapolation of the UNSAT-H model for the whole Pacific Northwest is not possible solely using the data of this LTSP site.

TABLE OF CONTENTS

LIST OF TABLES

Tables

LIST OF FIGURES

Figures

ACKNOWLEDGEMENTS

I would like to express my deepest gratitude and cordial thanks to my advisor Dr. Michael E. Barber for his full support, patience, encouragement, and expert guidance throughout my study and research. He gave me all of the tools I needed to succeed at this project, and will be eternally grateful to have worked with him. I also want to express my appreciation for Dr. Ramesh Goel and Dr. Steve Burian for having served on my committee. Their support, thoughtful questions and comments were valued greatly when I came to them for help.

I would like to extend my gratitude to the United States Department of Agriculture's National Institute of Food and Agriculture for funding this project. Additionally, my many thanks to Weyerhauser for allowing research to be conducted on their Long Term Soil Productivity (LTSP) site and climate data available for us to use.

I would also like to thank Scott Holub for all of his help with troubleshooting raw data from the LTSP site, answering my heaping amount of questions, and helping me analyze the data. Additionally, I want to send my warm thanks to Michael Fayer, developer of the computer code "UNSAT-H." He always helped me troubleshoot my code for the treatment plots, and would always lend a helping hand if I ever needed help understanding how the program worked. Thanks also to my fellow graduate students, indefinitely to Sulochan Dhungel, and staff at the Department of Civil and Environmental Engineering at the University of Utah for their support.

Finally, I would like to thank my mom, my sister, and my friends for their unconditional love and support during the last two years. They gave me the encouragement that I needed when I felt incompetent, and I would not have been able to complete graduate school without their support.

CHAPTER 1

INTRODUCTION

Sustainable production of bioenergy is necessary to meet future world-wide energy demands while helping to offset the global impacts of increased carbon dioxide from traditional fossil fuels (Aransiola et al., 2014; Beringer et al., 2011; Berndes, 2002; Johansson and Azar, 2007). The concept of sustainability, the ability to meet the needs of the present without compromising the ability to meet the needs of the future, continues to gain attention as human population growth creates ever greater pressure on diminishing natural resources (Mann et al., 2000).

According to the 2016 Federal Activities Report on the Bioeconomy released on February 2016, the Biomass R&D Technical Advisory Committee has recommended "targeting a potential 30% penetration of biomass carbon into the U.S. transportation market by 2030" (The Biomass Research and Development (R&D) Board, 2016). Scientists have been researching ways to produce bioenergy without adversely impacting food, land, and other environmental resources. The Northwest Advances Renewables Alliance (NARA), a broad alliance of private industry and educational institutions takes a holistic approach to building a supply chain within WA, OR, ID, and MT based on using forest residuals to make aviation biofuel. NARA's objective is to increase efficiency for each supply chain step from forestry operations to conversion processes; creating new bio

products; providing economic, environmental, and social sustainability analyses; engaging stakeholder groups; and improving bioenergy literacy for students, educators, professionals, and the general public. Forest residuals from logging operations will be used as feedstock to fulfill the project aims of creating a sustainable industry to produce aviation biofuels and important co-products. The Alliance is funded through a five-year grant in the amount of $40 million provided by the United States Department of Agriculture (USDA) National Institute of Food and Agriculture.

Key issues among the stakeholders include soil and water quality, loss of biodiversity, climate, market sustainability, and competition between industries with less expensive conventional biofuels. Many of these issues are currently being studied by different entities such as education, sustainability measurement, feedstock, conversion and outreach as part of the NARA teams. On November 14, 2016, Washington state-based Alaska Airlines made history by flying the first commercial flight from Seattle, WA to Washington, D.C. The plane used a 20% blend of the NARA aviation biofuel, which is chemically indistinguishable from regular jet A fuel. If the airline were able to replace 20% of its entire fuel supply, it would reduce greenhouse gas emissions by about 142,000 t of carbon dioxide. This is equivalent to taking approximately 30,000 passenger vehicles off the road for one year. The University of Utah is responsible for the assessing the hydrologic concerns of the water balance and is part of a larger effort by the sustainability measurement. This is specifically aimed at examining the potential repercussions of incremental woody biomass removal associated with various degrees of residual ground cover (or biomass) removal in the production of bio jetfuel in the Pacific Northwest.

Objectives

The overarching goal of this study is to investigate the potential hydrologic impacts of residual ground cover (biomass) removal in the production of biojet fuel in the Pacific Northwest. The region of interest for this project is the vadose zone of the subsurface. The vadose zone is the portion of the earth's surface that encompasses the soil and unsaturated sediments that lie above the water table. Test sites have been treated with two different types of compaction and three different types of biomass cover for investigation, totaling seven different types of ground treatment. These sites have equipment measuring volumetric water content and temperature on an hourly basis at respective depths in the vadose zone (10 cm, 20 cm, 30 cm, and 100 cm below ground surface). Specifically, the vadose zone investigation will include: 1) induced hydrologic variations due to deviation of evaporation and infiltration processes, 2) the effect of evaporation and infiltration processes based on the type and extent of biomass removal, and 3) the potential applicability of extending this site-scale study to a large, watershed-scale appropriate for the Pacific Northwest. Biomass crops, like conventional food and fiber crops, affect soil quality by causing changes in: organic matter, the relative flux of nutrients, erosion, and soil compaction resulting from equipment movement during planting, maintenance, and harvest. All of these changes are also affected by the biological activity of microfauna and macrofauna, which regulate nutrient dynamics, structure, and stability of the soil (Mann et al., 2000). The results for woody biomass such as Douglas Fir Trees in the Pacific Northwest could show different results and impacts, making this research necessary.

The following three objectives will be used to help achieve this goal:

(1) Collect and process data measured at the test plots and develop a predictive water

quantity model to evaluate site-scale regional impacts of small-scale biomass removal;

(2) To evaluate if there is a correlation between differences in land cover as a function of unique soil characteristics, such as: cation exchange capacity, clay content percentage, soil carbon percentage, slope of the land, microbial population, pH, electric conductivity;

(3) To determine the capability of extending site-scale regional impacts of small-scale biomass removal to watershed-scale semiarid regional impacts of large-scale biomass removal.

These objectives will help quantify the effects of woody biomass removal on the soil and water balance of the study site, and therefore demonstrate the sustainability of harvesting woody biomass forest residuals as a source of biomass for the NARA bioenergy feedstock. The vadose zone groundwater modeling software will mimic the onsite measured values of volumetric water content over time, and calculate for the infiltration/evaporation water budget values, and will be described in greater detail in Chapter 2.

Based on the different treatment removal technologies of two different forms of compaction and three different forms of biomass land cover, there could be potential impacts to water quantity and their timing of infiltration/evaporation, respectively. It has been previously stated that very severe compaction at high moisture contents cause soil deformation, thus decreasing soil water potential (Soane et. al., 1994). Furthermore, it has been studied previously that compaction impairs the conditions of the soil by increased soil bulk density, increased nitrification rates, reduced porosity and water infiltration rates,

damaged soil structure and aggregate stability (Mann et al., 2000). In some soils, even small deformations will cause large decreases in the saturated hydraulic conductivity of that particular soil. For the reasons listed, the literature would suggest that the compacted soil sites will promote more evaporation and less infiltration to the subsurface. Secondly, the seven different treatments are initially assumed to have fluctuations in parameters listed above, such as differences in microbial populations and saturated conductivity values to list a few of many variables. Lastly, to extrapolate the results of this investigation to a watershed-scale would aid in contributing to solutions for broadscale problems in large-scale biomass removal. To extrapolate the results would be to project, extend, or expand the simulated data into an area not known or experienced so as to arrive to a new knowledge of the unknown area by inferences based on an assumed continuity, correspondence, or other parallelism between it and what is known. This definition encompasses the process of "scaling up," or deriving inferences and rules that can be applied to broad scales on the basis of data collected at smaller scales (Miller et al., 2004). Therefore, the three study objectives described above will be evaluated using the following null hypotheses and test their validity:

i) H_o: Increased biomass removal from the LTSP site will have no impact on infiltration rates or the water budget of the subsurface.
ii) H_o: There is no distinction between differences in land cover as a function of unique soil characteristics, such as: slope, saturated conductivity, soil temperature, cation exchange capacity, and microbial populations present.
iii) H_o: Data from the site-scale regional impacts can be applied to watershed-scale regional impacts of large-scale biomass removal through the Pacific Northwest.

Description of the LTSP Sites and Treatment Process

Data for the investigations conducted in this thesis were collected from Weyerhaeuser's LTSP site (see Figure 1.1) in the southern Willamette Valley, OR (see Figure 1.2). To reduce redundancy in each chapter, a common description of study sites and biomass treatment options is provided below. As a part of Weyerhaeuser's effort to sustainably manage its more than six million acres of forested timberland in the U.S., it continues to conduct, evaluate, and support research associated with the North American LTSP program. The program was founded in 1989 as a "grass roots" proposal that grew to a national program of the USDA Forest Service, with its main goal to examine the long-term consequences of soil disturbance on fundamental forest productivity (http://www.fs.fed.us/psw/topics/forest_mgmt/ltsp/). This particular LTSP site near Springfield, OR was created to support the NARA project. A total of 28 one-acre plots were selected by Weyerhaeuser to aid in this investigation and round out an existing regional study, to extend into warmer and drier parts of the Douglas-fir ranges, as to contribute more understanding into the broader LTSP network.

Treatments were randomly assigned, and laid out in such that any plot could feasibly receive that particular random assignment. The original site selection criteria were for one harvest unit in the vicinity of Cottage Grove/Springfield, OR, on uniform soil with low rock content of an area large enough to contain the study plots with an appropriate buffer between plot to allow equipment accessibility and movement. The selected unit is East of Springfield, OR and South of the Mackenzie River on Weyerhaeuser ownership on the Booth Kelly 400 Rd. (Sec 1 18S 01W) at 44.032 Latitude and -122.76 Longitude.

These plots are part of a larger interconnected network for hydrologic analysis. The

site is between 1985 and 2190ft elevation on gentle slopes of 2 to 20%. Soil information was collected from Weyerhaeuser's NARA LTSP Plot Summary Analysis. The majority of the information used to characterize the soil class were the percent silt, percent sand, and percent clay values, cation exchange capacity, carbon organic matter amount, pH, and electric conductivity. The soil percentage values were then interpreted to determine the main soil class using the Natural Resources Conservation Service (NRCS) Soil Texture Calculator (http://www.nrcs.usda.gov/wps/portal/nrcs/detail/soils/survey/?cid=nrcs142p2_054167). Additionally, the soil percent-ages were input into the USDA ARS ROSETTA Model (https://www.ars.usda.gov/pacific-west-area/riverside-ca/us-salinity-laboratory/docs/rosetta-model/) to cross reference the soil class, as well as other fitting parameters, which will be discussed in greater detail in the Calibration and Validation of Hydraulic Parameters in UNSAT-H section.

The average annual precipitation at this location is 50.9" (1292.9 mm). Summers tend to be dry with less than one-third that of the wettest winter month, and with less than 1.54" (39.1 mm) of precipitation in a summer month (http://www.intellicast.com/Local/History.aspx? location=USOR0118). The month with the most precipitation on average is November with 8.44" (214.4 mm) of precipitation. The month with the least precipitation on average is July with 0.64" (16.3 mm) of precipitation. The warmest month, on average, is August with an average temperature of 82°F and the coolest month on average is December, with an average temperature of 46°F.

General LTSP "Core" Treatments consists of a factorial combination of compaction (C0, none; C1, moderate) and aboveground OM removal (OM0, bole/trunk only; OM1, whole tree; OM2, whole tree plus forest floor removal). Three levels of organic matter

removal and two levels of compaction results to total of 7 different treatment plots. Multiple passes with heavy machinery were used to compact soils. Seven different treatment combinations have been applied to 28 study plots; 4 replicate plots of each treatment. The different treatment types based on two different levels of compaction and three different levels of biomass land cover are categorized as follows, and presented via tabular form in Table 1.1, with their designated treatment type denoted by the letter in the top right corner. Additionally, Figure 1.3 depicts each LTSP study plot location on the ArcMap model, including the location of the soil moisture sensor probes and weather stations.

C0 – *No Compaction* – No ground trafficking on plot.

C1 – *Compaction* – Fixed traffic lanes where plot is leveled with forestry machinery.

OM0 – *Boles only* – Boles/Trunks only, meaning harvest consists of removing saw log top (5” minimum diameter), while all other limbs and tops remain on the site.

OM1 – *Total Tree* – Whole-tree type harvest where approximately 75+% of limb/top material is removed along with the boles/trunks. Remaining material will be dispersed and equal across plots.

OM2 – *Total Tree + Forest Floor* – Whole-tree type harvest where ~90-95% of limb/top material is removed along with the bole/trunk. Forest floor and legacy woody debris also removed.

Typical examples of the LTSP plots after woody biomass removal are shown in Figure 1.4 and Figure 1.5. Note the clearly visible compaction tracks caused by harvesting

activities in Figure 1.5. The most recent photo taken of the site was taken on July 11, 2016, and shows the tiny saplings planted earlier that summer, and can be seen in Figure 1.6 below.

The objectives of this study will be completed by collecting the necessary weather and soil characteristics data via Weyerhaeuser's LTSMP Site in Eugene, OR. The mean absolute error (MAE) was calculated for each plot for each season of the year over the course of two years between its measured and simulated value. UNSAT-H Version 3.0: Unsaturated Soil Water and Heat Flow Model, developed by the Pacific Northwest National Laboratory for the United States Department of Energy, will be used to develop a predictive water balance model that correlates with data collected from the soil moisture probes installed in the field. The kind of information that will then be predicted from the model will be quantified amounts of runoff, infiltration, evaporation, overall water balance, and so forth. That information will be used to determine the applicability to evaluate watershed-scale regional impacts. The overall outcome is a better indication of the amount of woody biomass that can be removed as forest residuals following conventional harvest without a reduction in productive capacity of the site. Productive capacity of the site will be determined using the infiltration/evaporation calculations; a lower evaporation rate coupled with higher infiltration rate dictates a high productive capacity, and therefore the favorable outcome. On the contrary, higher evaporation rates coupled with lower infiltration rates defines a low productive capacity, and therefore the nonfavorable outcome.

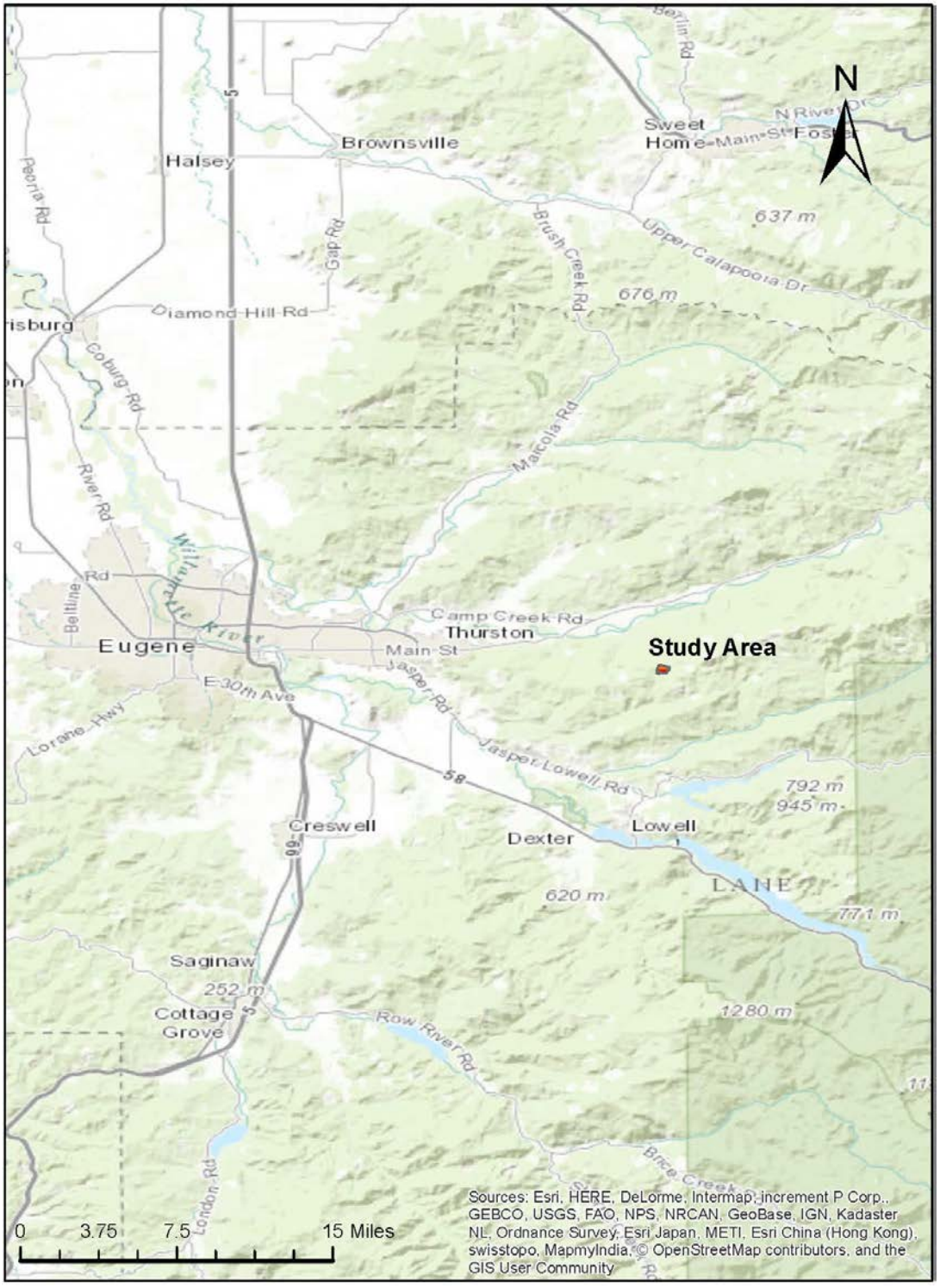

Figure 1.1 Location of LTSP Site in OR GIS Map

Figure 1.2 Location of LTSP Site via Satellite Imagery

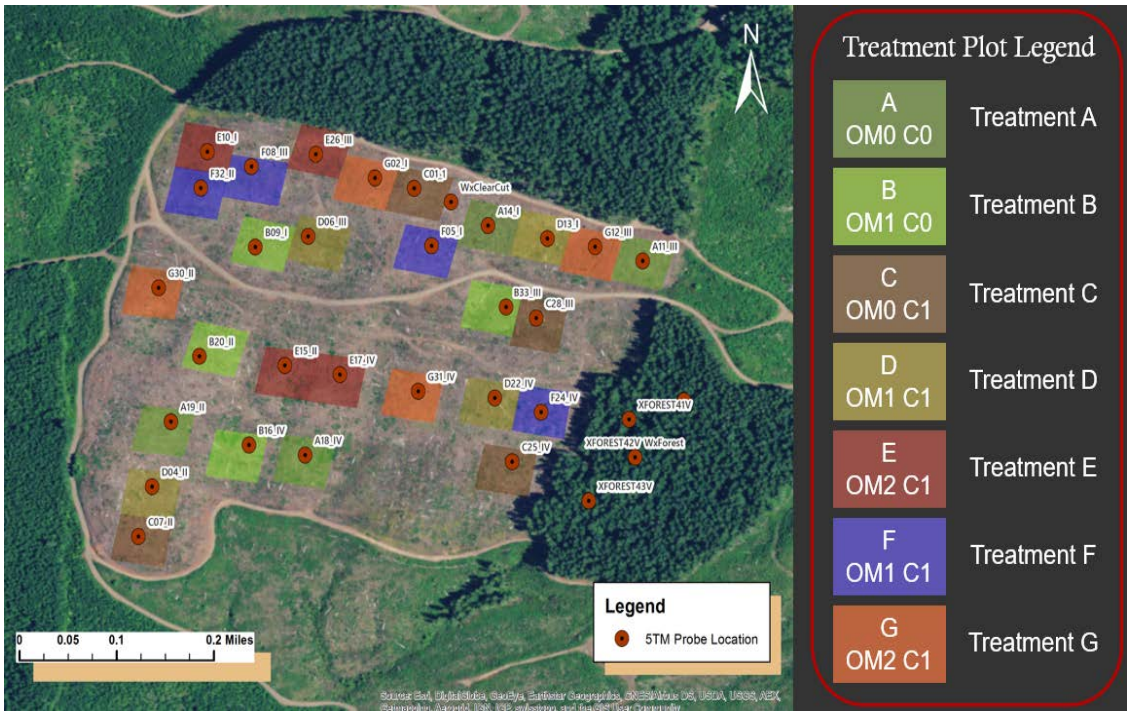

Figure 1.3 ArcMap Model of LTSP Study Plots and Location of Soil Moisture Probes

Table 1.1 Tabular Form of Treatment Removal Technologies

Compaction	C0	C1
Harvest	No Compaction	Moderate Compaction
OM0 – Bole only	OM0 C0 – Boles Removed, No Compaction **A**	OM0 C1 – Boles Removed, Moderate Compaction **C**
OM1 – Boles and crowns removed "Total Tree"	OM1 C0 – Boles and Crowns Removed / No Compaction **B**	OM1 C1 – Boles and Crowns Removed / Moderate Compaction **D/F**
OM2 – Boles, crowns, forest floor removed		OM2 C1 – Boles, Crowns, Forest Floor Removed / Moderate Compaction **E/G**

Figure 1.4 LTSP Site for Treatment A: (OM0 C0) No Compaction Bole Only

Figure 1.5 LTSP Site for Treatment G: (OM2 C1) Compaction Total Tree + FF

Figure 1.6 LTSP Site Picture Taken on July 11, 2016 by Weyerhaeuser. Copyright 2016 by Weyerhaeuser. Reprinted with permission.

CHAPTER 2

WATER BALANCE MODEL

Forest soils serve as underground reservoirs for water. Multiple studies provide evidence that forest-harvesting practices undoubtedly have a significant effect upon surface soil properties, and in semiarid regions where the clearing of land promotes desertification (Bonan, 1999). In rain-dominated portions of the Pacific Northwest, annual water yield may be enhanced by the removal of forest vegetation from small upland watersheds, yet questions still remain regarding the effects of logging operations on infiltration under the variety of climatic, physiographic, and vegetative conditions of this region. A particular study paired watersheds near Fort Bragg located in Northern California, and investigated the impacts of selected harvesting practices of a second-growth Douglas fir and redwood forest on peak infiltration. However, the effect of logging operations upon summer low-flow quantity and timing was not evaluated. This study found there was indeed an alteration of the amount and seasonal distribution of infiltration (Keppeler et al., 1990). The objective of this study is to examine the ecological environment through the measurement of soil moisture at the site, and develop a predictive water quantity and quality models based on each different type of removal (A-G). Based on this objective the following hypothesis will be tested: H_o: Increased biomass removal from the LTSP site will have no impact on infiltration rates or the water budget of the subsurface.

The interception of precipitation (rain and snow) by vegetation canopies is a major component of the surface water balance. Annual net interception losses in temperate forests were observed to range from 9 to 48% of gross precipitation in coniferous canopies. Additionally, previous studies of old-growth Douglas-fir ecosystems in Oregon found net interception losses to be 14% of gross precipitation for the time period between October-April, and 24% of gross precipitation for the time period between May-September (Link et al., 2004). Plant communities that exhibit low precipitation inputs during the growing season must rely on plant or soil water storage to provide the water necessary for growth processes. This soil water storage capability and uptake from the unsaturated zone govern various aspects of ecosystem functioning, and therefore are crucial for groundwater modeling. With this in mind, vadose zone groundwater modeling processes are technically more difficult due to roughly characterizing the extremely heterogeneous soil medium (Warren et al., 2005). Furthermore, modeling is required to determine and evaluate the water budget (infiltration/evaporation processes) of the site, due to insufficient data from the experimental devices not calculating these values. The groundwater model can then be used to study implications of climatic changes for future projections.

Methodology

Data Collection

Four soil moisture measurement probes were installed at each plot location on the map, respectively, totaling to approximately 112 probes for the whole LTSP site. The 5TM Soil Moisture and Temperature Sensor by Decagon Devices® was the chosen soil moisture and temperature probe selected for installation. Weyerhaeuser conducted the seven

different land alterations, at each plot, Weyerhaeuser installed four separate sensors at 10-cm, 20-cm, 30-cm, and 100-cm depths, respectively. For the 10-cm, 20-cm, and 30-cm depths, a trench wall was dug and the sensors were installed with a horizontal orientation to the surface. For the 100-cm depth, an auger hole was drilled into the subsurface and the sensors were installed with a vertical orientation to the surface. In three locations, the 100-cm depth was too gravely to install a 5TM sensor, therefore not collecting data at the 100-cm depth. A schematic of the installation configuration can be found in Figure 2.1.

The 5TM sensor was chosen because of its high accuracy by signal filtering; resulting measurements are then minimized in salinity and textural effects, making it accurate in most soils and even soilless media. An installation demo at short and long subsurface depths can be found on the Decagon Devices website (https://www.decagon.com/en/support/videos/ech2o-sensor-installation/). Additionally, there are two weather stations installed at the sites to measure: precipitation, air temperature, wind speed, relative humidity, and solar radiation at every hour. One weather station in the clear cut section, and the other weather station is located in the forested section. The data were collected and processed to get maximum and minimum daily air temperature [°F], daily average dewpoint temperature [°F], average wind speed per day at 2m height [mile/h], relative humidity and average solar radiation [Langleys/day]. Dew point temperature was calculated from relative humidity and the saturation vapor pressure.

Selection of the Model

An unsaturated flow recharge model has been used to estimate infiltration and evaporation of the groundwater, which will also help to predict water drainage rates for the

simulated conditions. Various numerical models such as Unsaturated-Zone Flow (UZF1), MODFLOW-2005, and UNSAT-H (Fayer, 2000) have been widely used to predict recharge estimates. All of these models use van Genuchten (1980) and Brooks-Corey (1964) water retention functions and the Mualem (1978) and Burdine (1953) hydraulic conductivity functions. All of these models simulate atmospheric interactions, plant transpiration, solute transport, heat transfer, and vapor flow using modified forms of Richard's Equation (Fayer, 2000). Additionally, UZF1 and MODFLOW-2005 contained 2-D and 3-D capabilities that were not used for this project. UZF1 and MODFLOW-2005 use kinematic wave approximations and UNSAT-H uses the finite difference method – this method tends to be more stable when solving problems where contrasts in hydraulic properties exist at layer interfaces (Benson et. al., 2007). UNSAT-H is a 1-D vertical or horizontal model which uses the finite difference method to solve for Richard's Equation (Benson et. al., 2007). Additionally, UNSAT-H is the only model which allows precipitation to be input as a daily amount (in), allowing evapotranspiration to occur throughout the day and provide a more accurate result than UZF1 and MODFLOW-2005. A 1-D numerical model was appropriate for the LTSP site, since it this is a region of relatively flat topography with small to negligible runoff. Thus, the UNSAT-H model was considered most appropriate for this study.

Calibration and Validation of Hydraulic Parameters in UNSAT-H

The UNSAT-H code must have mathematical descriptions of the hydraulic, vapor, and thermal properties of the soil and the air. To solve for the flow equation for liquid water, the code must be supplied with relationships for both water content and hydraulic

conductivity as functions of suction head. The soil water retention function and hydraulic conductivity function work together, constituting the set of hydraulic parameters and properties of the soil required by UNSAT-H. In the case of unsaturated flow, it is difficult to predict water content (θ), hydraulic conductivity (k), and suction head (h) due to the multidimensional, nonhomogeneous characteristics of soil (van Genuchten, 1980). There are many soil water retention relationships that have been determined, such as the linked polynomials, the Haverkamp function, the Brooks and Corey function, the van Genuchten function, and several special functions that account for water retention of very dry soils (Fayer, 2000). Therefore, Equation (2.1) illustrates how water content and hydraulic conductivity are functions of suction head according to the van Genuchten function and Mualem hydraulic conductivity model and has the form

$$\theta = \theta_r + (\theta_s - \theta_r)[1 + (\alpha h)^n]^{-m} \quad 2.1$$

where α, m, and n are curve-fitting parameters, and where it is assumed that m = 1 – 1/n (Mualem, 1976), θ_r is the residual water content, θ_s is the saturated water content. The conductivity function is based on the Mualem conductivity model (Mualem, 1978) and goes as follows in Equation (2.2).

$$K_L = K_S \frac{\{1-(\alpha h)^{n-2}[1+(\alpha h)^n]^{-m}\}^2}{[1+(\alpha h)^n]^{lm}} \quad 2.2$$

where K_L is the unsaturated hydraulic conductivity and K_S is the saturated hydraulic conductivity.

The van Genuchten model was chosen because of its widely used reputation and accuracy (Carsel et al., 1988). Also, the prediction of the parameters listed in Equation (2.1) and (2.2) is necessary for this study, due to an infiltration analysis of the soils not being conducted. There are pedotransfer functions (PTFs) to predict the values of water retention, and the saturated and unsaturated hydraulic conductivity (Schaap et al., 2001). ROSETTA is a computer program that utilizes five hierarchical PTFs, where it interprets and translates basic soil data into hydraulic properties, and additionally, provides the water retention parameters (θ_s, θ_r, K_L, and K_s) and curve fitting parameters (α, m, and n) according to van Genuchten (1980). The class average values of the seven hydraulic parameters for the twelve USDA textural classes can be seen in Table C.1 in Appendix C. This table effectively represents the first model of the hierarchical sequence. For the θ_r, θ_s, α, n, and K_s parameters, the values were generated by computing the average values for each textural class. The values in parentheses give one standard deviation uncertainties of the values. ROSETTA uses a combination of bootstrap and neural networks to calibrate the results and their respective uncertainty values. Additionally, calculating the coefficient of determination (R2) between predicted and measured/fitted hydraulic parameters and root mean square errors (RMSE) between measured and predicted water contents, saturated hydraulic conductivity, and unsaturated hydraulic conductivity.

Soil data containing the sand, silt, and clay percentages from the soil analysis conducted by Weyerhaeuser from each plot were input into ROSETTA. These parameters were averaged over 25 soil samples taken from each plot, where percentages were recorded over three depth profiles: 0-15 cm; 15-30 cm; and 30-100 cm below the soil surface. Table 2.1 gives the results from the ROSETTA simulation based on the soil texture percentages

for the soil depth profile of 0-15 cm. The results for each soil depth profile can be found in Tables C.3 and C.4 in Appendix C.

These values were entered initially, and then used to validate and calibrate the UNSAT-H model. Both statistical and graphical model techniques were reviewed for the calibration of the UNSAT-H simulations. For graphical techniques, curve fitting to simulate the measured data at the LTSP site for each respective plot as closely as possible for the changes in water content over time was used. For statistical model techniques, the mean absolute error (MAE) and percent bias (PBIAS) values were calculated between the observed and simulated values of water content at each given day. The constraining statistic model technique used for this study was PBIAS, and measures the average tendency of the simulated data to be larger or smaller than their observed water content counterparts. The optimal value of PBIAS is 0.0, with low-magnitude values indicating accurate model simulation. Positive values indicate model underestimation bias, and negative values indicate model overestimation bias (Gupta et al., 1999). PBIAS was chosen to calibrate the model because it has the ability to clearly indicate poor model performance (Gupta et al., 1999). The reported performance ratings and corresponding values developed were adapted from the work of Moriasi (2007), and include ranges of values used to establish general performance, which appear in Table 2.2. Model performance was evaluated as "satisfactory" for values PBIAS $\geq \pm$ 25%. For the general calibration, hydraulic conductivity and ranges for saturated and unsaturated volumetric water content values were altered to ensure the results for seasonal and two-year PBIAS statistical values were under 25%. Table 2.3 details the hydrologic soil parameters within UNSAT-H that were altered, along with its potential range of possible values.

ROSETTA Derived Values estimated by the computer software were used as the constraining values for θ using θ_{sat} - θ_r for each respective plot. USDA Baseline Values detailed in Table C.1 in Appendix C were used as the constraining values for k_s, α, and η for each respective plot, as well. θ_s and θ_r were central in the differences among volumetric water content values. Of all of the hydraulic parameters, the saturated hydraulic conductivity was the most influential and sensitive parameter, and was always the variable to adjust first. The second, third, and fourth most influential parameters were θ_s, α, and η, respectively, and in that order. With all of these parameters having the proper constraints on their values, the model was calibrated by changing these values gradually.

Performance was evaluated on the results of the simulation by calculating the MAE and PBIAS values, and can be found in Table 2.4 below. A "satisfactory" rating of ± 15% - ± 25% was preferred, therefore, multiple iterations of parameter changes were made until PBIAS values were under ± 25%. Seasonal PBIAS calculations can be found in Tables C.5-C.7 in Appendix C. The final hydraulic and curve-fitting parameters can be found for Selected Treatment Plots A-B in Table 2.5, and for all of the plots in Table C.5 in Appendix C.

Results

An example of the results from the UNSAT-H model for each treatment process having the letter designation A through C for two years of simulation can be found in Table 2.6, and for all of the plots in Appendix A (Table A.1). A time-series plot for two years of simulation for Plot A14I and its respective volumetric water content measurements (θ) can be found in Figure 2.2, and for all of the plots in Appendix D (Figures D.1 – D.28) for two

two years of simulation.

Discussion

The primary objective of this analysis is to understand the potential hydrologic impacts from woody biomass removal by modeling infiltration and evaporation-induced hydrologic variations, and to evaluate the best possible treatment type. In the following section, emphasis on specific soil characteristics and how their production can affect soil and water quality will be highlighted. Field studies applied at a plot scale, such as the LTSP site, and field experiments at a number of plots within a field plot was done at a fairly low-resolution level. There is much spatial heterogeneity in common existence, and field studies often overlook a rich abundance of information found at a higher resolution. Therefore, considerable consequences for the reliability of the models and thus for the validity of the concepts from these models exists (Raat et. al., 2002). Based on Equation (2.1), any attempt to solve for the value of one term will be limited by the accuracy of the other terms, and serve as a propagation of error throughout the results (Fayer et. al., 2000). Restating the first hypothesis below:

i) H_o: Increased biomass removal from the LTSP site will have no impact on infiltration rates or the water budget of the subsurface.

The water table was assumed to have a depth of 150 cm below the subsurface from soil survey results conducted by Weyerhaeuser. The total basal liquid flux (drainage) water amount that penetrates the water table. Once the water has traveled this vertical distance below the subsurface, it is assumed to have infiltrated the water table and thus impact the water budget. Total infiltration will be defined as the total amount of water that penetrates

the water table located at 150 cm. Any amount of water that resides above the water table, which water includes the current water moisture in the 0 to 150 cm soil profile is considered the “total infiltration.” For the purposes of this study, the total basal liquid flux (drainage) water amount is the only infiltration amount analyzed and of importance. In Table 2.7 is a tabular form of the actual evaporation (cm), total basal liquid flux (drainage) (cm), and the amount of rainfall evaporated (cm) for each plot.

To consolidate the results further, the average of each plot in the four replicate treatment options was done, including the standard deviation in each plot. These results can be found in Table 2.8. After the analysis of the amount of evaporation from each Treatment Type A-G, it was observed that there were statistically higher evaporation rates in Treatments C-F when compared to Treatments A-B, ranging from 12%-32% increases. Treatments D-F fall in the C1 compaction category, as well as the OM1 and OM2 harvest categories. It has been stated that very severe compaction at high moisture contents cause soil deformation, thus decreasing soil water potential (Soane et. al., 1994). Furthermore, it has been studied previously that compaction impairs the conditions of the soil by increased soil bulk density, increased nitrification rates, reduced porosity and water infiltration rates, damaged soil structure, and aggregate stability (Mann et al., 2000). In some soils, even small deformations will cause large decreases in the saturated hydraulic conductivity of that particular soil.

The LTSP site conveys the potential characteristics that are exhibited when topsoil is compacted: the water potential in the top layer is decreased due to increased evaporation. Furthermore, Treatment B exhibited the least average amount of evaporation compared to all other treatments. Treatment B contains the sites that were noncompacted and the crowns

removed. It can be noted that the lack of crowns impacts the amount of evaporation by lessening it. To investigate why the compacted sites had more evaporation, an infiltration analysis was conducted between a noncompacted plot, A19II, with a compacted plot, F08III. These two plots had similar soil types in the subsurface when compared with one another, and therefore chosen for this infiltration analysis. A peak rainfall event was chosen to ensure a significant response in volumetric water content changes. The peak rainfall event occurred on December 20, 2014 for a total of 7.4-cm of rainfall and continued on December 21, 2014 for a total of 5.14-cm of rainfall. The last day observed was December 22, 2014 with a total rainfall amount of 1.54-cm, bringing the total rainfall over the course of the three days to 14.08-cm of precipitation. Hourly volumetric water content (VWC) values were plotted at each port location, 10-cm, 20-cm, 30-cm, and 100-cm, respectively, with precipitation on the secondary axis. Plots A19II and F08III can be found below in Figure 2.3 and 2.4, respectively. For Plot A19II, there is a substantial increase in VWC before the main portion of the storm occurs. Possible sources of error could have risen from measurement error of the 5TM sensor at 100-cm. Additionally, percent change values were calculated from the daily average VWC values for each port location. A positive percentage change in VWC denotes an increase, meaning the soil is gaining water, while a negative percentage change in VWC denotes a decrease, meaning the soil is losing water. These values for Plot A19II and F08II were recorded in a tabular manner, and can be found in Tables 2.9 and 2.10, respectively.

There are differences between Treatment Plot A19II and F08III when comparing the percent change in VWC. With Plot A19II being the noncompacted plot, the percent change being positive in moisture content, that soil moisture is higher when compared to

plot F08III at every port location. Contrastingly, with plot F08III being the compacted plot, the percent change in moisture content in the soil is positive and higher when compared to plot A19II at every port location except for the 100-cm port. Furthermore, during the second day of rainfall (December 21, 2014), plot A19II exhibits a decrease in soil moisture solely in port 1 (10-cm) location; noting the negative percent change value equating to losing 1.30% of its moisture, while the other three ports continue to increase and gain soil moisture. In contrast, plot F08III loses moisture content at a confounding rate, with percent change values for port 1 (10-cm) and port 2 (20-cm) being -3.84% and -4.50%, respectively, equating to losing 3.84% and 4.50% of soil moisture at each location during the second day, respectively. Consequently, plot F08III displays the inability to retain soil moisture, most notably in the first 20-cm of the subsurface. This higher loss in moisture for plot F08III can be attributed to evaporation. With plot F08III being the compacted plot, the soil horizon on the top of the subsurface is most affected, and responds by not retaining soil moisture while simultaneously increasing soil moisture loss rates to evaporation. Furthermore, plot A19II has the ability to retain soil moisture better than plot F08III, even during peak rainfall events, therefore not exhibiting as much evaporation. The question still remains to see if cation exchange capacity, pH, clay content, and other hydrological parameters have an influence on these results.

To investigate why the compacted sites (C-G) are seeing more total basal liquid flux drainage, a soil study was conducted. This examination sought a potential correlation between clay, sand, and silt content percentage to drainage to the water table, by means of a multivariable linear regression. In the analysis, the independent variables were percent clay, sand, and silt content values, while the dependent variable was total basal liquid flux

drainage. Literature states that with the increase in clay content, there is a greater capacity to hold water when compared to sands and silts (Brooks and Corey, 1964; Penman et. al., 2007). A study suggests that on bare soils, raindrop impact breaks soil aggregates at the surface, and additionally a structural seal is formed at the surface. This seal is characterized by greater density, finer pores, and lower saturated hydraulic conductivities than the underlying soil, and it simultaneously decreases the soil infiltration rate (Ben-Hur, et. al., 2004). If there is clay in the soil, it acts as a cement that holds the particles in this aggregate together.

Three regression analyses were done for different hydrologic parameters for the three soil profiles conducted by Weyerhaeuser during the 5TM sensor installation and soil analysis: 0-15 cm, 15-30 cm, and 30-100 cm. When the bin depth went across the 30-cm 5TM sensor, the two different values were averaged together to receive the 30-cm designated value. The statistical results for the analysis of each soil profile for total basal liquid flux drainage simulated values to: percent clay content percentage, pH, electrical conductivity (EC), cation exchange capacity (CEC), Soil Carbon content in Megagrams per hectare (SoilC), mean slope, saturated hydraulic conductivity, average temperature, the five major genus of bacteria present (Bacillus, Clostridium, Shewanella, Thermoanerobacter, and Lactobacillus) were calculated.

Organic matter is the material in soil that is directly derived from plants and animals, and it supports most important microfauna and microflora in the soil. For this study, soil carbon was used, and is measured in megagrams per hectare (Mg/ha), in other words, the dry mass per area. Through its breakdown and interaction with other soil constituents, it is largely responsible for much of the physical and chemical fertility of a

soil (Hazelton et. al., 2007). Furthermore, organic carbon content is perhaps the most widely measured indicator of soil quality or potential productivity, although how changes in soil carbon will affect other soil characteristics in different soils is not always predictable (Mann et al. 2000). Crop systems that result in increases in organic carbon generally yield gradual, positive changes in soil structure, water-holding capacity, and the storage and availability of nutrients, which in turn, lead to increased abundance and diversity of soil biota. Furthermore, Crop residues and their decomposition are the main factors determining the organic matter content of soils.

CEC is a measure of the soil's ability to hold positively charged ions. It is a very important soil property influencing soil structure stability, nutrient availability, soil pH, and the soil's reaction to fertilizers and other ameliorants. CEC is an inherent soil characteristic and is difficult to alter significantly. It influences the soil's ability to hold onto essential nutrients and provides a buffer against soil acidification. Soils with a higher clay fraction tend to have a higher CEC. Organic matter has a very high CEC (Hazleton and Murphy, 2007). If a particular soil has a high CEC value, the soil has been characterized to have a larger capacity to hold onto the negatively charged water molecule. The opposite is also true, if a particular soil has a lower CEC value, the soil has a lower capacity to hold water.

Soil pH is a measure of the concentration of hydrogen ions in the soil solution. The lower the pH of soil, the greater the acidity. pH should be maintained at above 5.5 in the topsoil and 4.8 in the subsurface. A well-maintained soil pH will maintain the value of the soil resource, maximize crop and pasture choice, and avoid production losses due to low pH (http://www.soilquality.org.au/factsheets/soil-acidity). Chemical reactions are lowest

when the solution or soil is close to a neutral pH of 7.0. The pH characterizes the chemical environment of the soil and may be used as a guide to suitability of soils for various pasture and crop species. Soil pH is also an indicator of the chemical processes that occur in the soil, and is a guide to likely deficiencies and/or toxicities (Slattery et al., 1999). Dragun (1998) also provides guidelines for interpreting soil pH values for environmental evaluation. Based on the pH of the site soil profiles for the (0-15 cm), (15-30 cm), and (30-100 cm) depths averaging at 5.1, 5.1, and 4.9, respectively, Dragun (1998) designated the subsurface as strongly acidic in all cases. Since these values do not fall under 4.8, the subsurface is still within a tolerable range.

The R square values, standard error values, coefficients, t-values, p-values, and ANOVA analyses can be found in Tables 2.11 – 2.13 below for each respective soil layer. Raw data before statistical analysis can be found in Tables C.9 – C.11 in Appendix C. It is evident that there is no statistically significant correlation between a higher clay content exhibiting less drainage values at any soil profile depth, illustrated by having p-values of 0.179, 0.653, and 0.156, respectively. Furthermore, for all of the soil profiles, the multivariable regression analyses show a small R-squared value for fit, and additionally had a large p-value greater than 0.05 for every parameter. Since these p-value statistics were all much greater than 0.05, it cannot be firmly concluded that these sites exhibit more drainage or less drainage according to these unique soil characteristic. The null hypothesis, H_o, is therefore rejected.

The next hypothesis that will be analyzed details the potential differences in land cover as a function of unique soil characteristics.

ii) H_o: There is no distinction between differences in land cover as a function of unique

soil characteristics.

Referring to Table C.5 in Appendix C, similar soil depth profiles and treatment types were compared in an ANOVA analysis to one another, so that mixed effects of differences in parameters are considered. Out of all of the ANOVA results indicated in Tables 2.11 – 2.13, the F critical value is less than 2.5, therefore indicating that all means are different in the analysis. Furthermore, the correlations were insignificant and did not even have a calculable p-value, meaning that there is a significant difference between the means of each group, respectively. The null hypothesis in summary is accepted. There was no clear defining distinction between the land cover applications when comparing it to the plot's unique soil characteristics. While it is true that most of the sites contained loams, clay loams, and clays, each plot had a different soil composition at each respective subsurface depth (Table C.5 in Appendix C and Figures F.1 – F.12 in Appendix F).

iii) H_o: Data from the site-scale regional impacts can be applied to watershed-scale regional impacts of large-scale biomass removal through the Pacific Northwest.

The null hypothesis in summary is rejected. Through research and investigation, site-scale regional impacts cannot be applied to watershed-scale regional impacts of large-scale biomass removal through the Pacific Northwest. At a watershed-scale, regional studies are insufficient in capturing differing soils, slopes, and aspect ratios.

As stated previously, since each treatment plot had a different soil composition, 28 different codes were written for all 28 plots with that specific soil composition. This includes differing values in volumetric water capacity, saturated hydraulic conductivity, Van Genuchten parameters, and soil layers. Since the soil is so diverse in the 28-acre plots, the soil diversity would only be greater in a larger area than the LTSP site. Furthermore,

coarse generalizations in soil and area would hinder the accuracy of the model, and would in effect, produce questionable results. Differing slopes in topography and elevation would also contribute to different results in scaling-up. The LTSP site slope values were calculated using a Digital Elevation Model (DEM) in ArcMap 10.2.2., and can be seen in Figure 2.5

As it can be observed, there are a few depressions in the soil (indicated by the dark green areas) and a few small hills in the topography (indicated by the dark red areas). The average slope values were calculated at each of the 28 different site plots, and their values with standard deviations are presented in Table 2.14.

The variability of the soil surface slope can affect the manner and rate at which water infiltrates. Additionally, topographic variation in slopes of terrain can produce local differences in solar radiation that can equate to tens of degrees of latitude. This phenomenon is seen more in mountains, but also occurs on hillslopes as well. The LTSP site slope values range between 1.38% and 6.62%. Since these mean values are low in value, slope does not influence the amount of infiltration or runoff of the land surface.

Lastly, aspect can affect the amount of evaporation occurring on the soil surface. Aspect is another term used to define the azimuth angle of the slope, and is the direction to which the slope is oriented (north = 0°, east = 90°, south = 180°, west = 270°). The azimuth of the Sun is the compass bearing of the Sun on the horizon, and is east in the morning, south in the Northern Hemisphere at solar noon, and in the west after noon (http://www.cgd.ucar.edu/tss/aboutus/staff/bonan/ecoclim/1sted/Chapter08.pdf). The aspect of the LTSP Site was calculated using the DEM discussed previously, and can be seen in Figure 2.6. As it can be observed, a majority of the plots are South or Southwest facing.

There is a complex relationship between slope, aspect, latitude, time of year, and solar radiation, but the main generalization concludes that north slopes receive less radiation. Furthermore, south and gentle slopes receive more radiation than steep slopes. A defining characteristic of the LTSP site is that it is majorly south-facing and has gentle slopes. Thus, the aspect was also not an influential parameter in differing results in evaporation rates.

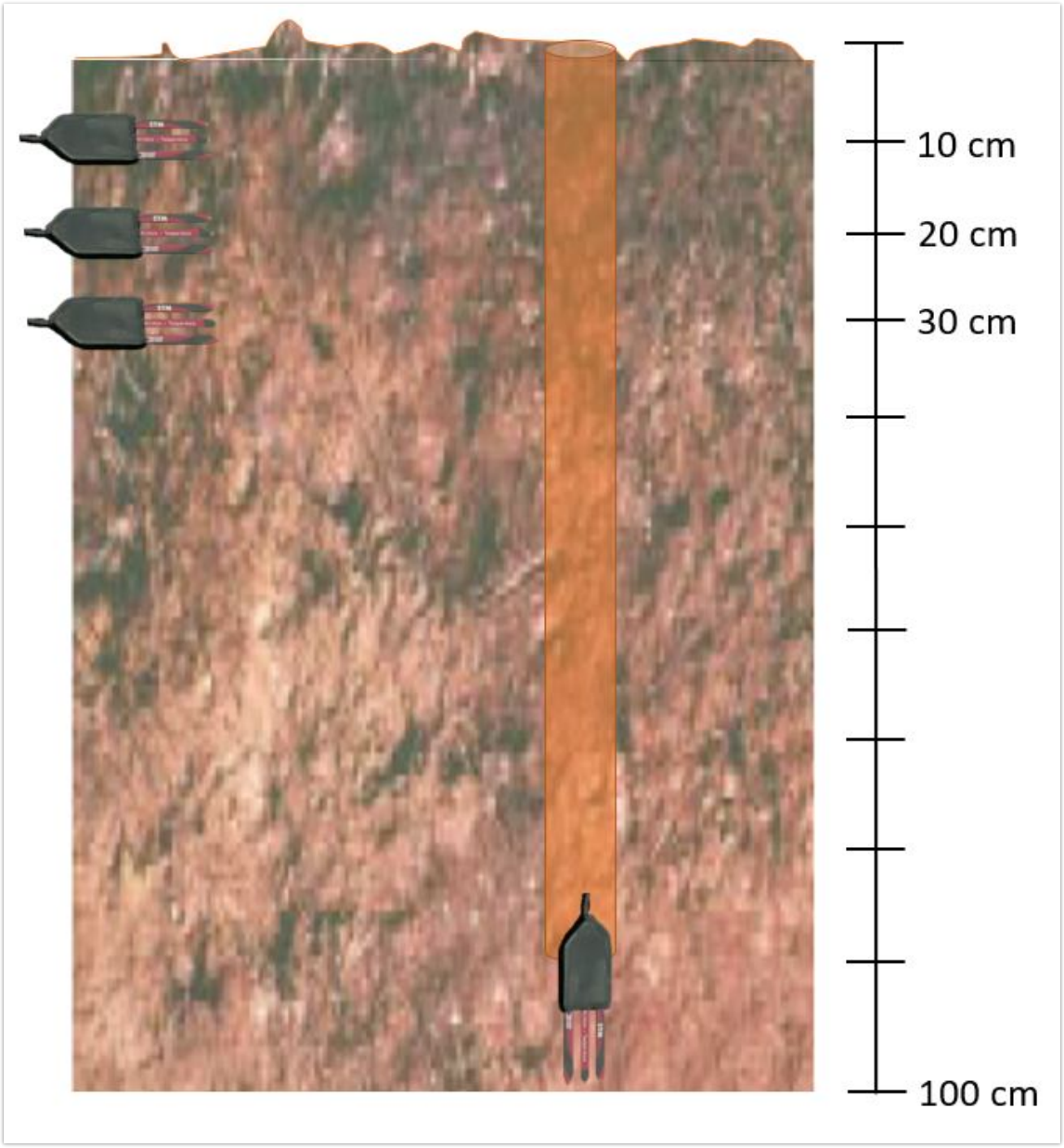

Figure 2.1 Soil Moisture and Temperature Sensor 5TM Installation Configuration

Table 2.1 ROSETTA Simulation Results for Each Plot for Hydraulic Parameters

Code	Description	θ_r [cm^3/cm^3]	θ_s [cm^3/cm^3]	α [1/cm]	η	K_s [cm/day]	K_o [cm/day]
11	A11III	0.080	0.437	0.010	1.457	10.73	2.733
14	A14I	0.077	0.431	0.010	1.469	10.53	2.740
18	A18IV	0.086	0.453	0.012	1.403	10.21	3.012
19	A19II	0.084	0.447	0.011	1.437	11.04	2.763
9	B09I	0.086	0.454	0.011	1.422	11.32	2.804
16	B16IV	0.074	0.430	0.008	1.511	12.69	2.295
20	B20II	0.080	0.437	0.011	1.436	9.05	2.980
33	B33III	0.080	0.437	0.010	1.457	10.73	2.733
1	C01I	0.077	0.431	0.010	1.469	10.53	2.740
7	C07II	0.078	0.432	0.010	1.455	9.68	2.863
25	C25IV	0.085	0.450	0.011	1.430	11.17	2.782
28	C28III	0.076	0.430	0.009	1.490	11.92	2.503
4	D04II	0.082	0.444	0.011	1.444	10.92	2.749
6	D06III	0.085	0.448	0.012	1.403	9.02	3.108
13	D13I	0.081	0.438	0.012	1.422	8.34	3.107
22	D22IV	0.082	0.446	0.009	1.471	11.99	2.452
10	E10I	0.081	0.439	0.011	1.443	10.00	2.854
15	E15II	0.075	0.429	0.009	1.482	11.32	2.622
17	E17IV	0.085	0.448	0.012	1.403	9.02	3.108
26	E26III	0.068	0.412	0.011	1.472	8.10	3.276
5	F05I	0.078	0.432	0.010	1.455	9.68	2.863
8	F08III	0.068	0.414	0.010	1.481	8.78	3.077
24	F24IV	0.078	0.437	0.009	1.499	12.36	2.311
32	F32III	0.082	0.439	0.012	1.409	7.78	3.236
2	G02I	0.069	0.417	0.009	1.509	12.07	2.581
12	G12III	0.086	0.451	0.012	1.396	9.32	3.117
30	G30II	0.075	0.429	0.009	1.482	11.32	2.622
31	G31IV	0.084	0.446	0.012	1.416	9.67	2.987

Table 2.2 General Performance Ratings for Recommended Statistics

Performance Rating	PBIAS (%)
Very good	PBIAS $< \pm 10$
Good	$\pm 10 \leq$ PBIAS $< \pm 15$
Satisfactory	$\pm 15 \leq$ PBIAS $< \pm 25$
Unsatisfactory	PBIAS $\geq \pm 25$

Table 2.3 Hydrologic Soil Parameters and Parameter Value Constraints

Parameter	Range	Test & Implementation
θ	θ_{sat} - θ_r	ROSETTA Derived Values in Table 2.1 & Table C.2 – C.4 in Appendix – C
k_s	k_s - k_o	USDA Baseline Values in Table C.1 in Appendix – C
α	α_{max} - α_{min}	USDA Baseline Values in Table C.1 in Appendix – C
η	η_{max} - η_{min}	USDA Baseline Values in Table C.1 in Appendix – C

Table 2.4 Performance Results for Two-Year Simulation of UNSAT-H

Plot	Treatment	MAE Node 1 (10cm)	MAE Node 2 (20 cm)	MAE Node 3 (30 cm)	MAE Node 4 (100 cm)	Percent Bias Node 1 [%]	Percent Bias Node 2 [%]	Percent Bias Node 3 [%]	Percent Bias Node 4 [%]
14	A-I	0.02	0.03	0.01	0.05	4.6%	9.4%	2.8%	19.5%
19	A-II	0.03	0.02	0.05	0.05	9.4%	4.0%	13.2%	5.9%
11	A-III	0.02	0.02	0.01	0.01	-1.5%	-3.0%	1.0%	-1.9%
18	A-IV	0.04	0.02	0.02	0.05	12.6%	0.4%	6.2%	12.2%
9	B-I	0.06	0.02	0.05	0.03	18.0%	1.0%	24.1%	7.2%
20	B-II	0.04	0.05	0.04	0.03	-11.5%	12.7%	3.4%	-0.3%
33	B-III	0.03	0.03	0.00	0.01	-6.7%	-7.9%	-0.5%	0.6%
16	B-IV	0.04	0.02	0.01	0.06	-12.7%	-4.5%	0.4%	3.4%
1	C-I	0.01	0.01	0.01	0.04	-0.4%	-1.2%	1.0%	-2.3%
7	C-II	0.03	0.02	0.02	0.01	-2.2%	5.2%	-5.8%	0.5%
28	C-III	0.02	0.03	0.04	0.06	-2.2%	6.8%	9.6%	6.0%
25	C-IV	0.04	0.02	0.02	0.02	10.9%	3.2%	4.2%	4.6%
13	D-I	0.02	0.01	0.01	0.03	4.1%	-2.3%	-1.7%	-1.9%
4	D-II	0.04	0.03	0.02	0.01	-4.5%	-5.4%	3.7%	-0.1%
6	D-III	0.05	0.02	0.02	0.05	-11.2%	3.3%	5.6%	-7.7%
22	D-IV	0.04	0.03	0.01	0.02	-8.7%	-6.6%	2.7%	0.6%
10	E-I	0.03	0.03	0.02	0.01	5.7%	6.8%	4.5%	0.9%
15	E-II	0.02	0.01	0.01	0.03	0.3%	-0.2%	0.9%	-1.5%
26	E-III	0.01	0.01	0.02	NA	0.2%	0.8%	-2.7%	NA
17	E-IV	0.03	0.01	0.01	0.01	-4.9%	2.1%	3.7%	-2.5%
5	F-I	0.02	0.01	0.01	NA	5.6%	3.4%	1.3%	NA
32	F-II	0.03	0.01	0.02	0.02	-4.1%	-0.5%	4.5%	-3.6%
8	F-III	0.02	0.02	0.02	0.01	4.9%	-4.3%	-2.9%	-1.7%

Table 2.4 (continued) Performance Results for Two-Year Simulation of UNSAT-H

Plot	Treatment	MAE Node 1 (10cm)	MAE Node 2 (20 cm)	MAE Node 3 (30 cm)	MAE Node 4 (100 cm)	Percent Bias Node 1 [%]	Percent Bias Node 2 [%]	Percent Bias Node 3 [%]	Percent Bias Node 4 [%]
24	F-IV	0.04	0.03	0.01	0.02	0.3%	0.9%	0.1%	-3.1%
2	G-I	0.02	0.01	0.01	NA	-6.1%	-1.0%	2.0%	NA
30	G-II	0.03	0.01	0.01	0.04	-0.7%	-1.8%	2.1%	-8.3%
12	G-III	0.04	0.02	0.02	NA	5.5%	6.1%	5.1%	NA
31	G-IV	0.01	0.01	0.01	0.01	0.3%	2.5%	3.2%	1.8%

Table 2.5 Hydraulic Parameters Entered for Each Soil Profile Depth for Treatment Plots A-B

Plot	Treatment	Soil Profile	θ_{sat}	θ_r	$\theta_{sat} - \theta_r$	Soil Class	α [1/cm]	η	K_s [cm/hr]
11	A-III	0-14.9 cm	0.3750	0.210	0.165	Clay Loam	0.01018	1.45686	2.07
11	A-III	15-24.9 cm	0.400	0.250	0.150	Clay Loam	0.01387	1.35759	1.60
11	A-III	25-64.9 cm	0.430	0.300	0.130	Clay Loam	0.01731	1.26876	1.42
11	A-III	65-150 cm	0.3800	0.3400	0.040	Clay	0.01731	1.26876	1.10
9	B-I	0-24.9 cm	0.470	0.250	0.220	Clay Loam	0.019	1.310	1.90
9	B-I	25-64.9 cm	0.280	0.160	0.120	Clay	0.0080	1.0900	1.43
9	B-I	65-150 cm	0.430	0.380	0.050	Clay	0.0080	1.0900	1.21
14	A-I	0-24.9 cm	0.38	0.25	0.13	Clay Loam	0.019	1.310	2.70
14	A-I	25-64.9 cm	0.4	0.34	0.06	Clay Loam	0.019	1.310	1.5
14	A-I	65-150 cm	0.3	0.25	0.05	Clay	0.0080	1.0900	2.65
18	A-IV	0-14.9 cm	0.32	0.15	0.17	Clay Loam	0.019	1.310	2.0
18	A-IV	15-64.9 cm	0.46	0.37	0.09	Clay Loam	0.019	1.310	1.35
18	A-IV	65-150 cm	0.45	0.37	0.08	Clay	0.0080	1.0900	0.85
19	A-II	0-14.9 cm	0.37	0.25	0.12	Clay Loam	0.019	1.310	1.7
19	A-II	15-64.9 cm	0.47	0.35	0.12	Clay Loam	0.019	1.310	1.1
19	A-II	65-150 cm	0.38	0.31	0.07	Clay	0.0080	1.0900	0.56
16	B-IV	0-14.9 cm	0.33	0.23	0.1	Loam	0.036	1.56	1.07
16	B-IV	15-24.9 cm	0.5	0.42	0.08	Clay Loam	0.019	1.310	0.82
16	B-IV	25-64.9 cm	0.35	0.29	0.06	Clay	0.0080	1.0900	0.6
16	B-IV	65-150 cm	0.48	0.4	0.08	Clay	0.0080	1.0900	0.6

Table 2.6 Results from UNSAT-H Program for Two Years of Simulation for Treatment Plots A-C

Plot	Treatment	Initial Water Storage [cm]	Potential Evaporation [cm]	Actual Evaporation [cm]	Total Basal Liquid Flux (drainage) [cm]	Total Final Moisture Storage [cm]	Total Runoff [cm]	Total Infiltration [cm]	Actual Rainfall [cm]
14	A-I	48.7	184.6	69.1	239.2	49.8	0	356.7	356.7
19	A-II	59.2	184.6	51.2	200.6	58.9	0	356.7	356.7
11	A-III	55.7	184.6	85.9	251.7	56.2	0	356.7	356.7
18	A-IV	63.8	184.6	76.3	246.2	64.0	12.1	344.6	356.7
9	B-I	58.0	184.6	78.2	186.0	57.6	0	356.7	356.7
16	B-IV	62.1	184.6	53.2	251.1	62.0	0	356.7	356.7
20	B-II	46.2	184.6	58.1	260.5	46.0	14.3	342.4	356.7
33	B-III	45.3	184.6	67.9	229.4	44.6	0	356.7	356.7
1	C-I	46.8	184.6	66.3	189.6	46.4	0.985	355.8	356.7
7	C-II	55.7	184.6	75.3	215.2	55.1	0	356.7	356.7
25	C-IV	64.7	184.6	73.1	258.4	64.3	0.112	356.6	356.7
28	C-III	74.7	184.6	74.3	247.5	74.7	0	356.7	356.7

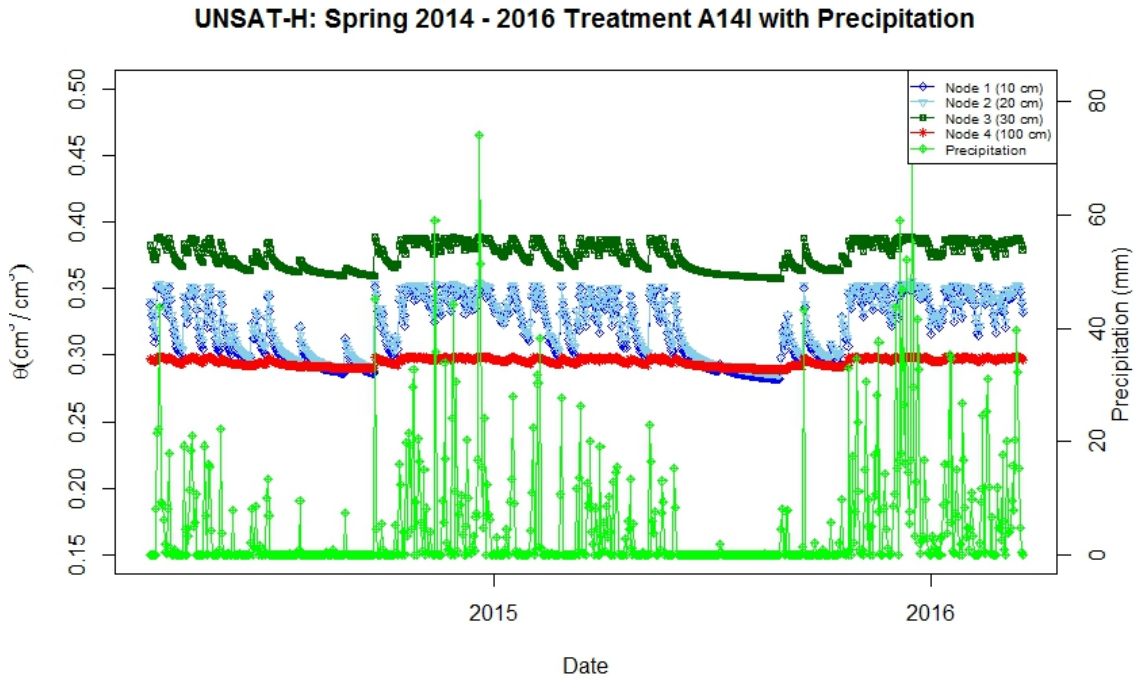

Figure 2.2 UNSAT-H Simulation for Two Years of Plot A14I - VWC with Precipitation

Table 2.7 Results of 2-Year Simulation for Water Budget for All LTSP Plots

Plot	Treatment	Actual Evaporation [cm]	Total Basal Liquid Flux (drainage) [cm]	Total Amount of Rainfall Evaporated [cm]
14	A-I	69.1	239.2	19%
19	A-II	51.2	200.6	14%
11	A-III	85.9	251.7	24%
18	A-IV	76.3	246.2	21%
9	B-I	78.2	186.0	22%
20	B-II	58.1	260.5	16%
33	B-III	67.9	229.4	19%
16	B-IV	53.2	251.1	15%
1	C-I	66.3	189.6	19%
7	C-II	75.3	215.2	21%
25	C-IV	73.1	258.4	21%
13	D-I	76.4	258.8	21%
4	D-II	83.4	265.1	23%
6	D-III	68.7	246.7	19%
22	D-IV	63.3	265.4	18%
15	E-II	85.0	267.2	24%
26	E-III	80.6	277.8	23%
17	E-IV	82.5	261.8	23%
5	F-I	81.3	269.3	23%
32	F-II	84.9	258.8	24%
8	F-III	87.3	264.5	24%
24	F-IV	86.2	267.1	24%
2	G-I	84.0	271.5	24%
30	G-II	89.4	260.5	25%
12	G-III	94.6	235.2	27%
31	G-IV	48.7	289.3	14%
Total for LTSP Site		2115.0	6991.2	21%

Table 2.8 Summary of Evaporation and Basal Liquid Flux Results by Treatment Type

Treatment	Average Evaporation [cm] (SD)	Evaporation - Percent Increase from Treatment B	Average Total Basal Liquid Flux (drainage) [cm]	Infiltration - Percent Increase from Treatment B	Average Amount of Rainfall Evaporated [cm]
A	70.6 (12.7)	10%	234.4 (20.0)	1.217	20%
B	64.4 (9.6)	NA	231.8 (28.7)	NA	18%
C	72.3 (3.5)	12%	227.7 (27.1)	-1.769	20%
D	72.9 (7.6)	13%	259.0 (7.5)	11.734	20%
E	84.4 (3.4)	31%	265.8 (7.9)	14.668	24%
F	84.9 (2.3)	32%	264.9 (3.9)	14.280	24%
G	79.2 (18.0)	23%	264.2 (19.6)	13.978	22%

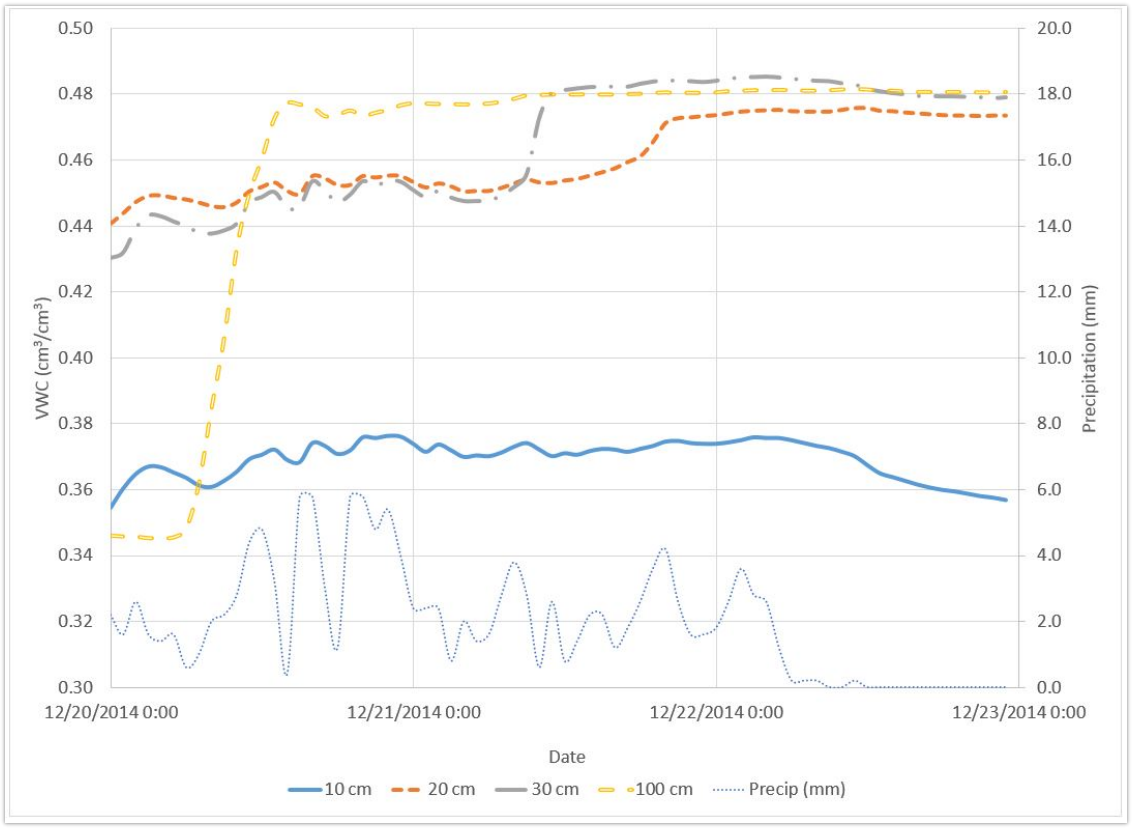

Figure 2.3 Treatment Plot A19II VWC during Peak Rainfall Event in December 2014

Table 2.9 Plot A19II Percent Change in VWC

A19II					
Date	Precip (cm)	Port 1 (10 cm)	Port 2 (20 cm)	Port 3 (30 cm)	Port 4 (100 cm)
12/20/2014	7.40	0.368	0.450	0.445	0.423
12/21/2014	5.14	0.372	0.458	0.469	0.479
	Percent Change	1.11%	1.60%	5.10%	11.8%
12/21/2014	5.14	0.372	0.458	0.469	0.479
12/22/2014	1.54	0.367	0.474	0.482	0.481
	Percent Change	-1.30%	3.68%	2.87%	0.40%

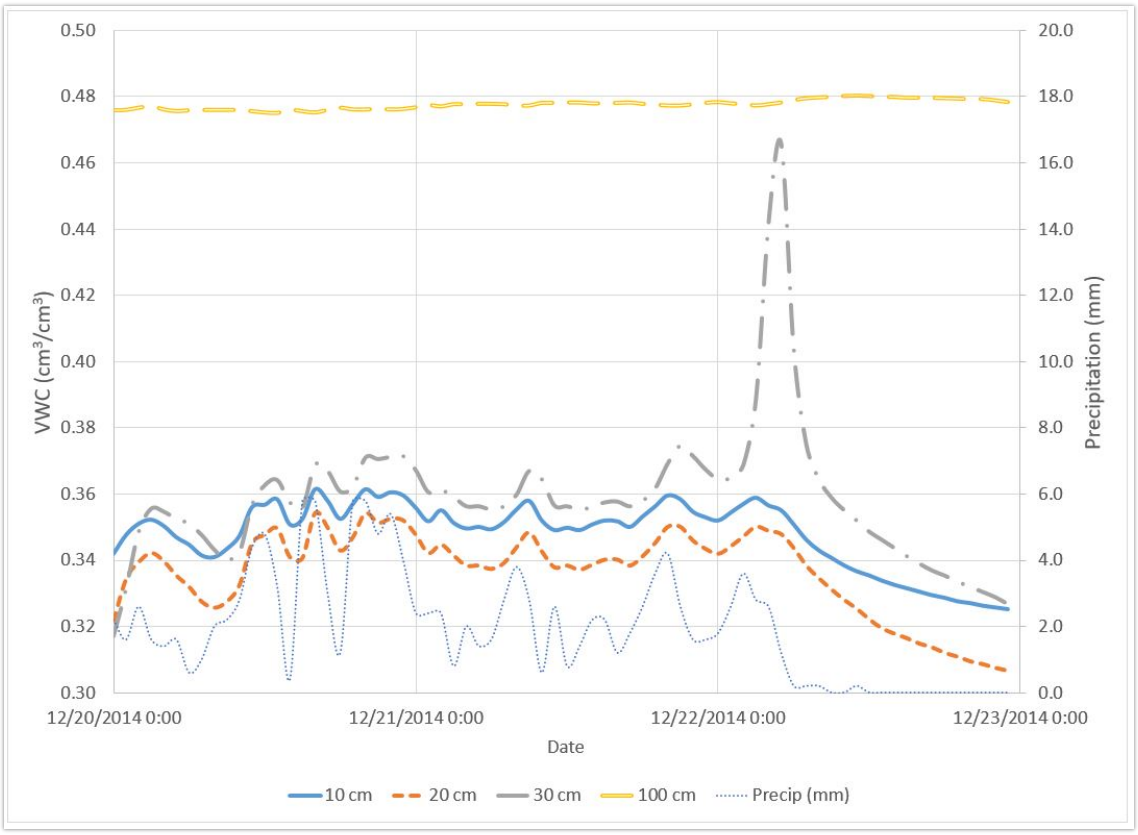

Figure 2.4 Treatment Plot F08III VWC during Peak Rainfall Event in December 2014

Table 2.10 Plot F08III Percent Change in VWC

F08III					
Date	Precip (cm)	Port 1 (10 cm)	Port 2 (20 cm)	Port 3 (30 cm)	Port 4 (100 cm)
12/20/2014	7.40	0.352	0.341	0.355	0.476
12/21/2014	5.14	0.353	0.342	0.361	0.478
	Percent Change	0.183%	0.309%	1.59%	0.40%
12/21/2014	5.14	0.353	0.342	0.361	0.478
12/22/2014	1.54	0.339	0.327	0.360	0.479
	Percent Change	-3.84%	-4.50%	-0.18%	0.30%

Table 2.11 Regression and ANOVA Statistical Results Between All Parameters for (0-15 cm) Soil Profile

Regression Statistics						
R Square	0.624					
Standard Error	21.525					
Observations	28					
Parameter	*Coefficients*	*Standard Error*	*t Stat*	*P-value*		
Intercept	600.770	371.717	1.616	0.128		
Clay (%)	-2.753	1.946	-1.414	0.179		
pH (0-15cm) <2mm	-38.594	45.322	-0.852	0.409		
EC (0-15cm) <2mm	-65.906	198.928	-0.331	0.745		
CEC (0-15cm) <2mm	-1.263	1.106	-1.141	0.273		
SoilC (0-15cm) (Mg/ha)	0.387	1.180	0.328	0.748		
Mean Slope (%)	4.954	3.827	1.295	0.216		
Saturated Conductivity (cm/hr)	-9.150	11.677	-0.784	0.446		
Average Temperature (°C)	3.318	10.303	0.322	0.752		
Genus of Bacteria: Bacillus (205)	-5.943	3.364	-1.767	0.099		
Genus of Bacteria: Clostridium (185)	3.980	3.796	1.048	0.312		
Genus of Bacteria: Shewanella (68)	-8.342	6.197	-1.346	0.200		
Genus of Bacteria: Thermoanerobacter (43)	1.319	4.632	0.285	0.780		
Genus of Bacteria: Lactobacillus (44)	7.827	3.767	2.078	0.057		
ANOVA Analysis	*SS*	*df*	*MS*	*F*	*P-value*	*F crit*
Between Groups	1510892	13	116222	2083	0	1.75
Within Groups	21092	378	55.8			
Total	1531984	391				

Table 2.12 Regression and ANOVA Statistical Results Between All Parameters for (15-30 cm) Soil Profile

Regression Statistics						
R Square	0.602					
Standard Error	22.136					
Observations	28					
Parameter	*Coefficients*	*Standard Error*	*t Stat*	*P-value*		
Intercept	272.845	329.635	0.828	0.422		
Clay (%)	-0.546	1.188	-0.460	0.653		
pH (15-30 cm) <2mm	39.767	48.115	0.827	0.422		
EC (15-30 cm) <2mm	-306.323	459.017	-0.667	0.515		
CEC (15-30 cm) <2mm	-1.519	1.467	-1.035	0.318		
SoilC (15-30 cm) (Mg/ha)	-0.785	1.143	-0.687	0.503		
Mean Slope (%)	5.254	3.270	1.606	0.130		
Saturated Conductivity (cm/hr)	-6.040	9.287	-0.650	0.526		
Average Temperature (°C)	-0.077	12.107	-0.006	0.995		
Genus of Bacteria: Bacillus (205)	-6.950	3.777	-1.840	0.087		
Genus of Bacteria: Clostridium (185)	4.670	3.934	1.187	0.255		
Genus of Bacteria: Shewanella (68)	-9.486	6.501	-1.459	0.167		
Genus of Bacteria: Thermoanerobacter (43)	3.279	5.033	0.652	0.525		
Genus of Bacteria: Lactobacillus (44)	6.752	3.588	1.882	0.081		
ANOVA Analysis	*SS*	*df*	*MS*	*F*	*P-value*	*F crit*
Between Groups	1503164	13	115628	2063	0	1.75
Within Groups	21188	378	56.1			
Total	1524352	391				

Table 2.13 Regression and ANOVA Statistical Results Between All Parameters for (30-100 cm) Soil Profile

Regression Statistics						
R Square	0.656					
Standard Error	20.6					
Observations	28					
Parameter	*Coefficients*	*Standard Error*	*t Stat*	*P-value*		
Intercept	335.914	416.735	0.806	0.434		
Clay (%)	-1.691	1.128	-1.499	0.156		
pH (30-100 cm) <2mm	17.860	76.575	0.233	0.819		
EC (30-100 cm) <2mm	-508.780	816.421	-0.623	0.543		
CEC (30-100 cm) <2mm	-1.242	0.822	-1.511	0.153		
SoilC (30-100 cm) (Mg/ha)	-0.091	0.408	-0.224	0.826		
Mean Slope (%)	5.704	3.584	1.591	0.134		
Saturated Conductivity (cm/hr)	-25.200	18.273	-1.379	0.190		
Average Temperature (°C)	3.400	9.628	0.353	0.729		
Genus of Bacteria: Bacillus (205)	-4.177	3.287	-1.271	0.225		
Genus of Bacteria: Clostridium (185)	3.767	3.766	1.000	0.334		
Genus of Bacteria: Shewanella (68)	-6.385	6.360	-1.004	0.332		
Genus of Bacteria: Thermoanerobacter (43)	-0.805	4.519	-0.178	0.861		
Genus of Bacteria: Lactobacillus (44)	4.836	3.827	1.264	0.227		
ANOVA Analysis	*SS*	*df*	*MS*	*F*	*P-value*	*F crit*
Between Groups	1622774	13	124828	1713	0	1.75
Within Groups	27538	378	73			
Total	1650312	391				

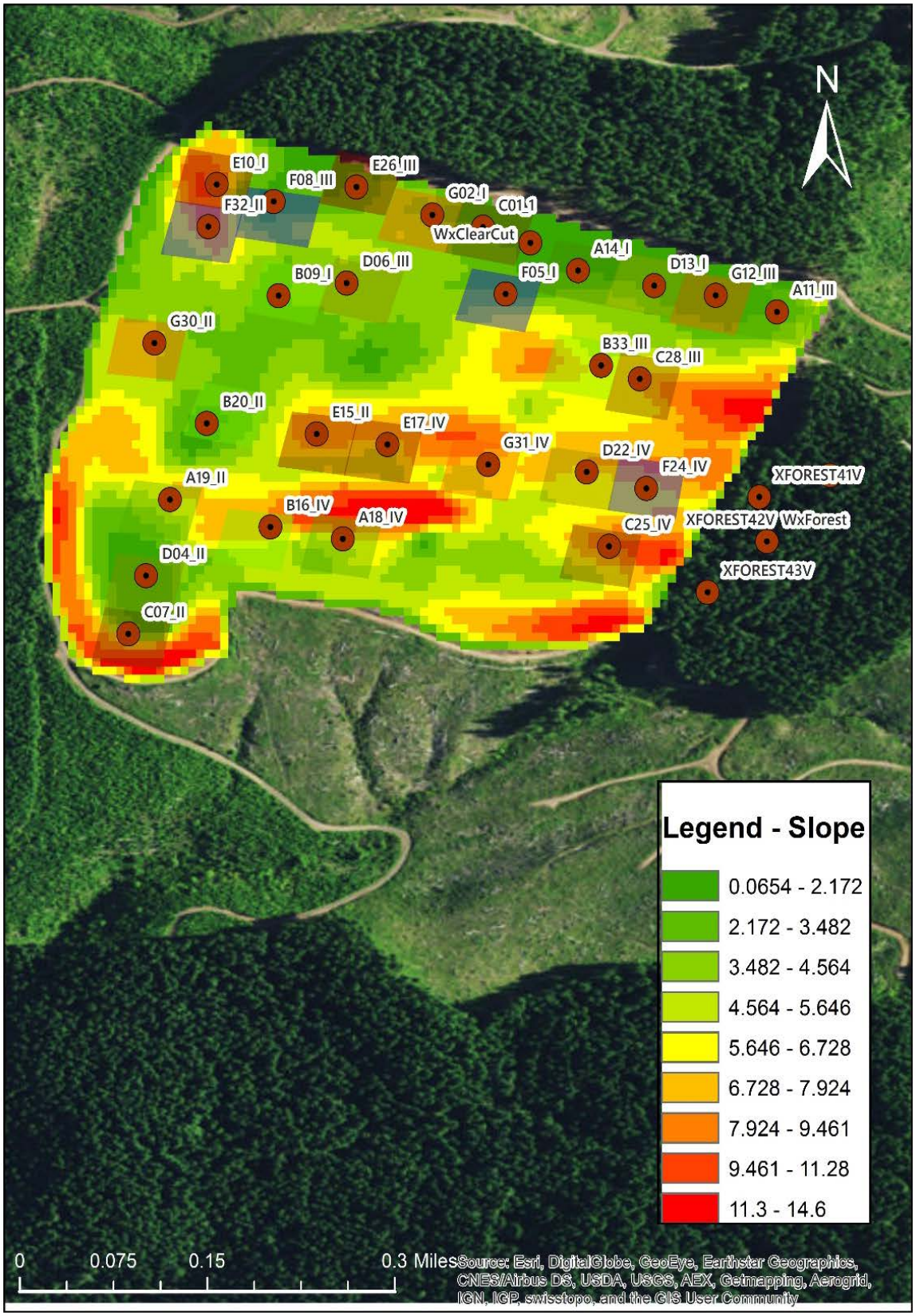

Figure 2.5 LTSP Site Depicting Calculated Slope Values in Percentage

Table 2.14 Average Slope Values for Each LTSP Plot

Plot	Mean Slope (%)	Standard Deviation
A11III	2.65	1.16
A14I	1.96	0.85
A18IV	5.89	2.40
A19II	4.40	1.68
B09I	2.92	0.68
B16IV	5.18	1.78
B20II	2.52	0.95
B33III	5.47	1.62
C01I	1.93	0.72
C07II	5.96	3.64
C25IV	5.93	2.10
C28III	5.52	1.65
D04II	1.43	0.68
D06III	3.45	0.89
D13I	1.70	1.06
D22IV	5.65	1.57
E10I	6.62	2.07
E15II	5.47	1.61
E17IV	5.47	1.42
E26III	2.47	0.87
F05I	3.70	1.43
F08III	3.07	1.11
F24IV	5.77	1.44
F32II	5.52	1.79
G02I	3.10	0.95
G12III	1.38	0.66
G30II	4.02	1.10
G31IV	5.75	1.62

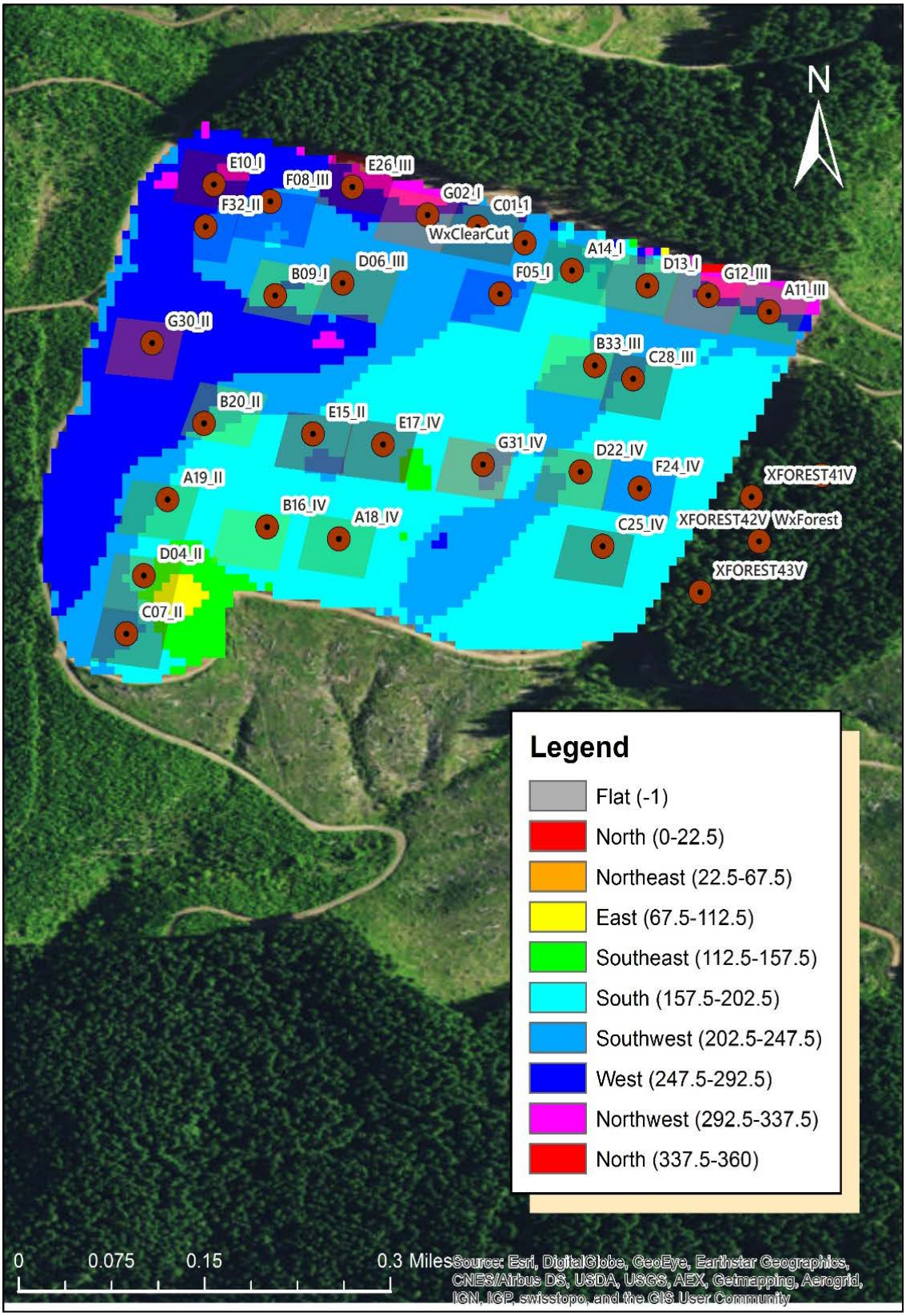

Figure 2.6 LTSP Site Depicting Calculated Aspect Values in Azimuth Angle

CHAPTER 3

OVERALL CONCLUSION AND SUMMARY

Twenty-eight UNSAT-H code files were written and modeled for each of the twenty-eight one-acre sites. It has been witnessed in a previous study of Douglas-Fir tree biomass removal, spatial patterns of forest floor water content could not be related directly to throughfall water patterns (Raat et al., 2002). Soil water evaporation and drainage significantly affect soil water content and moisture redistribution (Yanful et al., 2003). In terms of changes to runoff and sediment production, maximum impact coincides with the period immediately after track construction and harvesting but these effects decrease significantly over the 5-year time frame, well within the interlogging cutting cycle of 30-40 years in this region. (Croke et al., 2001).

Overall, to conclude that one treatment type is different from another only lies in the compaction application to the soil being noncompacted versus compacted. The evidence stands from the UNSAT-H modeling that for compacted sites, those sites will exhibit more evaporation from the surface. Furthermore, sites with no compaction and crowns removed exhibited the least amount of evaporation. It is recommended that the crowns be removed as well to ensure the least amount of evaporation occurs as to disrupt the water budget of the site the least. A relationship between soil hydrologic parameters and drainage values to the water table could not be determined. NARA is advised to not

compact the sites, and to remove the slash and crowns present at the plot to have the least amount of impact on the water budget of the site. Future studies on this project are possible, and include: plant modeling within UNSAT-H on the LTSP site to see if and how regrowth of the Douglas Fir saplings affect the water budget, and additional research into drainage rates to other treatment technologies and procedures other than solely the soil hydrologic parameters.

APPENDIX A

SUMMARY OF UNSAT-H SIMULATION RESULTS FOR TWO YEARS OF MODELING

Table A.1 Summary of UNSAT-H Simulation Results for Each Plot for 2-Year Simulation

Plot	Treatment	Initial Water Storage [cm]	Potential Evaporation [cm]	Actual Evaporation [cm]	Total Basal Liquid Flux (drainage) [cm]	Total Final Moisture Storage [cm]	Total Runoff [cm]	Total Infiltration [cm]	Actual Rainfall [cm]
14	A-I	48.7	184.6	69.1	239.2	49.8	0	356.7	356.7
19	A-II	59.2	184.6	51.2	200.6	58.9	0	356.7	356.7
11	A-III	55.7	184.6	85.9	251.7	56.2	0	356.7	356.7
18	A-IV	63.8	184.6	76.3	246.2	64.0	12.099	344.6	356.7
9	B-I	58.0	184.6	78.2	186.0	57.6	0	356.7	356.7
20	B-II	46.2	184.6	58.1	260.5	46.0	14.303	342.4	356.7
33	B-III	45.3	184.6	67.9	229.4	44.6	0	356.7	356.7
16	B-IV	62.1	184.6	53.2	251.1	62.0	0	356.7	356.7
1	C-I	46.8	184.6	66.3	189.6	46.4	0.985	355.8	356.7
7	C-II	55.7	184.6	75.3	215.2	55.1	0	356.7	356.7
28	C-III	74.7	184.6	74.3	247.5	74.7	0	356.7	356.7
25	C-IV	64.7	184.6	73.1	258.4	64.3	0.112	356.6	356.7
13	D-I	63.5	184.6	76.4	258.8	62.9	0.0	356.7	356.7
4	D-II	60.5	184.6	83.4	265.1	59.9	7.6	349.1	356.7
6	D-III	54.6	184.6	68.7	246.7	55.8	12.5	344.2	356.7
22	D-IV	59.2	184.6	63.3	265.4	58.7	0.0	356.7	356.7
10	E-I	59.9	184.6	89.6	256.5	60.0	9.1	347.6	356.7
15	E-II	61.3	184.6	85.0	267.2	60.1	0.0	356.7	356.7
26	E-III	56.5	184.6	80.6	277.8	54.8	0.0	356.7	356.7
17	E-IV	61.2	184.6	82.5	261.8	60.3	11.4	345.3	356.7

Table A.1 Continued

Plot	Treatment	Initial Water Storage [cm]	Potential Evaporation [cm]	Actual Evaporation [cm]	Total Basal Liquid Flux (drainage) [cm]	Total Final Moisture Storage [cm]	Total Runoff [cm]	Total Infiltration [cm]	Actual Rainfall [cm]
5	F-I	57.7	184.6	81.3	269.3	57.2	0.0	356.7	356.7
32	F-II	59.2	184.6	84.9	258.8	58.5	11.1	345.7	356.7
8	F-III	58.8	184.6	87.3	264.5	57.8	5.8	350.9	356.7
24	F-IV	55.6	184.6	86.2	267.1	54.7	2.2	354.6	356.7
2	G-I	53.2	184.6	84.0	271.5	52.8	0.0	356.7	356.7
30	G-II	49.0	184.6	89.4	260.5	48.7	6.0	350.7	356.7
12	G-III	58.8	184.6	94.6	235.2	59.0	11.5	345.2	356.7
31	G-IV	65.3	184.6	48.7	289.3	64.9	17.0	339.7	356.7

Table A.2 VWC Measurements for Spring 2015-2016 for Treatment A, Plot 11

Date	VWC at P1 (10 cm) [m^3/m^3]	VWC at P2 (20 cm) [m^3/m^3]	VWC at P3 (30 cm) [m^3/m^3]	VWC at P4 (100 cm) [m^3/m^3]
3/20/2015	0.325018	0.348797	0.381871	0.372252
3/21/2015	0.354047	0.377301	0.417578	0.372887
3/22/2015	0.34882	0.371413	0.395945	0.374176
3/23/2015	0.354239	0.373672	0.408358	0.374212
3/24/2015	0.349954	0.371006	0.401524	0.37561
3/25/2015	0.339651	0.359134	0.391713	0.374487
3/26/2015	0.33487	0.356218	0.387946	0.373423
3/27/2015	0.331718	0.352856	0.385606	0.372981
3/28/2015	0.350944	0.372374	0.394707	0.372539
3/29/2015	0.336392	0.359835	0.38997	0.372852
3/30/2015	0.330867	0.354056	0.386397	0.373
3/31/2015	0.350754	0.369765	0.400255	0.372714
4/1/2015	0.346518	0.366394	0.397346	0.373799
4/2/2015	0.339645	0.35933	0.391493	0.373974
4/3/2015	0.334403	0.354252	0.388369	0.373533
4/4/2015	0.343457	0.360311	0.388465	0.373055
4/5/2015	0.341713	0.361367	0.388324	0.372742
4/6/2015	0.347101	0.369708	0.394696	0.372557
4/7/2015	0.343729	0.366604	0.393906	0.372557
4/8/2015	0.349987	0.372382	0.411151	0.373376
4/9/2015	0.335542	0.357603	0.392008	0.37413
4/10/2015	0.333196	0.353489	0.387851	0.373662
4/11/2015	0.349132	0.368514	0.397094	0.373
4/12/2015	0.341786	0.362482	0.394281	0.373046
4/13/2015	0.34069	0.359842	0.393348	0.373248
4/14/2015	0.360756	0.381605	0.421528	0.374164
4/15/2015	0.347651	0.366397	0.401241	0.37631
4/16/2015	0.33782	0.35661	0.391306	0.374487
4/17/2015	0.334002	0.3528	0.387515	0.373671
4/18/2015	0.331259	0.350589	0.385214	0.37323
4/19/2015	0.32885	0.348756	0.383479	0.372945
4/20/2015	0.326453	0.347042	0.381952	0.372788
4/21/2015	0.32449	0.345108	0.380806	0.372391
4/22/2015	0.322546	0.343176	0.379833	0.371845
4/23/2015	0.322182	0.341987	0.378965	0.371781
4/24/2015	0.333253	0.34564	0.379637	0.371159
4/25/2015	0.354388	0.376958	0.39285	0.371039

Table A.2 Continued

Date	VWC at P1 (10 cm) [m^3/m^3]	VWC at P2 (20 cm) [m^3/m^3]	VWC at P3 (30 cm) [m^3/m^3]	VWC at P4 (100 cm) [m^3/m^3]
4/26/2015	0.348431	0.37066	0.397808	0.370834
4/27/2015	0.338805	0.358811	0.389952	0.371308
4/28/2015	0.334753	0.354486	0.387014	0.371836
4/29/2015	0.337686	0.352794	0.386068	0.371781
4/30/2015	0.33399	0.35337	0.384708	0.371892
5/1/2015	0.330781	0.351104	0.38355	0.372123
5/2/2015	0.327929	0.34904	0.382315	0.372262
5/3/2015	0.32508	0.34698	0.381144	0.372299
5/4/2015	0.322078	0.345048	0.380048	0.372262
5/5/2015	0.319522	0.34302	0.379108	0.372132
5/6/2015	0.317467	0.341425	0.378273	0.372049
5/7/2015	0.315811	0.339946	0.377479	0.371994
5/8/2015	0.314386	0.338925	0.376773	0.372012
5/9/2015	0.31314	0.338005	0.376093	0.372003
5/10/2015	0.311633	0.337156	0.375528	0.371929
5/11/2015	0.338213	0.358328	0.38467	0.370955
5/12/2015	0.360304	0.384402	0.417334	0.370657
5/13/2015	0.344524	0.365792	0.395885	0.374943
5/14/2015	0.341073	0.361941	0.389022	0.374679
5/15/2015	0.341011	0.362244	0.389296	0.373937
5/16/2015	0.350791	0.372291	0.401163	0.373992
5/17/2015	0.338601	0.359447	0.390293	0.374295
5/18/2015	0.333172	0.353778	0.386441	0.374194
5/19/2015	0.329538	0.350478	0.384226	0.373864
5/20/2015	0.326894	0.348135	0.382545	0.373579
5/21/2015	0.326982	0.344335	0.381846	0.372981
5/22/2015	0.353857	0.374597	0.398208	0.372594
5/23/2015	0.35083	0.373603	0.406152	0.373852
5/24/2015	0.337628	0.35813	0.389874	0.375264
5/25/2015	0.333055	0.35295	0.386111	0.374624
5/26/2015	0.330182	0.350498	0.383954	0.374139
5/27/2015	0.327467	0.348389	0.382306	0.373992
5/28/2015	0.325213	0.346704	0.380869	0.373855
5/29/2015	0.32321	0.345286	0.379753	0.373708
5/30/2015	0.321327	0.343922	0.378812	0.37357
5/31/2015	0.319307	0.342531	0.378002	0.373423
6/1/2015	0.340587	0.359869	0.379161	0.372354

Table A.2 Continued

Date	VWC at P1 (10 cm) [m^3/m^3]	VWC at P2 (20 cm) [m^3/m^3]	VWC at P3 (30 cm) [m^3/m^3]	VWC at P4 (100 cm) [m^3/m^3]
6/2/2015	0.353206	0.376658	0.388075	0.372178
6/3/2015	0.346129	0.368566	0.39154	0.372391
6/4/2015	0.336022	0.358052	0.386909	0.373119
6/5/2015	0.33115	0.352989	0.384252	0.373589
6/6/2015	0.328016	0.350003	0.382377	0.3738
6/7/2015	0.324947	0.347737	0.380949	0.373882
6/8/2015	0.322404	0.345873	0.379664	0.373864
6/9/2015	0.319555	0.343922	0.378614	0.373864
6/10/2015	0.316245	0.341675	0.377605	0.373809
6/11/2015	0.313255	0.339609	0.376692	0.373754
6/12/2015	0.31069	0.337824	0.375874	0.373699
6/13/2015	0.308032	0.336081	0.375081	0.373662
6/14/2015	0.305813	0.334637	0.374322	0.373653
6/15/2015	0.303828	0.333584	0.373644	0.373515
6/16/2015	0.301758	0.33243	0.373064	0.373442
6/17/2015	0.29971	0.331228	0.372603	0.373414
6/18/2015	0.297637	0.330249	0.372123	0.373258
6/19/2015	0.295366	0.329266	0.371549	0.373221
6/20/2015	0.29324	0.328281	0.37102	0.373138
6/21/2015	0.290764	0.327203	0.370471	0.373027
6/22/2015	0.288331	0.326166	0.369968	0.372981
6/23/2015	0.285944	0.325114	0.369426	0.372945
6/24/2015	0.283742	0.324548	0.36894	0.372834
6/25/2015	0.281627	0.323846	0.368461	0.372779
6/26/2015	0.279936	0.323445	0.367953	0.372714
6/27/2015	0.278185	0.323233	0.367558	0.372566
6/28/2015	0.275411	0.322461	0.367039	0.372557
6/29/2015	0.272929	0.321462	0.366727	0.372557
6/30/2015	0.270085	0.320528	0.366197	0.372557
7/1/2015	0.266885	0.319534	0.365741	0.372594
7/2/2015	0.2641	0.318696	0.36518	0.372622
7/3/2015	0.259811	0.317376	0.364522	0.372613
7/4/2015	0.255294	0.316017	0.363815	0.372668
7/5/2015	0.252195	0.314846	0.363422	0.372566
7/6/2015	0.249098	0.313706	0.362836	0.372502
7/7/2015	0.24661	0.312584	0.362442	0.372419
7/8/2015	0.244234	0.311645	0.361979	0.372493

Table A.2 Continued

Date	VWC at P1 (10 cm) [m^3/m^3]	VWC at P2 (20 cm) [m^3/m^3]	VWC at P3 (30 cm) [m^3/m^3]	VWC at P4 (100 cm) [m^3/m^3]
7/9/2015	0.242976	0.311295	0.361796	0.372382
7/10/2015	0.242964	0.311119	0.362211	0.372123
7/11/2015	0.238932	0.30883	0.361535	0.372336
7/12/2015	0.238083	0.307644	0.361129	0.372336
7/13/2015	0.237231	0.307054	0.360519	0.372317
7/14/2015	0.236044	0.306476	0.360072	0.372188
7/15/2015	0.233922	0.305872	0.359507	0.372114
7/16/2015	0.231978	0.305042	0.358971	0.372114
7/17/2015	0.229864	0.304078	0.358482	0.372114
7/18/2015	0.228255	0.303135	0.358002	0.372105
7/19/2015	0.226551	0.302442	0.357325	0.372068
7/20/2015	0.224572	0.301494	0.356734	0.372012
7/21/2015	0.222283	0.300531	0.356083	0.371929
7/22/2015	0.219905	0.299481	0.355539	0.371883
7/23/2015	0.217605	0.298294	0.354905	0.371883
7/24/2015	0.215749	0.297248	0.354358	0.371716
7/25/2015	0.213793	0.296138	0.353841	0.37167
7/26/2015	0.211936	0.294827	0.353511	0.37167
7/27/2015	0.211012	0.293832	0.353102	0.371633
7/28/2015	0.210008	0.292845	0.352561	0.371456
7/29/2015	0.209436	0.292413	0.35212	0.371447
7/30/2015	0.208522	0.292129	0.351366	0.371373
7/31/2015	0.206983	0.291509	0.350469	0.371197
8/1/2015	0.204893	0.290354	0.349447	0.371197
8/2/2015	0.202446	0.288982	0.348655	0.371206
8/3/2015	0.201359	0.287818	0.348502	0.371225
8/4/2015	0.200507	0.286788	0.348003	0.371225
8/5/2015	0.19913	0.285755	0.347268	0.371206
8/6/2015	0.197828	0.284541	0.346664	0.371225
8/7/2015	0.19681	0.283424	0.34612	0.371141
8/8/2015	0.195805	0.282482	0.345616	0.371132
8/9/2015	0.195118	0.281729	0.345348	0.371011
8/10/2015	0.194061	0.280693	0.344791	0.371011
8/11/2015	0.193306	0.279834	0.34443	0.371002
8/12/2015	0.192856	0.279062	0.344047	0.370983
8/13/2015	0.191697	0.278108	0.343352	0.370844
8/14/2015	0.190293	0.276969	0.342979	0.370816

Table A.2 Continued

Date	VWC at P1 (10 cm) [m^3/m^3]	VWC at P2 (20 cm) [m^3/m^3]	VWC at P3 (30 cm) [m^3/m^3]	VWC at P4 (100 cm) [m^3/m^3]
8/15/2015	0.190131	0.275853	0.342791	0.370779
8/16/2015	0.188705	0.274499	0.341895	0.370779
8/17/2015	0.187893	0.273545	0.341205	0.370779
8/18/2015	0.187275	0.272601	0.340555	0.370732
8/19/2015	0.186656	0.271655	0.339852	0.370611
8/20/2015	0.185383	0.270588	0.33902	0.370565
8/21/2015	0.183942	0.269345	0.338407	0.370537
8/22/2015	0.182645	0.267845	0.337729	0.370555
8/23/2015	0.18174	0.266686	0.336901	0.370453
8/24/2015	0.180783	0.265388	0.336198	0.370341
8/25/2015	0.179807	0.264046	0.335622	0.370332
8/26/2015	0.179046	0.263481	0.334916	0.370229
8/27/2015	0.178366	0.263131	0.334197	0.370108
8/28/2015	0.178067	0.262348	0.333692	0.370108
8/29/2015	0.182718	0.263543	0.33619	0.369987
8/30/2015	0.188174	0.270229	0.3437	0.369529
8/31/2015	0.190858	0.283029	0.346024	0.369707
9/1/2015	0.189419	0.280128	0.343612	0.369837
9/2/2015	0.224823	0.302321	0.346588	0.369099
9/3/2015	0.207856	0.297216	0.345862	0.368733
9/4/2015	0.20753	0.293933	0.347931	0.368818
9/5/2015	0.233068	0.324732	0.361674	0.368442
9/6/2015	0.217632	0.31349	0.356437	0.368761
9/7/2015	0.213425	0.307688	0.354308	0.368724
9/8/2015	0.211135	0.304101	0.353252	0.368752
9/9/2015	0.210024	0.301625	0.352722	0.36863
9/10/2015	0.2086	0.299492	0.35202	0.368564
9/11/2015	0.207715	0.297734	0.351256	0.368536
9/12/2015	0.206875	0.296565	0.350297	0.368536
9/13/2015	0.205503	0.295354	0.349447	0.368536
9/14/2015	0.203027	0.29356	0.348675	0.368536
9/15/2015	0.20008	0.291657	0.348085	0.368536
9/16/2015	0.198972	0.289868	0.34786	0.368536
9/17/2015	0.320444	0.360999	0.402993	0.367246
9/18/2015	0.290431	0.346638	0.378243	0.36813
9/19/2015	0.269767	0.337415	0.372602	0.371057
9/20/2015	0.26141	0.332438	0.370303	0.372141

Table A.2 Continued

Date	VWC at P1 (10 cm) [m^3/m^3]	VWC at P2 (20 cm) [m^3/m^3]	VWC at P3 (30 cm) [m^3/m^3]	VWC at P4 (100 cm) [m^3/m^3]
9/21/2015	0.256887	0.3292	0.368723	0.372649
9/22/2015	0.251803	0.326197	0.367425	0.372908
9/23/2015	0.246806	0.32331	0.366244	0.373037
9/24/2015	0.244375	0.321316	0.365247	0.373212
9/25/2015	0.24217	0.319624	0.364417	0.373221
9/26/2015	0.242479	0.318217	0.364053	0.372898
9/27/2015	0.23811	0.317033	0.362827	0.373
9/28/2015	0.236116	0.315443	0.362211	0.373
9/29/2015	0.234461	0.314121	0.361642	0.372991
9/30/2015	0.233177	0.313094	0.361061	0.372862
10/1/2015	0.231172	0.311865	0.360324	0.372779
10/2/2015	0.229672	0.310818	0.35976	0.372742
10/3/2015	0.230184	0.310317	0.359692	0.372474
10/4/2015	0.227767	0.309241	0.358971	0.372548
10/5/2015	0.226076	0.308208	0.358345	0.372391
10/6/2015	0.224229	0.307337	0.3576	0.372336
10/7/2015	0.223122	0.306688	0.357059	0.372225
10/8/2015	0.222073	0.305955	0.356655	0.372114
10/9/2015	0.220267	0.305113	0.356123	0.372068
10/10/2015	0.221292	0.304707	0.356554	0.371706
10/11/2015	0.224778	0.311213	0.357501	0.37154
10/12/2015	0.222283	0.309076	0.356843	0.37167
10/13/2015	0.221156	0.307254	0.356715	0.37167
10/14/2015	0.220448	0.306014	0.356606	0.37167
10/15/2015	0.219739	0.304792	0.356142	0.37166
10/16/2015	0.218439	0.303601	0.355668	0.371531
10/17/2015	0.219481	0.303207	0.356033	0.371262
10/18/2015	0.217362	0.302585	0.355014	0.371243
10/19/2015	0.226683	0.325582	0.356461	0.370713
10/20/2015	0.26138	0.340763	0.362519	0.370546
10/21/2015	0.253045	0.329282	0.361564	0.370611
10/22/2015	0.247339	0.324455	0.360227	0.370825
10/23/2015	0.242879	0.320311	0.359458	0.370834
10/24/2015	0.238946	0.317113	0.358511	0.371002
10/25/2015	0.272096	0.343866	0.378979	0.370387
10/26/2015	0.29566	0.349302	0.377915	0.370117
10/27/2015	0.28122	0.341123	0.373293	0.371131

Table A.2 Continued

Date	VWC at P1 (10 cm) [m^3/m^3]	VWC at P2 (20 cm) [m^3/m^3]	VWC at P3 (30 cm) [m^3/m^3]	VWC at P4 (100 cm) [m^3/m^3]
10/28/2015	0.314471	0.365874	0.389429	0.371206
10/29/2015	0.316548	0.361215	0.385149	0.372141
10/30/2015	0.316653	0.360333	0.382596	0.373708
10/31/2015	0.318301	0.362131	0.393188	0.373873
11/1/2015	0.336203	0.376148	0.409166	0.489163
11/2/2015	0.331598	0.366857	0.392347	0.380244
11/3/2015	0.312671	0.350603	0.383658	0.37838
11/4/2015	0.301487	0.343879	0.378667	0.376601
11/5/2015	0.296209	0.34029	0.376255	0.375729
11/6/2015	0.292375	0.338121	0.374395	0.375255
11/7/2015	0.304374	0.350161	0.380934	0.374743
11/8/2015	0.343311	0.386988	0.425935	0.381452
11/9/2015	0.329716	0.366082	0.391195	0.382006
11/10/2015	0.314101	0.352817	0.383271	0.377081
11/11/2015	0.32572	0.362428	0.387211	0.376001
11/12/2015	0.316817	0.365337	0.384517	0.375838
11/13/2015	0.334262	0.399893	0.385349	0.375565
11/14/2015	0.330489	0.393773	0.382427	0.375537
11/15/2015	0.345254	0.40677	0.394497	0.375109
11/16/2015	0.343036	0.403177	0.39533	0.376165
11/17/2015	0.344478	0.405818	0.400885	0.37651
11/18/2015	0.345906	0.408246	0.405664	0.439911
11/19/2015	0.360612	0.425074	0.43132	0.456567
11/20/2015	0.336812	0.3955	0.395227	0.382583
11/21/2015	0.328715	0.391997	0.389673	0.375555
11/22/2015	0.324168	0.390314	0.38717	0.374771
11/23/2015	0.322697	0.387649	0.385746	0.374121
11/24/2015	0.355028	0.421829	0.414809	0.373579
11/25/2015	0.342948	0.407782	0.398922	0.375209
11/26/2015	0.333901	0.401355	0.39415	0.375419
11/27/2015	0.327266	0.394536	0.390306	0.375182
11/28/2015	0.322717	0.391055	0.387844	0.374762
11/29/2015	0.319171	0.388352	0.385851	0.374423
11/30/2015	0.317479	0.386486	0.38476	0.373836
12/1/2015	0.319244	0.384957	0.384802	0.373055
12/2/2015	0.349188	0.418943	0.415388	0.372372
12/3/2015	0.347094	0.414112	0.404338	0.373506

Table A.2 Continued

Date	VWC at P1 (10 cm) [m^3/m^3]	VWC at P2 (20 cm) [m^3/m^3]	VWC at P3 (30 cm) [m^3/m^3]	VWC at P4 (100 cm) [m^3/m^3]
12/4/2015	0.35408	0.424523	0.427488	0.379647
12/5/2015	0.334261	0.401076	0.395089	0.376699
12/6/2015	0.344312	0.408896	0.397371	0.374761
12/7/2015	0.360221	0.431938	0.434858	0.423621
12/8/2015	0.344532	0.408867	0.402263	0.378689
12/9/2015	0.354235	0.424921	0.427463	0.471964
12/10/2015	0.354449	0.420155	0.414579	0.377486
12/11/2015	0.35311	0.420213	0.417017	0.376682
12/12/2015	0.358648	0.431295	0.43936	0.412565
12/13/2015	0.351422	0.417959	0.422151	0.464681
12/14/2015	0.341571	0.400312	0.401135	0.375518
12/15/2015	0.341968	0.400802	0.399148	0.373928
12/16/2015	0.348878	0.411702	0.410135	0.373616
12/17/2015	0.365997	0.446959	0.471258	0.510868
12/18/2015	0.356709	0.425464	0.431654	0.47127
12/19/2015	0.350248	0.415638	0.41186	0.376536
12/20/2015	0.350261	0.415137	0.418474	0.374944
12/21/2015	0.354928	0.423747	0.43066	0.379097
12/22/2015	0.362109	0.43855	0.452458	0.407736
12/23/2015	0.348021	0.410917	0.412349	0.391169
12/24/2015	0.34347	0.402569	0.40478	0.374221
12/25/2015	0.339188	0.39746	0.401411	0.373083
12/26/2015	0.336527	0.396139	0.398836	0.372225
12/27/2015	0.336026	0.396734	0.400206	0.372215
12/28/2015	0.354049	0.423515	0.430549	0.373191
12/29/2015	0.346245	0.408787	0.410535	0.375045
12/30/2015	0.343886	0.405982	0.405947	0.373864
12/31/2015	0.343573	0.403682	0.401837	0.372751
1/1/2016	0.341861	0.398209	0.397981	0.372465
1/2/2016	0.339504	0.393958	0.394931	0.372382
1/3/2016	0.348475	0.393868	0.3957	0.372067
1/4/2016	0.373938	0.421899	0.420103	0.37166
1/5/2016	0.372561	0.420456	0.420635	0.372815
1/6/2016	0.360715	0.405202	0.403458	0.373322
1/7/2016	0.356456	0.399915	0.399252	0.372686
1/8/2016	0.35288	0.397305	0.396694	0.372243
1/9/2016	0.355322	0.395622	0.396378	0.371771

Table A.2 Continued

Date	VWC at P1 (10 cm) [m^3/m^3]	VWC at P2 (20 cm) [m^3/m^3]	VWC at P3 (30 cm) [m^3/m^3]	VWC at P4 (100 cm) [m^3/m^3]
1/10/2016	0.355062	0.398245	0.395149	0.371447
1/11/2016	0.353429	0.395244	0.394907	0.371122
1/12/2016	0.367382	0.41112	0.404734	0.370899
1/13/2016	0.371907	0.418519	0.422209	0.370806
1/14/2016	0.367569	0.410765	0.408651	0.37356
1/15/2016	0.371639	0.417745	0.420948	0.374166
1/16/2016	0.374402	0.41968	0.419195	0.37402
1/17/2016	0.37735	0.425173	0.435149	0.432976
1/18/2016	0.36653	0.409787	0.409476	0.397305
1/19/2016	0.385283	0.434728	0.445953	0.432623
1/20/2016	0.368004	0.411196	0.41084	0.406865
1/21/2016	0.358361	0.401172	0.400775	0.373211
1/22/2016	0.364469	0.404533	0.400851	0.372178
1/23/2016	0.37634	0.419008	0.415459	0.371929
1/24/2016	0.375512	0.418523	0.416963	0.373541
1/25/2016	0.363803	0.406727	0.405188	0.373791
1/26/2016	0.357589	0.399147	0.400102	0.372954
1/27/2016	0.356053	0.398056	0.397437	0.372197
1/28/2016	0.37096	0.416309	0.421522	0.374459
1/29/2016	0.376603	0.421216	0.420154	0.3759
1/30/2016	0.374922	0.416939	0.414438	0.375546
1/31/2016	0.367443	0.4086	0.407543	0.374331
2/1/2016	0.365357	0.404961	0.404338	0.373322
2/2/2016	0.367574	0.40907	0.404888	0.372788
2/3/2016	0.370691	0.412756	0.409148	0.372769
2/4/2016	0.376088	0.422207	0.42635	0.374036
2/5/2016	0.36163	0.403851	0.404265	0.374524
2/6/2016	0.373953	0.416523	0.416801	0.37391
2/7/2016	0.361712	0.403022	0.403451	0.37369
2/8/2016	0.356416	0.39917	0.399162	0.373101
2/9/2016	0.35293	0.396694	0.396163	0.372806
2/10/2016	0.349689	0.394437	0.394153	0.372354
2/11/2016	0.34783	0.392089	0.392766	0.371818
2/12/2016	0.35307	0.392352	0.392688	0.371512
2/13/2016	0.369922	0.411006	0.397689	0.371187
2/14/2016	0.384625	0.433824	0.447231	0.454824
2/15/2016	0.366394	0.407418	0.405953	0.378804

Table A.2 Continued

Date	VWC at P1 (10 cm) [m^3/m^3]	VWC at P2 (20 cm) [m^3/m^3]	VWC at P3 (30 cm) [m^3/m^3]	VWC at P4 (100 cm) [m^3/m^3]
2/16/2016	0.359639	0.401441	0.398993	0.373992
2/17/2016	0.367594	0.409733	0.410649	0.373576
2/18/2016	0.380174	0.423658	0.425206	0.379407
2/19/2016	0.373816	0.414903	0.411192	0.379811
2/20/2016	0.364701	0.405599	0.403209	0.374322
2/21/2016	0.366585	0.405505	0.401402	0.373543
2/22/2016	0.367138	0.407572	0.403154	0.373073
2/23/2016	0.359513	0.401544	0.398859	0.372898
2/24/2016	0.355686	0.397907	0.396146	0.372742
2/25/2016	0.352841	0.395656	0.394094	0.372548
2/26/2016	0.353496	0.393288	0.39352	0.372243
2/27/2016	0.377198	0.420723	0.40989	0.371577
2/28/2016	0.365991	0.406891	0.402129	0.372058
2/29/2016	0.362754	0.404124	0.400078	0.372419
3/1/2016	0.365232	0.403491	0.399205	0.372345
3/2/2016	0.363657	0.404085	0.398853	0.372262
3/3/2016	0.372916	0.414196	0.402925	0.372151
3/4/2016	0.361286	0.404614	0.399668	0.372428
3/5/2016	0.365886	0.404537	0.399894	0.372372
3/6/2016	0.373813	0.41781	0.416628	0.373457
3/7/2016	0.369434	0.407301	0.403121	0.37446
3/8/2016	0.369814	0.409544	0.403498	0.373919
3/9/2016	0.377312	0.420492	0.413246	0.373717
3/10/2016	0.379141	0.421585	0.417101	0.374907
3/11/2016	0.369053	0.409015	0.405775	0.375337
3/12/2016	0.387101	0.431729	0.43241	0.376525
3/13/2016	0.385141	0.429757	0.435138	0.38248
3/14/2016	0.390191	0.439394	0.448521	0.475282
3/15/2016	0.38683	0.434347	0.438217	0.415303
3/16/2016	0.378081	0.418133	0.414728	0.376117
3/17/2016	0.365718	0.404248	0.404848	0.374615
3/18/2016	0.359884	0.400606	0.399677	0.373478

APPENDIX B

THE BASIS OF UNSAT-H

UNSAT-H uses a finite-difference implementation of a modified form of Richards' equation that describes unsaturated liquid and vapor flow in soil layers, while additionally having the option for water removal through plant roots (i.e., transpiration) (Khire et. al., 1997). A recharge model was made for assessing the water dynamics of the arid site, and in particular, estimating recharge fluxes by simulating soil water infiltration, redistribution, evaporation, plant transpiration, deep drainage, and soil heat flow.

Infiltration is the process of water entry into soil. Once water has infiltrated the soil, the soil water balance equation that forms the basis of the UNSAT-H conceptual model is

$$\Delta S_w = \mathrm{I} - \mathrm{E} - \mathrm{T} - \mathrm{D} \qquad \text{B.1}$$

where ΔS_w is the change in soil water storage during an interval of time. The water storage equates to the average volumetric water content of the soil multiplied by the depth of the soil. This equation simply states that the change in the amount of water stored in the soil profile is equal to the total infiltration, I, minus the amount of water that is lost to evaporation, E, transpiration, T, and drainage, D.

The first term in Equation (B.1) is I, the soil infiltratability (i.e., the instantaneous infiltration rate), and is a function of several factors: the time from the onset of precipitation, the initial water content, the hydraulic properties of the surface soil, and the hydraulic properties of layers deeper within the profile. At the start of the infiltration rate, the infiltratability is maximal. In time, this rate will decrease asymptotically to approaching the value of the saturated conductivity of the surface soil. As the wetted depth of the soil increases, the infiltration rate decreases asymptotically and approaches the saturated

conductivity of the most impeding layer within the soil profile conditions. The UNSAT-H model simulates infiltration as a two-step process. First, the infiltration rate is set equal to the precipitation rate during each time step. In this case, the infiltration is controlled by the supply of water (i.e., supply-controlled or flux-controlled), and is most typical in arid environments. In the second stage, infiltration is controlled by the soil profile conditions. Many algebraic equations have been developed to estimate infiltration rates during this second stage, however the UNSAT-H conceptual model does not use an infiltration equation. Instead, the infiltration in this second stage is determined directly by calculating the ability of the soil profile to transmit water downward. In this case, if the surface soil saturates, the solution of that time step is repeated using a Dirichlet boundary condition (with the surface node saturated). The resulting flux from the surface into the profile is the infiltration rate.

Runoff/overland flow occurs when the precipitation rate exceeds the infiltration rate, in which water accumulates on the soil surface. There has not been observable surface runoff from the site plots, apart from plot 12 producing a “moderate sized puddle” when precipitation is heavy. Weyerhaeuser also stated that minor subsurface flow occurs, and has been attributed with rodent holes and root channels. During the installation of zero-tension lysimeters, the holes would fill with water during heavy rain through horizontal flow. Overland flow is not addressed by the UNSAT-H conceptual model due to being a one-dimensional model. Since overland flow is a multidimensional process that a one-dimensional model cannot describe, UNSAT-H can be applied only to areas for which local run-on/off processes can be represented by a uniform precipitation rate over the entire area of interest, or to areas in which overland flow is prevented (i.e., lysimeters).

Evaporation is modeled in UNSAT-H as an integrated form of Fick's law of diffusion, and simply justifies that the evaporation rate is equal to the deficit in vapor density between the soil surface and the atmosphere divided by the atmospheric boundary-layer resistance (the region of the atmosphere that is directly affected by the shearing forces originating at the surface). In the second process, water flow, a decrease in the supply of water to the surface leads to surface drying. Since a drier surface is indicative of a lower vapor density, the evaporation is reduced due to the vapor density deficit being smaller. However, an increased water supply to the soil surface would have the opposite effect. The third process is controlled by both the atmospheric vapor density and the atmospheric boundary-layer resistance by transporting water vapor from the surface to the atmosphere. Commonly, the soil surface is wetter (higher vapor density) than air. But there are instances, however, such as during the early morning when the temperature approaches the dew point or after rainfall, the increased atmospheric vapor density decreases the surface-air vapor deficit and, therefore, decreases evaporation. Other causes for the transfer of water vapor from the soil surface to the atmosphere result from decreased wind speed or reduced eddy diffusion from high atmospheric stability.

For infiltration events, the upper boundary condition for water flow can be a flux, where it can be specified as an hourly flux that is equivalent to a precipitation rate. If the suction head of the surface node should become less than the minimum suction head, the upper boundary becomes a constant head that is equivalent to the minimum suction head. During this condition, infiltration is calculated as the sum of the change in storage of the surface node and the flux between the surface node and the node below it. In contrast, the infiltration event could be modeled as a Constant head, and this condition continues until

the precipitation rate becomes less than the potential infiltration rate, and the suction head of the surface node exceeds the minimum suction head.

Transpiration from plants is an optional addition to the model. Transpiration was not modeled due to simulating virtually bare groundcover and no trees present on site. After preliminary investigation revealed a lack of root development, the saplings are too young to drastically alter the water content measurements and subsurface groundwater flow.

The final term of Equation (B.1) is drainage, which is the movement of water downward through the bottom of the zone being simulated. The bottom of the vadose zone was set to 150 cm below the surface throughout the entire site. Even though it is known that there are water table depth fluctuations through seasons of the year, the data requirements for physically based models to simulate water table fluctuation are enormous and are difficult and costly to satisfy in many cases (Coulibaly et al., 2001; Warren et al., 2005). Of interest is the drainage water that reaches the water table; this water was considered to have completely infiltrated into the groundwater system as there exists little chance of it being drawn upward again, and it is also known as groundwater recharge. Thus, recharge was defined as drainage below the 150-cm depth bottom boundary.

The following two relations are the basis of the modified Richards' equation: the water flux inside the soil is proportional to the water potential gradient, which is the basis of Darcy's Law, and the change in water content at a specific location is due to the convergence/divergence of water fluxes at another location, the basis of continuity. Additionally, the modified equation allows estimation of the initial soil moisture contents from sparse observations of related quantities (Ren, 2005). Since the modified Richards' equation begins with Darcy's Law, the one-dimensional differential form goes as:

$$q_L = -K_s \frac{\delta H}{\delta z} \quad \text{B.2}$$

where q_L is the flux density of water (cm/hr), K_s is the saturated hydraulic conductivity (cm/hr), H is the hydraulic potential and z is the depth below the soil surface. Darcy's Law can be extended to unsaturated flow by replacing K_s with liquid conductivity, K_L, as a function of matric potential, ψ, resulting in:

$$q_L = -K_L(\varphi) \frac{\delta H}{\delta z} \quad \text{B.3}$$

Equation (B.3) must be combined with the continuity equation to describe transient flow, stating that the change in water content of a volume of soil equates to the difference between flux into and out of the soil (Fayer et al., 2000). For one-dimensional flow, the continuity equation is:

$$\frac{\delta \theta}{\delta t} = -\frac{\delta q_L}{\delta z} \quad \text{B.4}$$

where θ is the volumetric water content (cm^3/cm^3), and t is time (h). The equation for transient flow in the unsaturated zone for groundwater thus yields:

$$\frac{\delta \theta}{\delta t} = -\frac{\delta}{\delta z}\left[-K_L(\varphi) \frac{\delta H}{\delta z}\right] \quad \text{B.5}$$

It should be noted that UNSAT-H has two sign conventions that relate to heads. The first type is gravitational head: a point in the soil where the elevation of the point with respect to (w.r.t.) the soil surface and is negative. Therefore z is replaced with $-z$. Matric head is the second type, and is usually denoted with a negative number for unsaturated soil conditions. In UNSAT-H, matric head is replaced with suction head, h, which is the negative of matric head. Therefore, a positive suction head represents matric head and a negative suction head represents a pressure head. The calculation of hydraulic head then changes from $H = \psi + Z$ to the UNSAT-H form:

$$H = -(h + z) \tag{B.6}$$

Using the chain rule of differentiation to Equation (B.4), $\frac{\delta\theta}{\delta t}$ can be replaced by $C(h)\frac{\delta h}{\delta t}$ where C(h) represents $\frac{\delta\theta}{\delta t}$. Through derivation using the chain rule, Equation (B.4) becomes:

$$C(h)\frac{\delta h}{\delta t} = \frac{\delta}{\delta z}\left[K_L(h)\left(\frac{\delta h}{\delta z} + 1\right)\right] - S(z,t) \tag{B.7}$$

where $\frac{\delta H}{\delta z} = \frac{\delta h}{\delta z} + 1$, through differentiation of Equation (B.5). S(z,t) is a sink term added to determine later uptake by plants as a function of depth and time.

The assumptions that led to Equation (B.7) are: the fluid is treated as incompressible, the air phase is continuous and at constant pressure, flow is one-dimensional, liquid water flow is isothermal, and the pore-air pressure is at atmospheric

pressure (Lam et al., 1987), and vapor flow is negligible. In the case of unsaturated flow, it is difficult to predict water content (θ), hydraulic conductivity (k), and suction head (h) due to the multidimensional, nonhomogeneous characteristics of soil (van Genuchten, 1980). There are many soil water retention relationships that have been determined, such as the linked polynomials, the Haverkamp function, the Brooks and Corey function, the van Genuchten function, and several special functions that account for water retention of very dry soils (Fayer, 2000). The van Genuchten model was chosen because of its widely used reputation and accuracy (Carsel et al., 1988). Therefore, Equation (B.8) illustrates how water content and hydraulic conductivity are functions of suction head according to the van Genuchten function and Mualem hydraulic conductivity model and has the form

$$\theta = \theta_r + (\theta_s - \theta_r)[1 + (\alpha h)^n]^{-m} \quad \text{B.8}$$

where α, m, and n are curve-fitting parameters, and where it is assumed that $m = 1 - 1/n$ (Mualem, 1976), and

$$K_L = K_S \frac{\{1-(\alpha h)^{n-2}[1+(\alpha h)^n]^{-m}\}^2}{[1+(\alpha h)^n]^{lm}} \quad \text{B.9}$$

where the conductivity function is based on the Mualem conductivity model (Mualem, 1978).

The next important concept to cover is the fundamental equation used to calculate the diffusion of water vapor in soils via Fick's Law of Diffusion, which can be written as

$$q_v = -\frac{D}{\rho_w}\frac{\partial \rho_v}{\partial z} \quad \text{B.10}$$

where q_v is the flux density of water vapor, cm h^{-1}, ρ_w is the density of liquid water, g cm^{-3}, D is the vapor diffusivity in soil, cm^2 h^{-1}, and ρ_v is the vapor density, g cm^{-3}. When applying Fick's Law to soils, the tortuous diffusion path and reduced cross-sectional area available for flow requires adjustments. The three-phase nature of soils requests the need for both adjustments, and are included in the new diffusivity term to be written as

$$D = \alpha(\theta_s - \theta)D_a \quad \text{B.11}$$

where α is the tortuosity factor, D_a is the diffusivity of water vapor in air, cm^2 s^{-1}, and the quantity $(\theta_s - \theta)$ represents the air-filled porosity. Generally, α is treated as a constant, and the most common formulation is to set α = 0.66 (Penman 2007). Fick's Law can also be written to explicitly include gradients for suction head and temperature by using the chain rule of differentiation, thus making Equation (B.10) become

$$q_v = -\frac{D}{\rho_w}\frac{\partial \rho_v}{\partial h}\frac{\partial h}{\partial z} - \frac{D}{\rho_w}\frac{\partial \rho_v}{\partial T}\frac{\partial T}{\partial z} \quad \text{B.12}$$

where T is the temperature, K. Consequently, the vapor density at a specific point in the soil can then be related to the saturated vapor density, ρ_{vs}, and relative humidity, H_R, by

$$\rho_v = \rho_{vs}H_R \quad \text{B.13}$$

Therefore, Equation (B.12) can be rewritten by substituting Equation (B.13) as the relative humidity and temperature function into the vapor density, using the product rule for differentiation and setting $\partial H_R/\partial T = 0$ for relative humidity conditions greater than 0.6 because the resulting temperature effect on H_R is so small:

$$q_v = -\left(\frac{D}{\rho_w}\rho_{vs}\frac{\partial H_R}{\partial z}\right) - \left(\frac{D}{\rho_w}H_R\frac{\partial \rho_{vs}}{\partial T}\frac{\partial T}{\partial z}\right) \quad \text{B.14}$$

Equation (B.14) unambiguously contains the effect of soil temperature on vapor diffusion. The first term characterizes isothermal vapor diffusion while the second term characterizes thermal vapor diffusion. Therefore, the relative humidity can be determined using the soil suction head (Campbell, 1985)

$$H_R = \exp\left[-\frac{hMg}{RT}\right] \quad \text{B.15}$$

where M is the molecular weight of water, g mol^{-1}, g is the gravitational constant, cm s^{-1}, and R is the universal gas constant, erg mol^{-1} K^{-1}. Although Equation (B.14) underpredicts water vapor flow, Philip and de Vries (1957) proposed that vapor is effectively transported through the liquid phase by condensation and evaporation processes operating within individual pores. By adding an enhancement factor, η, to the thermal vapor diffusion term these two processes will be accounted for. This leads to Equation (B.16)

$$q_v = \left(\frac{D}{\rho_w}\rho_{vs}\frac{Mg}{RT}H_R\frac{\partial h}{\partial z}\right) - \left(\frac{D}{\rho_w}\eta H_R\frac{\partial \rho_{vs}}{\partial T}\frac{\partial T}{\partial z}\right) \quad \text{B.16}$$

This law accounts for the effect of temperature gradients and enhanced vapor diffusion in soil.

To determine the surface and lower boundary of the soil column, boundary conditions are specified. For infiltration events, the upper boundary condition for water flow was set to a flux, which was set equal to the hourly flux equivalent to the precipitation rate. If the suction head of the surface node becomes less than the minimum suction head, the upper boundary becomes the value of the minimum suction head. Thus, the infiltration is then calculated as the sum of the change in storage of the surface node and the flux between the surface node and the node below it. This condition continues until the precipitation rate becomes less than the potential infiltration rate, and the suction head of the surface node therefore exceeds the minimum suction head, thus reverting it back to a flux boundary. Similarly, for evaporation events, the surface boundary condition was set to a flux. This condition required input through daily weather data, consisting of the daily maximum and minimum air temperatures, daily average dewpoint temperature, total daily solar radiation, and average daily wind speed. The maximum and minimum air temperatures were used to calculate the sinusoidal variation in air temperature, T_a, throughout that day, using

$$T_a = T_{mean} + T_{amp} \cos\left[\frac{2\pi}{24}(t_d - 15)\right] \quad \text{B.17}$$

where T_{mean} is the average of the maximum and minimum air temperatures, K; T_{amp} is the amplitude of the air temperature, K; and t_d is the time of day, hour. Equation (B.17) assumes the minimum daily temperature occurring at 0300 h and the maximum daily

temperature occurring at 1500 h. To ensure that no discontinuity at midnight occurs, before 0300 h, the maximum air temperature from the previous day is used in Equation (B.17), and the minimum air temperature from the next day is used after 1500 h in Equation (B.17). The dewpoint temperature, (and therefore, the atmospheric vapor density), wind speed and cloud cover are assumed to remain constant during the day. Since heat flow in the vadose zone is not being modeled, the boundary condition for evaportranspiration was a dependent variable of the PET rate. The UNSAT-H program can calculate the daily value using the form of the Penman equation reported by Doorenbos and Pruitt (1977), in which the units originally used were retained in the UNSAT-H model

$$PET = \frac{sR_{ni}}{s+\gamma} + \frac{\gamma}{s+\gamma} 0.27 \left(1 + \frac{U}{100}\right)(e_a - e_d) \qquad \text{B.18}$$

where s is the slope of the saturation vapor pressure-temperature curve, mb K^{-1}; R_{ni} is the isothermal net radiation, mm d^{-1}; γ is the psychrometric constant, mb K^{-1}; U is the 24-h wind run, km d^{-1}; e_a is the saturation vapor pressure at the mean air temperature, mb; and e_d is the actual vapor pressure, mb. This calculated PET value is distributed through the day according to the hourly factors that were generated with a sine wave function. For the hours between 0600 and 1800, 88% of the daily PET is applied sinusoidally. During the remaining time, hourly PET rates are 1% of the daily value.

The second boundary specified is the lower boundary. At a depth of 150 cm in the model, a unit gradient option was chosen due to corresponding to gravity-induced drainage and being most appropriate for applying soil profiles that extend below the root zone and drainage is not inhibited.

The mass balance error is calculated by first calculating the soil-water storage at the end of a time step using

$$S_w^j = \theta_1^j \left(\frac{z_2 - z_1}{2}\right) + \theta_n^j \left(\frac{z_n - z_{n-1}}{2}\right) + \sum_{i=2}^{n-1} \left[\theta_i^j \left(\frac{z_{i+1} - z_{i-1}}{2}\right)\right] \quad \text{B.19}$$

Then, the mass balance error (E_w) for the time step can be obtained using

$$E_w = I^j - E^j - T^j - D^j - \left(S_w^j - S_w^{j-1}\right) \quad \text{B.20}$$

where the terms I^j, E^j, T^j, D^j, and $\left(S_w^j - S_w^{j-1}\right)$ refer to the amounts of infiltration, evaporation, transpiration, drainage, and change in storage, respectively, having occurred during that particular time step.

The UNSAT-H model consists of three programs: DATAINH, UNSATH, and DATAOUT. The purpose of DATAINH is to process the input data in a way that the UNSATH program can recognize, therefore reducing the likelihood that UNSATH will fail to run from input errors. It is an interactive program that reads data from a *.*inp* file, checks for errors, and performs certain calculations. An example of the input file for Plot B09I is illustrated by Figure B.1.

Then, DATAINH writes the data in binary form to a file with the same name as the input file, but with the extension bin. This *.bin file created by DATAINH serves as the input file for UNSATH. The steps start with data input and end with the final summary output of the simulation to file *.res. Simulation data that is output to the *.res file include initial conditions, water content, water flow, temperatures, water balance terms, and at the

end of the file, the simulation end results. After the file has been made, DATAOUT can read the *.res file and create an output file in the *.out file format, but with a .out extension. An example of the .out file for Plot B09I is illustrated by Figure B.2.

```
Treatment_B091_Run2.INP: !VG 2 Year Model for - Treatment B09I Summarized
0,1,                                IPLANT,NGRAV
365,1,365,                          IFDEND,IDTBEG,IDTEND
2014,2,0,1,0,                       IYS,NYEARS,ISTEAD,IFLIST,NFLIST !IFLIST=1 - Included Meteorological Data in separate file
0,24.0,                             NPRINT,STOPHR
1,3,1,1.0E-4,                       ISMETH,INMAX,ISWDIF,DMAXBA
1.0,1.0E-10,0.0,                    DELMAX,DELMIN,OUTTIM
2.0,1.0E-05,0.0,0.0,0.0,            RFACT,RAINIF,DHTOL,DHMAX,DHFACT
4,3,0.5,                            KOPT,KEST,WIF
0,1,2,1,                            ITOPBC,IEVOPT,NFHOUR,LOWER
0.0,1.0E+05,0.0,0.83,               HIRRI,HDRY,HTOP,RHA
1,0,1,                              IETOPT,ICLOUD,ISHOPT
1,1.0,                              IRAIN,HPR
0,0,0,0,0,                          IHYS,AIRTOL,HYSTOL,HYSMXH,HYFILE
0,0,0,                              IHEAT,ICONVH,DMAXHE
0,0,0,0,                            UPPERH,TSMEAN,TSAMP,QHCTOP
0,0.0,0.0,                          LOWERH,QHLEAK,TGRAD
1,0.66,284.625,0.229,               IVAPOR,TORT,TSOIL,VAPDIF
3,101,                               MATN,NPT
1,  0.000,1,  0.100,1,  0.200,1,  0.500,
1,  1.000,1,  2.000,1,  3.000,1,  4.000,
1,  5.000,1,  6.000,1,  7.000,1,  8.000,
1,  9.000,1, 10.000,1, 11.000,1, 12.000,
1, 13.000,1, 14.000,1, 15.000,1, 16.000,
1, 17.000,1, 18.000,1, 19.000,1, 20.000,
1, 21.000,1, 22.000,1, 22.500,1, 23.000,
1, 23.500,1, 24.000,1, 24.500,1, 24.700,
1, 24.800,1, 24.900,2, 25.000,2, 25.100,
2, 25.200,2, 25.500,2, 26.000,2, 27.000,
2, 28.000,2, 29.000,2, 30.000,2, 31.000,
2, 32.000,2, 33.000,2, 34.000,2, 35.000,
2, 36.000,2, 38.000,2, 40.000,2, 42.000,
2, 44.000,2, 46.000,2, 48.000,2, 50.000,
2, 52.000,2, 54.000,2, 56.000,2, 58.000,
2, 60.000,2, 61.000,2, 62.000,2, 62.500,
2, 63.000,2, 63.500,2, 64.000,2, 64.500,
2, 64.700,2, 64.800,2, 64.900,3, 65.000,
3, 65.100,3, 65.200,3, 65.500,3, 66.000,
3, 67.000,3, 68.000,3, 69.000,3, 70.000,
3, 71.000,3, 72.000,3, 74.000,3, 76.000,
3, 78.000,3, 80.000,3, 83.000,3, 86.000,
3, 90.000,3, 95.000,3,100.000,3,105.000,
3,110.000,3,115.000,3,120.000,3,125.000,
3,130.000,3,135.000,3,140.000,3,145.000,
3,150.000,
Layer 1 (0-24.9cm) Clay Loam Retention
0.470,0.250,0.019,1.310,                  THET,THTR,VGA,VGN
Layer 1 (0-24.9cm) Clay Loam Conductivity
2,1.965,0.019,1.310,0.5,                KMODEL,SK,VGA,VGN,EPIT
Layer 2 (25-64.9cm) Kinney Cobbly Loam Retention
0.280,0.16,0.008,1.090,                   THET,THTR,VGA,VGN
Layer 2 (25-64.9cm) Kinney Cobbly Loam Conductivity
2,1.430,0.008,1.090,0.5,                KMODEL,SK,VGA,VGN,EPIT
Layer 3 (65-150cm) Silty Clay Loam Retention
0.43,0.38,0.008,1.090,                    THET,THTR,VGA,VGN
Layer 3 (65-150cm) Silty Clay Loam Conductivity
2,1.209,0.008,1.090,0.5,                KMODEL,SK,VGA,VGN,EPIT
0,                                      NDAY
1.12E+02,1.12E+02,1.12E+02,1.11E+02,
1.11E+02,1.10E+02,1.08E+02,1.07E+02,
1.06E+02,1.05E+02,1.03E+02,1.02E+02,
1.01E+02,9.96E+01,9.84E+01,9.72E+01,
9.59E+01,9.47E+01,9.35E+01,9.23E+01,
9.10E+01,8.94E+01,8.67E+01,8.52E+01,
8.40E+01,8.29E+01,8.23E+01,8.17E+01,
8.12E+01,8.06E+01,8.00E+01,7.98E+01,
7.97E+01,7.96E+01,7.94E+01,7.92E+01,
7.90E+01,7.84E+01,7.74E+01,7.54E+01,
7.36E+01,7.18E+01,7.02E+01,6.85E+01,
6.70E+01,6.56E+01,6.42E+01,6.28E+01,
6.15E+01,5.91E+01,5.69E+01,5.48E+01,
5.28E+01,5.09E+01,4.92E+01,4.74E+01,
4.58E+01,4.42E+01,4.26E+01,4.11E+01,
3.96E+01,3.88E+01,3.81E+01,3.77E+01,
3.74E+01,3.70E+01,3.66E+01,3.63E+01,
3.61E+01,3.60E+01,3.60E+01,3.59E+01,
3.59E+01,3.59E+01,3.58E+01,3.57E+01,
3.56E+01,3.54E+01,3.52E+01,3.50E+01,
3.49E+01,3.47E+01,3.44E+01,3.41E+01,
3.38E+01,3.35E+01,3.31E+01,3.27E+01,
3.21E+01,3.15E+01,3.10E+01,3.05E+01,
3.00E+01,2.95E+01,2.91E+01,2.88E+01,
2.85E+01,2.82E+01,2.80E+01,2.78E+01,
2.78E+01,
0.25,637.5,2.0,1018.96,                              ALBEDO,ALT,ZU,PMB

metdatone
dat
```

Figure B.1 Input .inp file for Treatment B091 for 2-Year Simulation

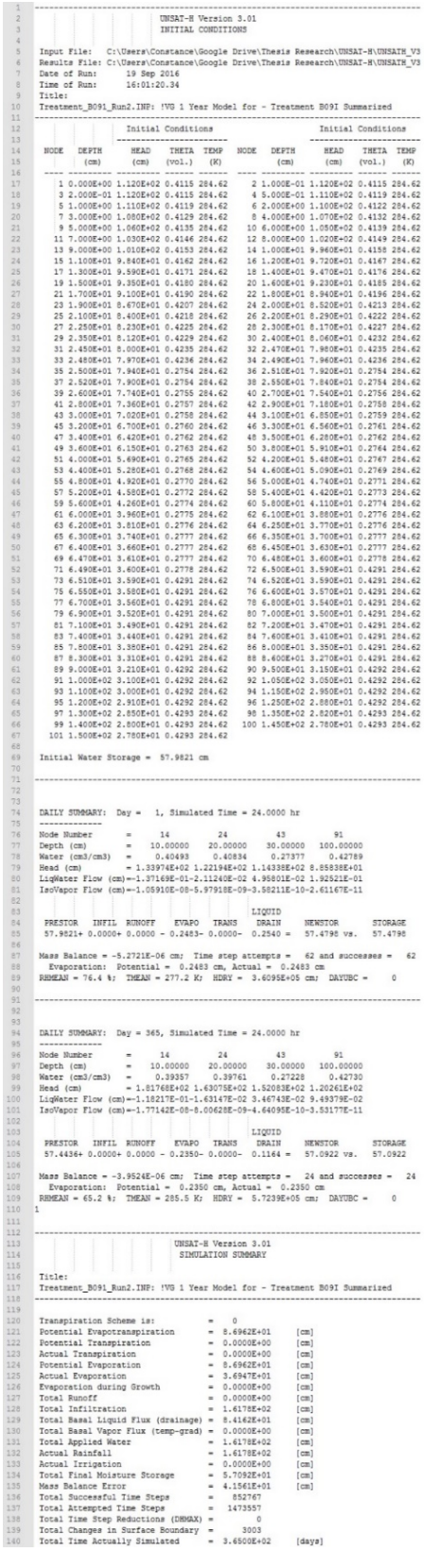

```
------------------------------------------------------------------------------
                    UNSAT-H Version 3.01
                    INITIAL CONDITIONS

 Input File:   C:\Users\Constance\Google Drive\Thesis Research\UNSAT-H\UNSATH_V3
 Results File: C:\Users\Constance\Google Drive\Thesis Research\UNSAT-H\UNSATH_V3
 Date of Run:       19 Sep 2016
 Time of Run:       16:01:20.34
 Title:
 Treatment_B09I_Run2.INP: TVG 1 Year Model for - Treatment B09I Summarized
------------------------------------------------------------------------------
                 Initial Conditions                          Initial Conditions
                ---------------------                       ---------------------
  NODE   DEPTH      HEAD    THETA  TEMP   NODE   DEPTH      HEAD    THETA  TEMP
         (cm)       (cm)   (vol.)   (K)          (cm)      (cm)   (vol.)   (K)
 ---- --------- --------- ------- ------ ---- --------- --------- ------- ------
    1 0.000E+00 1.120E+02 0.4115 284.62     2 1.000E-01 1.120E+02 0.4115 284.62
    3 2.000E-01 1.120E+02 0.4115 284.62     4 5.000E-01 1.110E+02 0.4119 284.62
    5 1.000E+00 1.110E+02 0.4119 284.62     6 2.000E+00 1.100E+02 0.4122 284.62
    7 3.000E+00 1.080E+02 0.4129 284.62     8 4.000E+00 1.070E+02 0.4132 284.62
    9 5.000E+00 1.060E+02 0.4135 284.62    10 6.000E+00 1.050E+02 0.4139 284.62
   11 7.000E+00 1.030E+02 0.4146 284.62    12 8.000E+00 1.020E+02 0.4149 284.62
   13 9.000E+00 1.010E+02 0.4153 284.62    14 1.000E+01 9.960E+01 0.4158 284.62
   15 1.100E+01 9.840E+01 0.4162 284.62    16 1.200E+01 9.720E+01 0.4167 284.62
   17 1.300E+01 9.590E+01 0.4171 284.62    18 1.400E+01 9.470E+01 0.4176 284.62
   19 1.500E+01 9.350E+01 0.4180 284.62    20 1.600E+01 9.230E+01 0.4185 284.62
   21 1.700E+01 9.100E+01 0.4190 284.62    22 1.800E+01 8.940E+01 0.4196 284.62
   23 1.900E+01 8.670E+01 0.4207 284.62    24 2.000E+01 8.520E+01 0.4213 284.62
   25 2.100E+01 8.400E+01 0.4218 284.62    26 2.200E+01 8.290E+01 0.4222 284.62
   27 2.250E+01 8.230E+01 0.4225 284.62    28 2.300E+01 8.170E+01 0.4227 284.62
   29 2.350E+01 8.120E+01 0.4229 284.62    30 2.400E+01 8.060E+01 0.4232 284.62
   31 2.450E+01 8.000E+01 0.4235 284.62    32 2.470E+01 7.980E+01 0.4235 284.62
   33 2.480E+01 7.970E+01 0.4236 284.62    34 2.490E+01 7.960E+01 0.4236 284.62
   35 2.500E+01 7.940E+01 0.2754 284.62    36 2.510E+01 7.920E+01 0.2754 284.62
   37 2.520E+01 7.900E+01 0.2754 284.62    38 2.550E+01 7.840E+01 0.2754 284.62
   39 2.600E+01 7.740E+01 0.2755 284.62    40 2.700E+01 7.540E+01 0.2756 284.62
   41 2.800E+01 7.360E+01 0.2757 284.62    42 2.900E+01 7.180E+01 0.2758 284.62
   43 3.000E+01 7.020E+01 0.2758 284.62    44 3.100E+01 6.850E+01 0.2759 284.62
   45 3.200E+01 6.700E+01 0.2760 284.62    46 3.300E+01 6.560E+01 0.2761 284.62
   47 3.400E+01 6.420E+01 0.2762 284.62    48 3.500E+01 6.280E+01 0.2762 284.62
   49 3.600E+01 6.150E+01 0.2763 284.62    50 3.800E+01 5.910E+01 0.2764 284.62
   51 4.000E+01 5.690E+01 0.2765 284.62    52 4.200E+01 5.480E+01 0.2767 284.62
   53 4.400E+01 5.280E+01 0.2768 284.62    54 4.600E+01 5.090E+01 0.2769 284.62
   55 4.800E+01 4.920E+01 0.2770 284.62    56 5.000E+01 4.740E+01 0.2771 284.62
   57 5.200E+01 4.580E+01 0.2772 284.62    58 5.400E+01 4.420E+01 0.2773 284.62
   59 5.600E+01 4.260E+01 0.2774 284.62    60 5.800E+01 4.110E+01 0.2774 284.62
   61 6.000E+01 3.960E+01 0.2775 284.62    62 6.100E+01 3.880E+01 0.2776 284.62
   63 6.200E+01 3.810E+01 0.2776 284.62    64 6.250E+01 3.770E+01 0.2776 284.62
   65 6.300E+01 3.740E+01 0.2777 284.62    66 6.350E+01 3.700E+01 0.2777 284.62
   67 6.400E+01 3.660E+01 0.2777 284.62    68 6.450E+01 3.630E+01 0.2777 284.62
   69 6.470E+01 3.610E+01 0.2777 284.62    70 6.480E+01 3.600E+01 0.2778 284.62
   71 6.490E+01 3.600E+01 0.2778 284.62    72 6.500E+01 3.590E+01 0.4291 284.62
   73 6.510E+01 3.590E+01 0.4291 284.62    74 6.520E+01 3.590E+01 0.4291 284.62
   75 6.550E+01 3.580E+01 0.4291 284.62    76 6.600E+01 3.570E+01 0.4291 284.62
   77 6.700E+01 3.560E+01 0.4291 284.62    78 6.800E+01 3.540E+01 0.4291 284.62
   79 6.900E+01 3.520E+01 0.4291 284.62    80 7.000E+01 3.500E+01 0.4291 284.62
   81 7.100E+01 3.490E+01 0.4291 284.62    82 7.200E+01 3.470E+01 0.4291 284.62
   83 7.400E+01 3.440E+01 0.4291 284.62    84 7.600E+01 3.410E+01 0.4291 284.62
   85 7.800E+01 3.380E+01 0.4291 284.62    86 8.000E+01 3.350E+01 0.4291 284.62
   87 8.300E+01 3.310E+01 0.4291 284.62    88 8.600E+01 3.270E+01 0.4291 284.62
   89 9.000E+01 3.210E+01 0.4292 284.62    90 9.500E+01 3.150E+01 0.4292 284.62
   91 1.000E+02 3.100E+01 0.4292 284.62    92 1.050E+02 3.050E+01 0.4292 284.62
   93 1.100E+02 3.000E+01 0.4292 284.62    94 1.150E+02 2.950E+01 0.4292 284.62
   95 1.200E+02 2.910E+01 0.4292 284.62    96 1.250E+02 2.880E+01 0.4292 284.62
   97 1.300E+02 2.850E+01 0.4293 284.62    98 1.350E+02 2.820E+01 0.4293 284.62
   99 1.400E+02 2.800E+01 0.4293 284.62   100 1.450E+02 2.780E+01 0.4293 284.62
  101 1.500E+02 2.780E+01 0.4293 284.62

 Initial Water Storage =  57.9821 cm

------------------------------------------------------------------------------


 DAILY SUMMARY:  Day =   1, Simulated Time = 24.0000 hr
 ------------
 Node Number       =      14          24          43          91
 Depth (cm)        =    10.00000    20.00000    30.00000   100.00000
 Water (cm3/cm3)   =     0.40493     0.40834     0.27377     0.42789
 Head (cm)         = 1.33974E+02 1.22194E+02 1.14338E+02 8.85838E+01
 LiqWater Flow (cm)=-1.37169E-01-2.11240E-02 4.95801E-02 1.92521E-01
 IsoVapor Flow (cm)=-1.08910E-08-5.97918E-09-3.58211E-10-2.61167E-11

                                                    LIQUID
  PRESTOR    INFIL  RUNOFF    EVAPO   TRANS    DRAIN     NEWSTOR       STORAGE
  57.9821+ 0.0000+ 0.0000 - 0.2483- 0.0000-  0.2540 =   57.4798 vs.   57.4798

 Mass Balance = -5.2721E-06 cm;  Time step attempts =   62 and successes =   62
   Evaporation:  Potential =  0.2483 cm, Actual =  0.2483 cm
 RHMEAN = 76.4 %;  TMEAN = 277.2 K;  HDRY =  3.6095E+05 cm;  DAYUBC =     0

------------------------------------------------------------------------------


 DAILY SUMMARY:  Day = 365, Simulated Time = 24.0000 hr
 ------------
 Node Number       =      14          24          43          91
 Depth (cm)        =    10.00000    20.00000    30.00000   100.00000
 Water (cm3/cm3)   =     0.39357     0.39761     0.27228     0.42730
 Head (cm)         = 1.81766E+02 1.63075E+02 1.52083E+02 1.20261E+02
 LiqWater Flow (cm)=-1.18217E-01-1.63147E-02 3.46743E-02 9.49379E-02
 IsoVapor Flow (cm)=-1.77142E-08-8.00628E-09-4.64095E-10-3.53177E-11

                                                    LIQUID
  PRESTOR    INFIL  RUNOFF    EVAPO   TRANS    DRAIN     NEWSTOR       STORAGE
  57.4436+ 0.0000+ 0.0000 - 0.2350- 0.0000-  0.1164 =   57.0922 vs.   57.0922

 Mass Balance = -3.9524E-06 cm;  Time step attempts =   24 and successes =   24
   Evaporation:  Potential =  0.2350 cm, Actual =  0.2350 cm
 RHMEAN = 65.2 %;  TMEAN = 285.5 K;  HDRY =  5.7239E+05 cm;  DAYUBC =     0
1


------------------------------------------------------------------------------
                    UNSAT-H Version 3.01
                     SIMULATION SUMMARY

 Title:
 Treatment_B09I_Run2.INP: TVG 1 Year Model for - Treatment B09I Summarized
------------------------------------------------------------------------------

 Transpiration Scheme is:            =    0
 Potential Evapotranspiration        =  8.6962E+01     [cm]
 Potential Transpiration             =  0.0000E+00     [cm]
 Actual Transpiration                =  0.0000E+00     [cm]
 Potential Evaporation               =  8.6962E+01     [cm]
 Actual Evaporation                  =  3.6947E+01     [cm]
 Evaporation during Growth           =  0.0000E+00     [cm]
 Total Runoff                        =  0.0000E+00     [cm]
 Total Infiltration                  =  1.6178E+02     [cm]
 Total Basal Liquid Flux (drainage)  =  8.4162E+01     [cm]
 Total Basal Vapor Flux (temp-grad)  =  0.0000E+00     [cm]
 Total Applied Water                 =  1.6178E+02     [cm]
 Actual Rainfall                     =  1.6178E+02     [cm]
 Actual Irrigation                   =  0.0000E+00     [cm]
 Total Final Moisture Storage        =  5.7092E+01     [cm]
 Mass Balance Error                  =  4.1561E+01     [cm]
 Total Successful Time Steps         =    852767
 Total Attempted Time Steps          =   1473557
 Total Time Step Reductions (DMAX)   =         0
 Total Changes in Surface Boundary   =      3003
 Total Time Actually Simulated       =  3.6500E+02     [days]
```

Figure B.2 Output .out File for Treatment B09I for First Year of Simulation

APPENDIX C

HYDROLOGIC PARAMETER INPUT

INFORMATION FOR UNSAT-H

Table C.1 Seven Hydraulic Parameters for All Twelve USDA Textural Classes Described by ROSETTA

Texture Class	N	θ_r [cm^3/cm^3]		θ_s [cm^3/cm^3]		log(α) [log(1/cm)]		log(n) [log(10)]		K_s [log(cm/day)]	
Clay	84	0.10	(0.11)	0.459	(0.08)	-1.83	(0.68)	0.098	(0.07)	1.169	(0.92)
Clay Loam	140	0.08	(0.08)	0.442	(0.08)	-1.80	(0.69)	0.151	(0.12)	0.913	(1.09)
Loam	242	0.06	(0.07)	0.399	(0.10)	-1.95	(0.73)	0.168	(0.13)	1.081	(0.92)
Loamy Sand	201	0.05	(0.04)	0.390	(0.07)	-1.46	(0.47)	0.242	(0.16)	2.022	(0.64)
Sand	308	0.05	(0.03)	0.375	(0.06)	-1.45	(0.25)	0.502	(0.18)	2.808	(0.59)
Sandy Clay	11	0.12	(0.11)	0.385	(0.05)	-1.48	(0.57)	0.082	(0.06)	1.055	(0.89)
Sandy Clay Loam	87	0.06	(0.08)	0.384	(0.06)	-1.68	(0.71)	0.124	(0.12)	1.120	(0.85)
Sandy Loam	476	0.04	(0.05)	0.387	(0.09)	-1.57	(0.56)	0.161	(0.11)	1.583	(0.66)
Silt	6	0.05	(0.04)	0.489	(0.08)	-2.18	(0.30)	0.225	(0.13)	1.641	(0.27)
Silt Clay	28	0.11	(0.12)	0.481	(0.08)	-1.79	(0.64)	0.121	(0.10)	0.983	(0.57)
Silty Clay Loam	172	0.09	(0.08)	0.482	(0.09)	-2.08	(0.59)	0.182	(0.13)	1.046	(0.76)
Silt Loam	330	0.07	(0.07)	0.439	(0.09)	-2.3	(0.57)	0.221	(0.14)	1.261	(0.74)

Table C.2 ROSETTA Software Results for All Plots for 0-15 cm Soil Depth Profile

Code	Description	θ_r [cm^3/cm^3]	θ_s [cm^3/cm^3]	α [1/cm]	η	K_s [cm/day]	TEXTURE
1	C01I	0.077	0.431	0.010	1.469	10.53	CLAY LOAM
2	G02I	0.069	0.417	0.009	1.509	12.07	LOAM
4	D04II	0.082	0.444	0.011	1.444	10.92	CLAY LOAM
5	F05I	0.078	0.432	0.010	1.455	9.68	CLAY LOAM
6	D06III	0.085	0.448	0.012	1.403	9.02	CLAY LOAM
7	C07II	0.078	0.432	0.010	1.455	9.68	CLAY LOAM
8	F08III	0.068	0.414	0.010	1.481	8.78	LOAM
9	B09I	0.086	0.454	0.011	1.422	11.32	CLAY LOAM
10	E10I	0.081	0.439	0.011	1.443	10.00	CLAY LOAM
11	A11III	0.080	0.437	0.010	1.457	10.73	CLAY LOAM
12	G12III	0.086	0.451	0.012	1.396	9.32	CLAY LOAM
13	D13I	0.081	0.438	0.012	1.422	8.34	CLAY LOAM
14	A14I	0.077	0.431	0.010	1.469	10.53	CLAY LOAM
15	E15II	0.075	0.429	0.009	1.482	11.32	CLAY LOAM
16	B16IV	0.074	0.430	0.008	1.511	12.69	LOAM
17	E17IV	0.085	0.448	0.012	1.403	9.02	CLAY LOAM
18	A18IV	0.086	0.453	0.012	1.403	10.21	CLAY LOAM
19	A19II	0.084	0.447	0.011	1.437	11.04	CLAY LOAM
20	B20II	0.080	0.437	0.011	1.436	9.05	CLAY LOAM
22	D22IV	0.082	0.446	0.009	1.471	11.99	CLAY LOAM
24	F24IV	0.078	0.437	0.009	1.499	12.36	CLAY LOAM
25	C25IV	0.085	0.450	0.011	1.430	11.17	CLAY LOAM
26	E26III	0.068	0.412	0.011	1.472	8.10	LOAM

Table C.2 Continued

Code	Description	θ_r [cm^3/cm^3]	θ_s [cm^3/cm^3]	α [1/cm]	η	K_s [cm/day]	TEXTURE
28	C28III	0.076	0.430	0.009	1.490	11.92	CLAY LOAM
30	G30II	0.075	0.429	0.009	1.482	11.32	CLAY LOAM
31	G31IV	0.084	0.446	0.012	1.416	9.67	CLAY LOAM
32	F32III	0.082	0.439	0.012	1.409	7.78	CLAY LOAM
33	B33III	0.080	0.437	0.010	1.457	10.73	CLAY LOAM

Table C.3 ROSETTA Software Results for All Plots for 15-30 cm Soil Depth Profile

Code	Description	θ_r [cm^3/cm^3]	θ_s [cm^3/cm^3]	α [1/cm]	η	K_s [cm/day]	TEXTURE
1	C01I	0.072	0.425	0.007	1.538	13.52	LOAM
2	G02I	0.076	0.432	0.009	1.498	12.29	CLAY LOAM
4	D04II	0.086	0.449	0.013	1.390	8.49	CLAY LOAM
5	F05I	0.086	0.451	0.012	1.396	9.32	CLAY LOAM
6	D06III	0.085	0.450	0.012	1.409	9.93	CLAY LOAM
7	C07II	0.086	0.449	0.013	1.390	8.49	CLAY LOAM
8	F08III	0.078	0.429	0.013	1.418	6.67	CLAY LOAM
9	B09I	0.092	0.468	0.014	1.338	10.84	CLAY
10	E10I	0.089	0.460	0.013	1.376	10.42	CLAY LOAM
11	A11III	0.088	0.453	0.014	1.358	8.23	CLAY LOAM
12	G12III	0.091	0.466	0.012	1.393	12.20	CLAY LOAM
13	D13I	0.084	0.444	0.012	1.409	8.76	CLAY LOAM
14	A14I	0.083	0.440	0.013	1.395	7.36	CLAY LOAM
15	E15II	0.086	0.452	0.011	1.416	10.74	CLAY LOAM
16	B16IV	0.084	0.448	0.011	1.423	10.53	CLAY LOAM
17	E17IV	0.086	0.453	0.012	1.403	10.21	CLAY LOAM
18	A18IV	0.091	0.466	0.012	1.393	12.20	CLAY LOAM
19	A19II	0.091	0.466	0.012	1.393	12.20	CLAY LOAM
20	B20II	0.090	0.463	0.012	1.400	11.91	CLAY LOAM
22	D22IV	0.086	0.453	0.012	1.403	10.21	CLAY LOAM
24	F24IV	0.091	0.466	0.012	1.393	12.20	CLAY LOAM
25	C25IV	0.090	0.463	0.012	1.400	11.91	CLAY LOAM

Table C.3 Continued

Code	Description	θ_r [cm^3/cm^3]	θ_s [cm^3/cm^3]	α [1/cm]	η	K_s [cm/day]	TEXTURE
26	E26III	0.082	0.440	0.011	1.429	9.23	CLAY LOAM
28	C28III	0.087	0.457	0.010	1.434	11.93	CLAY LOAM
30	G30II	0.087	0.458	0.010	1.454	12.15	CLAY LOAM
31	G31IV	0.090	0.464	0.012	1.387	11.80	CLAY LOAM
32	F32III	0.090	0.465	0.011	1.406	12.19	CLAY LOAM
33	B33III	0.069	0.417	0.009	1.509	12.07	LOAM

Table C.4 ROSETTA Software Results for All Plots for 30-100 cm Soil Depth Profile

Code	Description	θ_r [cm^3/cm^3]	θ_s [cm^3/cm^3]	α [1/cm]	η	K_s [cm/day]	TEXTURE
1	C01I	0.090	0.461	0.013	1.363	10.00	CLAY
2	G02I	0.089	0.453	0.015	1.328	7.87	CLAY
4	D04II	0.098	0.489	0.018	1.250	20.67	CLAY
5	F05I	0.095	0.477	0.016	1.296	13.08	CLAY
6	D06III	0.091	0.463	0.015	1.328	9.55	CLAY
7	C07II	0.097	0.485	0.017	1.261	18.76	CLAY
8	F08III	0.077	0.426	0.012	1.423	6.56	CLAY LOAM
9	B09I	0.098	0.488	0.018	1.257	19.99	CLAY
10	E10I	0.097	0.484	0.018	1.249	19.34	CLAY
11	A11III	0.096	0.479	0.017	1.269	16.16	CLAY
12	G12III	0.094	0.472	0.017	1.286	12.62	CLAY

Table C.4 Continued

Code	Description	θ_r [cm^3/cm^3]	θ_s [cm^3/cm^3]	α [1/cm]	η	K_s [cm/day]	TEXTURE
13	D13I	0.095	0.478	0.017	1.277	14.97	CLAY
14	A14I	0.090	0.459	0.016	1.317	8.87	CLAY
15	E15II	0.092	0.465	0.016	1.306	10.13	CLAY
16	B16IV	0.095	0.475	0.017	1.282	13.74	CLAY
17	E17IV	0.092	0.466	0.014	1.333	10.11	CLAY
18	A18IV	0.098	0.490	0.017	1.261	20.39	CLAY
19	A19II	0.099	0.494	0.017	1.269	21.43	CLAY
20	B20II	0.096	0.483	0.016	1.286	15.51	CLAY
22	D22IV	0.094	0.473	0.014	1.337	12.44	CLAY
24	F24IV	0.097	0.487	0.015	1.318	16.61	CLAY
25	C25IV	0.098	0.488	0.015	1.308	17.09	CLAY
26	E26III	0.084	0.442	0.014	1.370	6.85	CLAY LOAM
28	C28III	0.097	0.486	0.015	1.304	16.33	CLAY
30	G30II	0.095	0.477	0.016	1.296	13.08	CLAY
31	G31IV	0.098	0.490	0.016	1.281	18.97	CLAY
32	F32III	0.096	0.480	0.017	1.282	15.16	CLAY
33	B33III	0.093	0.469	0.017	1.291	11.62	CLAY

Table C.5 Summary of Soil Information Input in UNSAT-H for Each Soil Profile and Each Plot

Plot	Treatment	Soil Profile	θ_{sat}	θ_r	$\theta_{sat} - \theta_r$	Soil Class	α [1/cm]	N	K_s [cm/hr]
14	A-I	0-24.9 cm	0.38	0.25	0.13	Clay Loam	0.019	1.310	2.72
14	A-I	25-64.9 cm	0.40	0.34	0.06	Clay Loam	0.019	1.310	1.50
14	A-I	65-150 cm	0.30	0.25	0.05	Clay	0.008	1.090	2.65
19	A-II	0-14.9 cm	0.37	0.24	0.13	Clay Loam	0.036	1.560	2.50
19	A-II	15-24.9 cm	0.47	0.35	0.12	Clay Loam	0.019	1.310	1.80
19	A-II	25-64.9 cm	0.46	0.30	0.16	Clay	0.008	1.090	1.50
19	A-II	65-150 cm	0.38	0.31	0.07	Clay	0.008	1.090	0.90
11	A-III	0-14.9 cm	0.38	0.21	0.17	Clay Loam	0.010	1.457	2.07
11	A-III	15-24.9 cm	0.40	0.25	0.15	Clay Loam	0.014	1.358	1.60
11	A-III	25-64.9 cm	0.43	0.30	0.13	Clay Loam	0.017	1.269	1.42
11	A-III	65-150 cm	0.38	0.34	0.04	Clay	0.017	1.269	1.10
18	A-IV	0-14.9 cm	0.32	0.15	0.17	Clay Loam	0.019	1.310	2.00
18	A-IV	15-64.9 cm	0.46	0.37	0.09	Clay Loam	0.019	1.310	1.35
18	A-IV	65-150 cm	0.45	0.37	0.08	Clay	0.008	1.090	0.85
9	B-I	0-24.9 cm	0.47	0.25	0.22	Clay Loam	0.019	1.310	1.97
9	B-I	25-64.9 cm	0.28	0.16	0.12	Clay	0.008	1.090	1.43
9	B-I	65-150 cm	0.43	0.38	0.05	Clay	0.008	1.090	1.21
20	B-II	0-14.9 cm	0.45	0.25	0.20	Clay Loam	0.036	1.560	2.33
20	B-II	15-24.9 cm	0.45	0.35	0.10	Clay Loam	0.020	1.350	1.90
20	B-II	25-64.9 cm	0.30	0.23	0.07	Clay	0.019	1.310	1.50
20	B-II	65-150 cm	0.30	0.25	0.05	Clay	0.008	1.090	0.74
33	B-III	0-14.9 cm	0.39	0.25	0.14	Clay Loam	0.019	1.310	2.50
33	B-III	15-24.9 cm	0.47	0.31	0.16	Loam	0.036	1.560	2.35

Table C.5 Continued

Plot	Treatment	Soil Profile	θ_{sat}	θ_r	$\theta_{sat} - \theta_r$	Soil Class	α [1/cm]	N	K_s [cm/hr]
33	B-III	25-64.9 cm	0.35	0.30	0.05	Clay	0.008	1.090	1.81
33	B-III	65-150 cm	0.27	0.24	0.03	Clay	0.019	1.310	1.30
16	B-IV	0-14.9 cm	0.33	0.15	0.18	Loam	0.040	1.600	2.50
16	B-IV	15-24.9 cm	0.48	0.40	0.08	Clay Loam	0.036	1.560	1.90
16	B-IV	25-64.9 cm	0.36	0.30	0.06	Clay Loam	0.025	1.250	1.55
16	B-IV	65-150 cm	0.48	0.37	0.12	Clay	0.008	1.090	1.20
1	C-I	0-14.9 cm	0.37	0.20	0.17	Clay Loam	0.019	1.310	1.18
1	C-I	15-24.9 cm	0.41	0.31	0.10	Loam	0.036	1.560	0.91
1	C-I	25-64.9 cm	0.38	0.33	0.05	Clay	0.008	1.090	1.24
1	C-I	65-150 cm	0.28	0.20	0.08	Clay	0.008	1.090	1.54
7	C-II	0-14.9 cm	0.40	0.25	0.15	Clay Loam	0.019	1.310	3.13
7	C-II	15-24.9 cm	0.42	0.33	0.09	Clay Loam	0.019	1.310	2.73
7	C-II	25-64.9 cm	0.35	0.25	0.10	Clay Loam	0.019	1.310	2.23
7	C-II	65-150 cm	0.39	0.36	0.03	Clay	0.008	1.090	1.47
28	C-III	0-14.9 cm	0.42	0.30	0.12	Clay Loam	0.019	1.310	2.00
28	C-III	15-64.9 cm	0.48	0.37	0.11	Clay Loam	0.019	1.310	1.80
28	C-III	65-150 cm	0.55	0.45	0.10	Clay	0.008	1.090	1.10
25	C-IV	0-14.9 cm	0.47	0.30	0.17	Clay Loam	0.019	1.310	1.50
25	C-IV	15-24.9 cm	0.47	0.35	0.12	Clay Loam	0.019	1.310	0.91
25	C-IV	25-64.9 cm	0.43	0.35	0.08	Clay Loam	0.019	1.310	1.30
25	C-IV	65-150 cm	0.44	0.40	0.04	Clay	0.008	1.090	1.00
13	D-I	0-24.9 cm	0.43	0.30	0.13	Clay Loam	0.019	1.310	2.50
13	D-I	25-64.9 cm	0.40	0.30	0.10	Clay Loam	0.019	1.310	1.50

Table C.5 Continued

Plot	Treatment	Soil Profile	θ_{sat}	θ_r	θ_{sat} - θ_r	Soil Class	α [1/cm]	N	K_s [cm/hr]
13	D-I	65-150 cm	0.45	0.39	0.06	Clay	0.008	1.090	1.00
4	D-II	0-14.9 cm	0.48	0.15	0.33	Clay Loam	0.019	1.310	1.80
4	D-II	15-24.9 cm	0.45	0.25	0.20	Clay Loam	0.019	1.310	1.90
4	D-II	25-64.9 cm	0.40	0.30	0.10	Clay Loam	0.008	1.090	1.40
4	D-II	65-150 cm	0.42	0.40	0.02	Clay	0.014	1.333	0.80
6	D-III	0-14.9 cm	0.46	0.20	0.26	Loam	0.036	1.560	3.00
6	D-III	15-64.9 cm	0.42	0.25	0.17	Clay Loam	0.019	1.310	2.50
6	D-III	65-150 cm	0.37	0.35	0.02	Clay	0.008	1.090	0.60
22	D-IV	0-14.9 cm	0.38	0.20	0.18	Clay Loam	0.025	1.350	1.65
22	D-IV	15-24.9 cm	0.45	0.35	0.10	Clay Loam	0.036	1.560	2.50
22	D-IV	25-64.9 cm	0.44	0.40	0.04	Clay	0.010	1.150	1.85
22	D-IV	65-150 cm	0.39	0.36	0.03	Clay	0.008	1.090	1.00
10	E-I	0-14.9 cm	0.40	0.20	0.20	Clay Loam	0.012	1.446	3.00
10	E-I	15-64.9 cm	0.43	0.30	0.13	Clay Loam	0.017	1.381	1.50
10	E-I	65-150 cm	0.42	0.38	0.04	Clay	0.023	1.295	0.80
15	E-II	0-14.9 cm	0.40	0.20	0.20	Clay Loam	0.009	1.482	3.50
15	E-II	15-24.9 cm	0.40	0.30	0.10	Clay Loam	0.011	1.416	3.00
15	E-II	25-64.9 cm	0.43	0.35	0.08	Clay	0.016	1.306	2.50
15	E-II	65-150 cm	0.42	0.40	0.02	Clay	0.016	1.306	1.50
26	E-III	0-14.9 cm	0.40	0.25	0.15	Loam	0.011	1.472	2.00
26	E-III	15-24.9 cm	0.35	0.30	0.05	Clay Loam	0.011	1.429	1.80
26	E-III	25-64.9 cm	0.40	0.30	0.10	Clay Loam	0.014	1.370	1.60
26	E-III	65-150 cm	0.40	0.30	0.10	Clay Loam	0.014	1.370	1.60

Table C.5 Continued

Plot	Treatment	Soil Profile	θ_{sat}	θ_r	$\theta_{sat} - \theta_r$	Soil Class	α [1/cm]	N	K_s [cm/hr]
17	E-IV	0-14.9 cm	0.40	0.20	0.20	Clay Loam	0.012	1.403	3.00
17	E-IV	15-24.9 cm	0.40	0.30	0.10	Clay Loam	0.012	1.403	2.50
17	E-IV	25-64.9 cm	0.43	0.35	0.08	Clay	0.014	1.333	1.50
17	E-IV	65-150 cm	0.42	0.40	0.02	Clay	0.014	1.333	0.80
5	F-I	0-14.9 cm	0.45	0.35	0.10	Clay Loam	0.010	1.455	1.50
5	F-I	15-64.9 cm	0.40	0.30	0.10	Clay Loam	0.012	1.396	1.00
5	F-I	65-150 cm	0.40	0.30	0.10	Clay	0.016	1.296	1.00
32	F-II	0-14.9 cm	0.35	0.15	0.20	Clay Loam	0.012	1.409	2.50
32	F-II	15-24.9 cm	0.40	0.30	0.10	Clay Loam	0.011	1.406	2.00
32	F-II	25-64.9 cm	0.43	0.35	0.08	Clay	0.017	1.282	1.50
32	F-II	65-150 cm	0.41	0.36	0.05	Clay	0.017	1.282	0.80
8	F-III	0-14.9 cm	0.40	0.20	0.20	Loam	0.010	1.481	2.00
8	F-III	15-64.9 cm	0.35	0.20	0.15	Clay Loam	0.013	1.418	1.50
8	F-III	65-150 cm	0.45	0.42	0.03	Clay Loam	0.012	1.423	0.80
24	F-IV	0-14.9 cm	0.45	0.25	0.20	Clay Loam	0.009	1.499	1.55
24	F-IV	15-24.9 cm	0.35	0.25	0.10	Clay Loam	0.015	1.450	1.45
24	F-IV	25-64.9 cm	0.38	0.25	0.13	Clay	0.015	1.318	1.35
24	F-IV	65-150 cm	0.38	0.25	0.13	Clay	0.015	1.318	0.95
2	G-I	0-14.9 cm	0.40	0.25	0.15	Loam	0.015	1.328	2.00
2	G-I	15-24.9 cm	0.43	0.40	0.03	Clay Loam	0.009	1.498	1.50
2	G-I	25-64.9 cm	0.35	0.20	0.15	Clay	0.015	1.328	1.50
2	G-I	65-150 cm	0.40	0.20	0.20	Clay	0.015	1.328	1.00
30	G-II	0-14.9 cm	0.47	0.15	0.32	Clay Loam	0.019	1.310	2.50

Table C.5 Continued

Plot	Treatment	Soil Profile	θ_{sat}	θ_r	θ_{sat} - θ_r	Soil Class	α [1/cm]	N	K_s [cm/hr]
30	G-II	15-64.9 cm	0.40	0.25	0.15	Clay Loam	0.010	1.454	1.50
30	G-II	65-150 cm	0.30	0.25	0.05	Clay	0.016	1.296	0.80
12	G-III	0-14.9 cm	0.50	0.20	0.30	Clay Loam	0.012	1.396	2.50
12	G-III	15-24.9 cm	0.42	0.30	0.12	Clay Loam	0.012	1.393	2.50
12	G-III	25-64.9 cm	0.40	0.25	0.15	Clay	0.017	1.286	2.00
12	G-III	65-150 cm	0.40	0.20	0.20	Clay	0.008	1.090	0.80
31	G-IV	0-14.9 cm	0.47	0.35	0.12	Loam	0.036	1.560	2.00
31	G-IV	15-24.9 cm	0.45	0.37	0.08	Clay Loam	0.036	1.560	1.50
31	G-IV	25-64.9 cm	0.43	0.37	0.06	Clay	0.019	1.310	1.00
31	G-IV	65-150 cm	0.46	0.42	0.04	Clay	0.016	1.281	0.70

Table C.6 Seasonal PBIAS Calculated Values for Fall 2014 Season

Plot	Treatment	MAE Node 1 (10cm)	MAE Node 2 (20 cm)	MAE Node 3 (30 cm)	MAE Node 4 (100 cm)	Percent Bias Node 1 [%]	Percent Bias Node 2 [%]	Percent Bias Node 3 [%]	Percent Bias Node 4 [%]
14	A-I	0.0227	0.0420	0.0139	0.0450	6.8%	14.0%	3.7%	17.4%
19	A-II	0.0289	0.0210	0.0517	0.0593	-8.7%	4.9%	12.8%	-1.5%
11	A-III	0.0148	0.0128	0.0173	0.0107	2.5%	1.6%	3.0%	-2.7%
18	A-IV	0.0382	0.0121	0.0274	0.0436	15.6%	1.0%	6.6%	10.8%
9	B-I	0.0684	0.0260	0.0502	0.0289	19.7%	5.8%	22.4%	7.2%
20	B-II	0.0348	0.0496	0.0393	0.0378	-9.1%	13.2%	0.0%	-5.5%
33	B-III	0.0169	0.0285	0.0063	0.0082	-4.6%	-6.9%	-1.5%	-1.2%
16	B-IV	0.0495	0.0200	0.0131	0.0454	17.4%	-4.3%	2.5%	-3.6%
1	C-I	0.0162	0.0074	0.0069	0.0425	2.7%	0.2%	0.7%	-8.9%
7	C-II	0.0224	0.0309	0.0145	0.0052	4.9%	8.5%	-4.3%	-0.5%
28	C-III	0.0131	0.0296	0.0429	0.0462	-2.9%	6.4%	10.5%	-0.5%
25	C-IV	0.0512	0.0162	0.0180	0.0223	13.6%	3.1%	3.9%	1.5%
13	D-I	0.0225	0.0082	0.0100	0.0365	5.7%	-0.2%	-0.2%	-5.3%
4	D-II	0.0221	0.0119	0.0107	0.0081	-0.1%	-0.8%	1.9%	-1.9%
6	D-III	0.0442	0.0251	0.0294	0.0710	-11.8%	5.5%	5.8%	-14.1%
22	D-IV	0.0262	0.0197	0.0121	0.0208	-7.3%	-4.7%	2.7%	-1.2%
10	E-I	0.0344	0.0313	0.0251	0.0170	10.8%	8.5%	6.6%	0.8%
15	E-II	0.0183	0.0095	0.0115	0.0478	3.4%	1.4%	2.2%	-9.2%
26	E-III	0.0136	0.0074	0.0188	NA	3.3%	-0.2%	-4.9%	NA
17	E-IV	0.0127	0.0125	0.0179	0.0107	-2.2%	3.5%	4.6%	-2.3%
5	F-I	0.0275	0.0173	0.0102	NA	-2.3%	7.0%	4.7%	1.5%
32	F-II	0.0181	0.0126	0.0219	0.0291	3.4%	3.1%	5.6%	-4.9%
8	F-III	0.0241	0.0114	0.0142	0.0183	7.1%	0.8%	0.1%	-2.6%

Table C.6 Continued

Plot	Treatment	MAE Node 1 (10cm)	MAE Node 2 (20 cm)	MAE Node 3 (30 cm)	MAE Node 4 (100 cm)	Percent Bias Node 1 [%]	Percent Bias Node 2 [%]	Percent Bias Node 3 [%]	Percent Bias Node 4 [%]
24	F-IV	0.0106	0.0046	0.0050	0.0274	-0.6%	-0.8%	-1.2%	-4.9%
2	G-I	0.0195	0.0040	0.0288	NA	-5.2%	-5.2%	-0.9%	7.9%
30	G-II	0.0127	0.0072	0.0173	0.0555	0.3%	-1.2%	2.8%	-13.4%
12	G-III	0.0434	0.0293	0.0327	0.0614	7.9%	7.4%	6.3%	-10.0%
31	G-IV	0.0143	0.0203	0.0137	0.0136	2.4%	5.2%	2.9%	1.2%

Table C.7 Seasonal PBIAS Calculated Values for Spring 2015 Season

Plot	Treatment	MAE Node 1 (10cm)	MAE Node 2 (20 cm)	MAE Node 3 (30 cm)	MAE Node 4 (100 cm)	Percent Bias Node 1 [%]	Percent Bias Node 2 [%]	Percent Bias Node 3 [%]	Percent Bias Node 4 [%]
14	A-I	0.0106	0.0252	0.0100	0.0469	0.7%	8.4%	2.7%	18.8%
19	A-II	0.0481	0.0106	0.0422	0.0405	-14.1%	2.4%	10.3%	12.0%
11	A-III	0.0263	0.0147	0.0079	0.0036	-7.7%	-3.0%	0.5%	0.9%
18	A-IV	0.0249	0.0091	0.0236	0.0586	10.4%	-1.7%	5.8%	15.1%
9	B-I	0.0461	0.0161	0.0482	0.0304	13.3%	0.8%	21.6%	7.7%
20	B-II	0.0537	0.0422	0.0337	0.0144	-13.9%	11.2%	2.5%	4.4%
33	B-III	0.0367	0.0415	0.0040	0.0034	-10.0%	-10.2%	-1.1%	-0.7%
16	B-IV	0.0436	0.0323	0.0102	0.0507	-16.5%	-6.9%	-2.2%	0.3%
1	C-I	0.0148	0.0128	0.0034	0.0172	-3.7%	-3.3%	0.7%	3.7%
7	C-II	0.0449	0.0216	0.0246	0.0016	-11.6%	5.9%	-7.3%	0.1%
28	C-III	0.0204	0.0240	0.0373	0.0484	-5.2%	5.5%	9.2%	2.6%
25	C-IV	0.0214	0.0069	0.0148	0.0236	4.9%	0.2%	3.7%	5.3%
13	D-I	0.0114	0.0172	0.0089	0.0247	0.4%	-4.2%	-1.7%	-1.8%
4	D-II	0.0625	0.0252	0.0044	0.0147	-14.9%	-6.4%	-0.6%	-0.4%
6	D-III	0.0624	0.0191	0.0231	0.0422	-16.6%	5.3%	5.8%	-6.3%
22	D-IV	0.0546	0.0354	0.0070	0.0109	-15.6%	-8.4%	1.6%	2.1%
10	E-I	0.0251	0.0167	0.0171	0.0123	0.4%	4.5%	4.0%	3.1%
15	E-II	0.0225	0.0110	0.0052	0.0201	-4.3%	-2.6%	0.7%	-3.7%
26	E-III	0.0168	0.0037	0.0234	NA	-4.3%	-0.6%	-6.1%	NA
17	E-IV	0.0396	0.0087	0.0081	0.0147	-11.3%	-0.5%	2.0%	-3.4%
5	F-I	0.0171	0.0092	0.0058	NA	4.4%	2.4%	-0.5%	NA
32	F-II	0.0407	0.0159	0.0115	0.0112	-13.3%	-4.2%	2.9%	-0.1%
8	F-III	0.0146	0.0121	0.0143	0.0146	0.0%	-2.2%	-4.1%	-1.4%

Table C.7 Continued

Plot	Treatment	MAE Node 1 (10cm)	MAE Node 2 (20 cm)	MAE Node 3 (30 cm)	MAE Node 4 (100 cm)	Percent Bias Node 1 [%]	Percent Bias Node 2 [%]	Percent Bias Node 3 [%]	Percent Bias Node 4 [%]
24	F-IV	0.0305	0.0089	0.0095	0.0048	-7.4%	-2.6%	-2.8%	-0.3%
2	G-I	0.0331	0.0087	0.0091	NA	-8.8%	-2.0%	-1.3%	NA
30	G-II	0.0282	0.0116	0.0109	0.0141	-7.4%	-3.2%	2.2%	-2.9%
12	G-III	0.0348	0.0206	0.0227	NA	0.7%	5.6%	5.9%	NA
31	G-IV	0.0150	0.0075	0.0107	0.0112	-2.9%	0.6%	2.6%	2.4%

Table C.8 Seasonal PBIAS Calculated Values for Winter 2015 Season

Plot	Treatment	MAE Node 1 (10cm)	MAE Node 2 (20 cm)	MAE Node 3 (30 cm)	MAE Node 4 (100 cm)	Percent Bias Node 1 [%]	Percent Bias Node 2 [%]	Percent Bias Node 3 [%]	Percent Bias Node 4 [%]
14	A-I	0.0051	0.0266	0.0123	0.0489	0.5%	8.4%	3.3%	19.6%
19	A-II	0.0297	0.0128	0.0355	0.0642	-8.8%	2.9%	8.2%	-5.8%
11	A-III	0.0276	0.0445	0.0081	0.0063	-7.5%	-10.9%	-1.5%	-1.5%
18	A-IV	0.0526	0.0130	0.0267	0.0356	23.4%	-2.8%	6.5%	8.6%
9	B-I	0.0701	0.0109	0.0370	0.0247	20.1%	1.7%	15.4%	6.1%
20	B-II	0.0359	0.0334	0.0405	0.0391	-9.3%	8.5%	-6.1%	-6.4%
33	B-III	0.0163	0.0358	0.0072	0.0072	-4.4%	-8.5%	-2.0%	-2.3%
16	B-IV	0.0113	0.0177	0.0262	0.0343	3.0%	-3.8%	-7.0%	-6.0%
1	C-I	0.0106	0.0129	0.0075	0.0560	-2.3%	-3.3%	-1.9%	-12.9%
7	C-II	0.0548	0.0116	0.0222	0.0044	-13.3%	-2.7%	-6.4%	-0.7%
28	C-III	0.0113	0.0167	0.0445	0.0437	-2.8%	3.6%	10.8%	-1.2%
25	C-IV	0.0574	0.0184	0.0082	0.0225	15.5%	4.3%	1.8%	3.9%
13	D-I	0.0234	0.0074	0.0052	0.0517	6.3%	-1.7%	0.3%	-9.4%
4	D-II	0.0103	0.0089	0.0074	NA	-1.9%	1.3%	1.7%	NA
6	D-III	0.0150	0.0199	0.0221	0.0817	-4.2%	5.3%	2.9%	-16.9%
22	D-IV	0.0401	0.0294	0.0050	0.0226	-11.2%	-6.9%	0.6%	-2.7%
10	E-I	0.0433	0.0440	0.0301	0.0171	13.3%	12.5%	8.2%	2.0%
15	E-II	0.0137	0.0046	NA	0.0535	3.7%	0.4%	NA	-11.0%
26	E-III	0.0088	0.0089	0.0206	NA	-2.2%	-2.4%	-5.3%	NA
17	E-IV	0.0147	0.0083	0.0119	0.0159	-4.0%	2.3%	3.0%	-3.7%
5	F-I	0.0096	0.0128	0.0045	NA	2.2%	3.6%	0.2%	NA
32	F-II	0.0061	0.0073	0.0113	0.0426	-0.3%	-1.8%	2.8%	-9.6%
8	F-III	0.0153	0.0554	0.0092	0.0232	4.7%	-15.3%	-2.2%	-4.1%

Table C.8 Continued

Plot	Treatment	MAE Node 1 (10cm)	MAE Node 2 (20 cm)	MAE Node 3 (30 cm)	MAE Node 4 (100 cm)	Percent Bias Node 1 [%]	Percent Bias Node 2 [%]	Percent Bias Node 3 [%]	Percent Bias Node 4 [%]
24	F-IV	0.0156	0.0104	0.0088	0.0456	3.9%	-3.0%	-2.5%	-10.9%
2	G-I	0.0167	0.0075	0.0068	NA	-4.5%	-1.7%	-0.6%	NA
30	G-II	0.0188	0.0086	0.0170	0.0671	5.2%	-2.1%	4.4%	-17.3%
12	G-III	0.0594	0.3088	0.0356	NA	15.6%	7.6%	4.2%	NA
31	G-IV	0.0094	0.0096	0.0108	0.0127	0.0%	2.2%	1.9%	-0.9%

Table C.9 Data for Statistical Analysis for Unique Soil Parameters for (0-15 cm) Soil Profile

Plot	Clay (%)	pH (0-15cm) <2mm	EC (0-15cm) <2mm	CEC (0-15cm) <2mm	SoilC (0-15cm) Mg/ha	Mean Slope (%)	Saturated Conductivity (cm/hr)	Average Temperature (°C)	Genus of Bacteria (Bacillus - 205)	Genus of Bacteria (Clostridium - 185)	Genus of Bacteria (Shewanella - 68)	Total Basal Liquid Flux [cm]
A11III	30.0	5.2	0.16	35.7	62.0	2.654	2.07	11.6	27	26	11	251.67
A14I	28.0	5.2	0.27	36.5	67.2	1.965	2.72	12.0	27	26	11	239.24
A18IV	36.0	5.1	0.16	34.1	58.0	5.887	2.00	12.6	27	26	11	246.19
A19II	33.0	5.1	0.19	38.1	62.3	4.400	2.50	12.8	27	26	11	200.57
B09I	35.0	5.1	0.19	37.1	58.9	2.924	1.97	12.4	25	31	15	186.02
B16IV	26.0	5.3	0.16	39.0	59.3	5.183	2.50	13.7	25	31	15	251.11
B20II	31.0	5.1	0.17	31.7	64.2	2.523	2.33	13.3	25	31	15	260.54
B33III	30.0	5.1	0.20	37.0	56.7	5.468	2.50	12.8	25	31	15	229.44
C01I	28.0	5.4	0.14	36.1	55.1	1.930	1.18	12.3	33	21	6	189.58
C07II	29.0	5.3	0.16	27.9	60.5	5.963	3.13	12.4	33	21	6	215.24
C25IV	34.0	5.1	0.13	34.0	49.0	5.927	1.50	12.4	33	21	6	258.38
C28III	27.0	5.2	0.18	39.4	60.2	5.522	2.00	12.5	33	21	6	247.55
D04II	32.0	5.2	0.18	27.7	63.6	1.429	1.80	12.3	25	23	10	265.07
D06III	35.0	5.1	0.18	44.8	58.3	3.446	3.00	13.0	25	23	10	246.73
D13I	32.0	5.3	0.20	34.4	69.5	1.701	2.50	13.7	25	23	10	258.76
D22IV	31.0	5.4	0.17	36.9	48.6	5.647	1.65	13.3	25	23	10	265.36
E10I	31.0	5.1	0.15	37.5	64.8	6.620	3.00	13.5	21	14	4	256.54
E15II	27.0	5.1	0.24	33.9	52.8	5.474	3.50	14.2	21	14	4	267.25
E17IV	35.0	5.0	0.15	39.9	50.1	5.468	3.00	14.5	21	14	4	261.76
E26III	23.0	5.4	0.22	33.4	61.7	2.474	2.00	14.4	21	14	4	277.81

Table C.9 Continued

Plot	Clay (%)	pH (0-15cm) <2mm	EC (0-15cm) <2mm	CEC (0-15cm) <2mm	SoilC (0-15cm) Mg/ha	Mean Slope (%)	Saturated Conductivity (cm/hr)	Average Temperature (°C)	Genus of Bacteria (Bacillus - 205)	Genus of Bacteria (Clostridium - 185)	Genus of Bacteria (Shewanella - 68)	Total Basal Liquid Flux [cm]
F05I	29.0	5.4	0.17	31.8	64.3	3.703	1.50	13.3	20	17	4	269.33
F08III	23.0	5.4	0.21	37.9	61.0	3.069	2.00	13.5	20	17	4	264.47
F24IV	28.0	5.1	0.18	31.9	56.2	5.766	1.55	13.6	20	17	4	267.12
F32III	33.0	5.3	0.19	40.5	63.3	5.518	2.50	13.0	20	17	4	258.84
G02I	23.0	5.2	0.24	40.8	63.0	3.103	2.00	14.2	24	30	11	271.54
G12III	36.0	5.1	0.14	40.8	70.2	1.380	2.50	14.6	24	30	11	235.23
G30II	27.0	5.4	0.26	35.4	60.4	4.021	2.50	13.6	24	30	11	260.53
G31IV	34.0	5.0	0.18	30.2	57.3	5.752	2.00	14.2	24	30	11	289.33

Table C.10 Data for Statistical Analysis for Unique Soil Parameters for (15-30 cm) Soil Profile

Plot	Clay (%)	pH (0-15cm) <2mm	EC (0-15cm) <2mm	CEC (0-15cm) <2mm	SoilC (0-15cm) Mg/ha	Mean Slope (%)	Saturated Conductivity (cm/hr)	Average Temperature (°C)	Genus of Bacteria (Bacillus - 205)	Genus of Bacteria (Clostridium - 185)	Genus of Bacteria (Shewanella - 68)	Total Basal Liquid Flux [cm]
A11III	39.0	5.1	0.08	28.9	51.1	2.654	1.60	11.6	27	26	11	251.7
A14I	34.0	5.2	0.11	33.6	56.2	1.965	2.72	12.0	27	26	11	239.2
A18IV	39.0	5.0	0.08	33.0	42.4	5.887	1.35	12.6	27	26	11	246.2
A19II	39.0	4.9	0.08	37.8	55.9	4.400	1.80	12.8	27	26	11	200.6
B09I	43.0	5.0	0.11	35.9	54.8	2.924	1.97	12.4	25	31	15	186.0
B16IV	34.0	5.1	0.09	40.4	48.8	5.183	1.90	13.7	25	31	15	251.1
B20II	38.0	5.2	0.07	30.2	56.1	2.523	1.90	13.3	25	31	15	260.5
B33III	23.0	5.0	0.10	39.0	48.5	5.468	2.35	12.8	25	31	15	229.4
C01I	24.0	5.2	0.08	36.0	57.8	1.930	0.91	12.3	33	21	6	189.6
C07II	36.0	5.2	0.09	30.0	61.9	5.963	2.73	12.4	33	21	6	215.2
C25IV	38.0	4.9	0.08	35.8	48.5	5.927	0.91	12.4	33	21	6	258.4
C28III	35.0	5.0	0.08	41.3	50.5	5.522	1.80	12.5	33	21	6	247.5
D04II	36.0	5.0	0.09	29.0	57.5	1.429	1.90	12.3	25	23	10	265.1
D06III	35.0	5.1	0.09	44.5	49.3	3.446	2.50	13.0	25	23	10	246.7
D13I	34.0	5.2	0.08	34.3	60.4	1.701	2.50	13.7	25	23	10	258.8
D22IV	36.0	5.1	0.07	37.7	50.0	5.647	2.50	13.3	25	23	10	265.4
E10I	39.0	5.0	0.11	35.6	58.6	6.620	1.50	13.5	21	14	4	256.5
E15II	35.0	5.0	0.11	35.5	53.7	5.474	3.00	14.2	21	14	4	267.2
E17IV	36.0	4.9	0.08	41.8	44.5	5.468	2.50	14.5	21	14	4	261.8
E26III	32.0	5.4	0.09	32.2	57.4	2.474	1.80	14.4	21	14	4	277.8

Table C.10 Continued

Plot	Clay (%)	pH (0-15cm) <2mm	EC (0-15cm) <2mm	CEC (0-15cm) <2mm	SoilC (0-15cm) Mg/ha	Mean Slope (%)	Saturated Conductivity (cm/hr)	Average Temperature (°C)	Genus of Bacteria (Bacillus - 205)	Genus of Bacteria (Clostridium - 185)	Genus of Bacteria (Shewanella - 68)	Total Basal Liquid Flux [cm]
F05I	36.0	5.2	0.09	32.2	61.0	3.703	1.00	13.3	20	17	4	269.3
F08III	30.0	5.0	0.09	39.8	53.9	3.069	1.50	13.5	20	17	4	264.5
F24IV	39.0	5.1	0.08	33.9	51.2	5.766	2.00	13.6	20	17	4	267.1
F32II	38.0	4.9	0.11	39.6	52.9	5.518	2.00	13.0	20	17	4	258.8
G02I	27.0	5.1	0.09	38.5	60.6	3.103	1.50	14.2	24	30	11	271.5
G12III	39.0	4.9	0.07	35.6	43.9	1.380	2.50	14.6	24	30	11	235.2
G30II	34.0	5.2	0.11	33.9	53.3	4.021	1.50	13.6	24	30	11	260.5
G31IV	39.0	5.0	0.09	31.7	55.0	5.752	1.50	14.2	24	30	11	289.3

Table C.11 Data for Statistical Analysis for Unique Soil Parameters for (30-100 cm) Soil Profile

Plot	Clay (%)	pH (0-15cm) <2mm	EC (0-15cm) <2mm	CEC (0-15cm) <2mm	SoilC (0-15cm) Mg/ha	Mean Slope (%)	Saturated Conductivity (cm/hr)	Average Temperature (°C)	Genus of Bacteria (Bacillus - 205)	Genus of Bacteria (Clostridium - 185)	Genus of Bacteria (Shewanella - 68)	Total Basal Liquid Flux [cm]
A11III	51.0	4.8	0.02	47.3	94.1	2.654	1.25	11.6	27	26	11	251.7
A14I	43.0	5.0	0.03	34.6	133.6	1.965	2.00	12.0	27	26	11	239.2
A18IV	54.0	4.8	0.04	44.9	84.7	5.887	1.30	12.6	27	26	11	246.2
A19II	54.0	4.9	0.03	55.6	119.9	4.400	1.20	12.8	27	26	11	200.6
B09I	54.0	4.9	0.03	51.6	105.7	2.924	1.30	12.4	25	31	15	186.0
B16IV	49.0	4.9	0.02	46.1	78.9	5.183	1.35	13.7	25	31	15	251.1
B20II	50.0	5.0	0.03	36.8	126.3	2.523	1.15	13.3	25	31	15	260.5
B33III	47.0	4.8	0.04	47.3	86.5	5.468	1.50	12.8	25	31	15	229.4
C01I	40.0	4.9	0.04	37.5	115.6	1.930	1.35	12.3	33	21	6	189.6
C07II	53.0	5.0	0.02	30.9	97.1	5.963	1.85	12.4	33	21	6	215.2
C25IV	49.0	4.9	0.03	41.7	96.7	5.927	1.15	12.4	33	21	6	258.4
C28III	49.0	4.8	0.03	48.1	91.2	5.522	1.45	12.5	33	21	6	247.5
D04II	55.0	5.0	0.02	27.6	95.0	1.429	1.10	12.3	25	23	10	265.1
D06III	43.0	4.8	0.03	56.1	93.4	3.446	1.55	13.0	25	23	10	246.7
D13I	50.0	4.9	0.03	41.1	116.3	1.701	1.25	13.7	25	23	10	258.8
D22IV	44.0	4.8	0.02	40.2	78.6	5.647	1.40	13.3	25	23	10	265.4
E10I	54.0	4.8	0.03	41.0	110.1	6.620	1.20	13.5	21	14	4	256.5
E15II	45.0	5.0	0.03	38.2	111.7	5.474	2.00	14.2	21	14	4	267.2
E17IV	43.0	4.8	0.02	50.4	91.4	5.468	1.30	14.5	21	14	4	261.8
E26III	36.0	5.0	0.03	40.0	94.5	2.474	1.60	14.4	21	14	4	277.8

Table C.11 Continued

Plot	Clay (%)	pH (0-15cm) <2mm	EC (0-15cm) <2mm	CEC (0-15cm) <2mm	SoilC (0-15cm) Mg/ha	Mean Slope (%)	Saturated Conductivity (cm/hr)	Average Temperature (°C)	Genus of Bacteria (Bacillus - 205)	Genus of Bacteria (Clostridium - 185)	Genus of Bacteria (Shewanella - 68)	Total Basal Liquid Flux [cm]
F05I	48.0	5.0	0.03	36.2	117.0	3.703	1.00	13.3	20	17	4	269.3
F08III	29.0	4.9	0.03	58.7	87.9	3.069	1.20	13.5	20	17	4	264.5
F24IV	48.0	4.9	0.03	39.3	95.6	5.766	1.20	13.6	20	17	4	267.1
F32II	50.0	4.8	0.03	50.3	114.9	5.518	1.20	13.0	20	17	4	258.8
G02I	41.0	4.9	0.03	52.0	107.6	3.103	1.40	14.2	24	30	11	271.5
G12III	48.0	4.7	0.02	52.5	91.6	1.380	1.40	14.6	24	30	11	235.2
G30II	48.0	4.7	0.03	53.4	105.1	4.021	1.20	13.6	24	30	11	260.5
G31IV	52.0	4.9	0.03	36.1	100.8	5.752	0.85	14.2	24	30	11	289.3

APPENDIX D

GRAPHICAL SUMMARIES OF UNSAT-H

SIMULATION RESULTS FOR

TWO YEARS

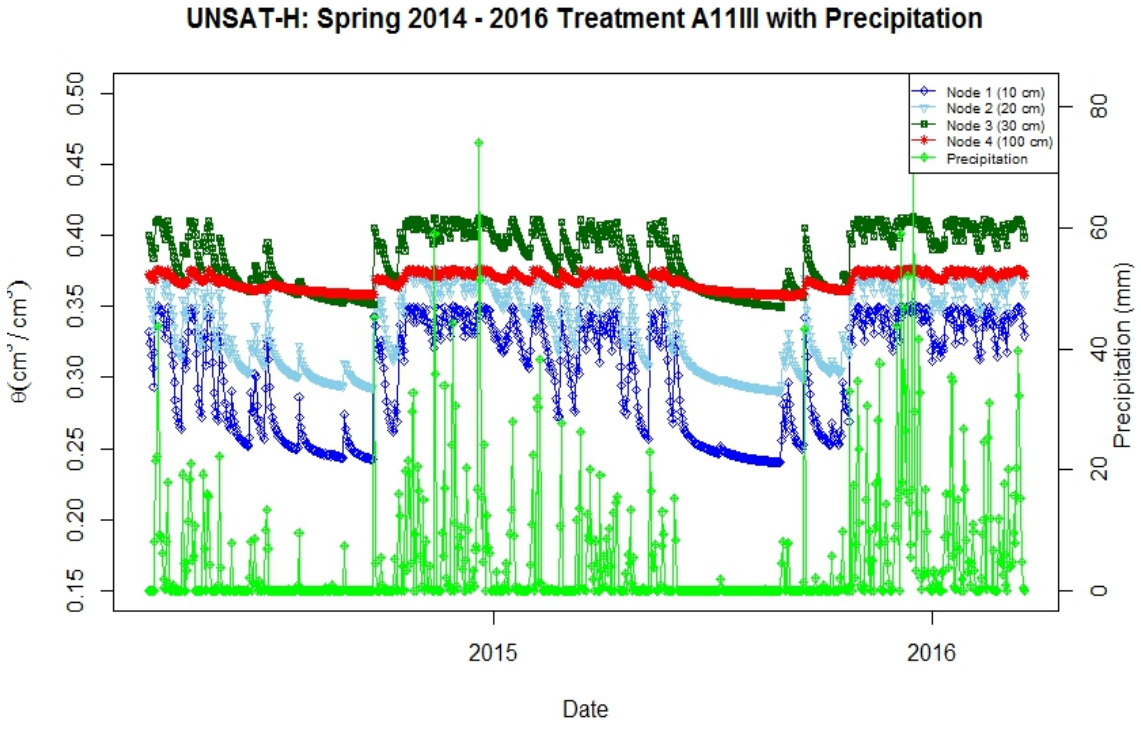

Figure D.1 Treatment Plot A11III Volumetric Water Content with Precipitation for 2-Year Simulation

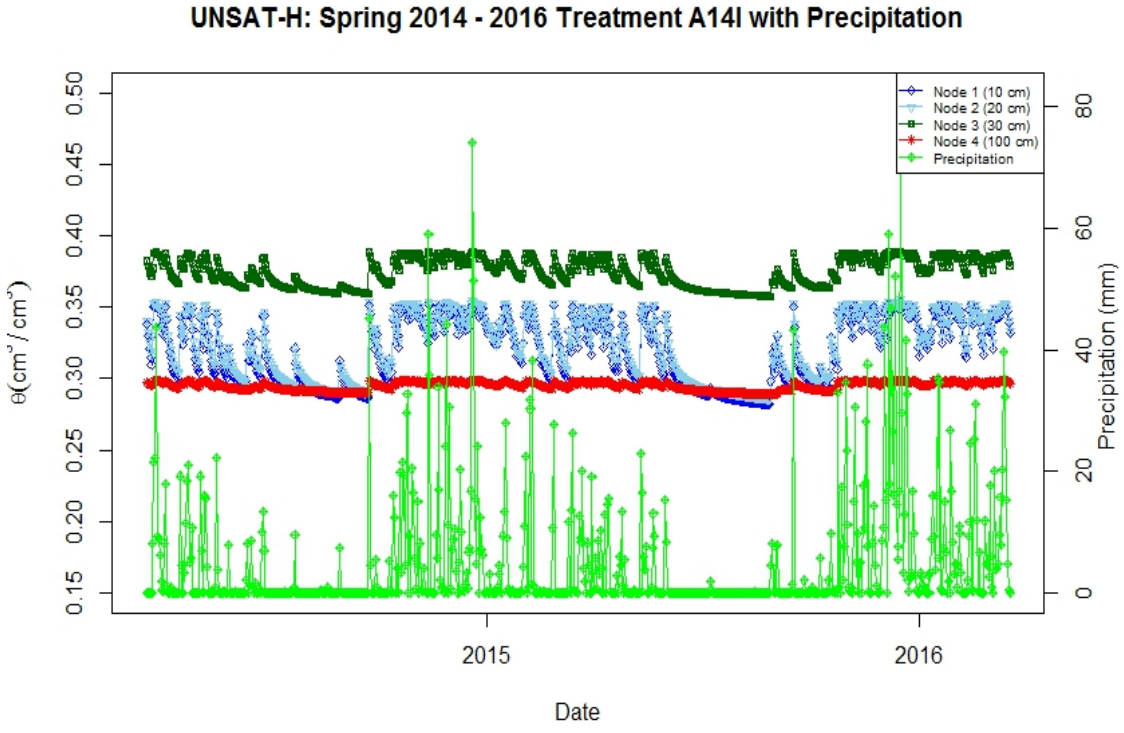

Figure D.2 Treatment Plot A14I Volumetric Water Content with Precipitation for 2-Year Simulation

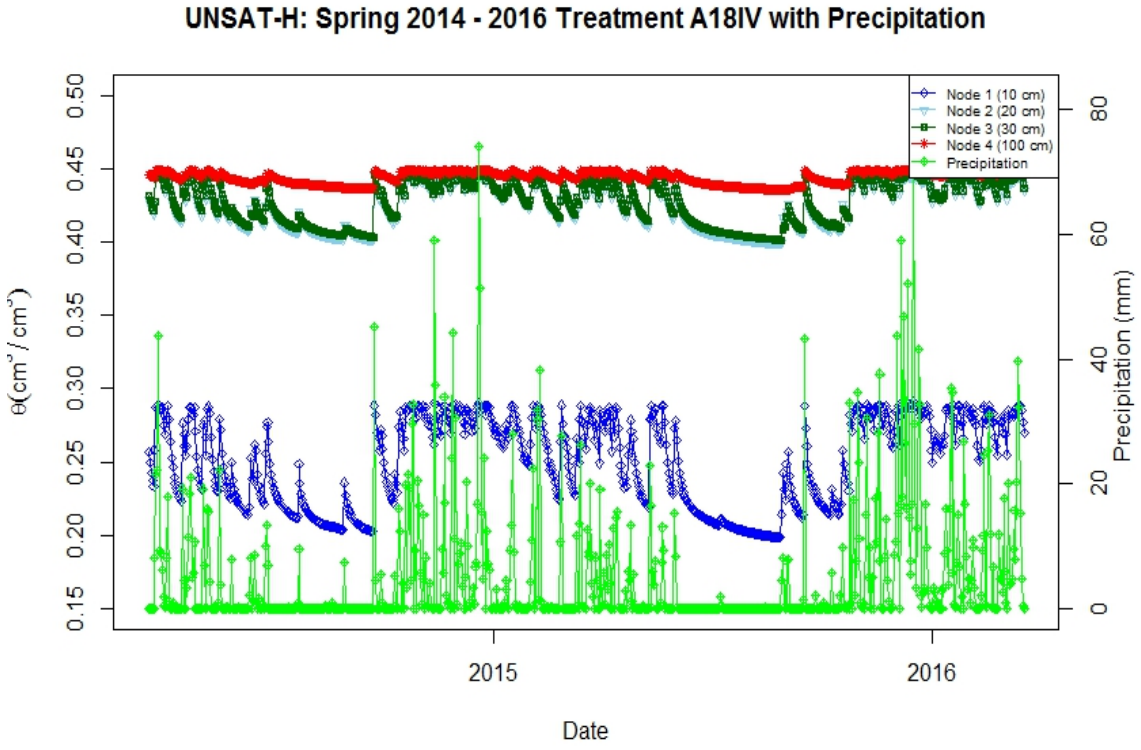

Figure D.3 Treatment Plot A18IV Volumetric Water Content with Precipitation for 2-Year Simulation

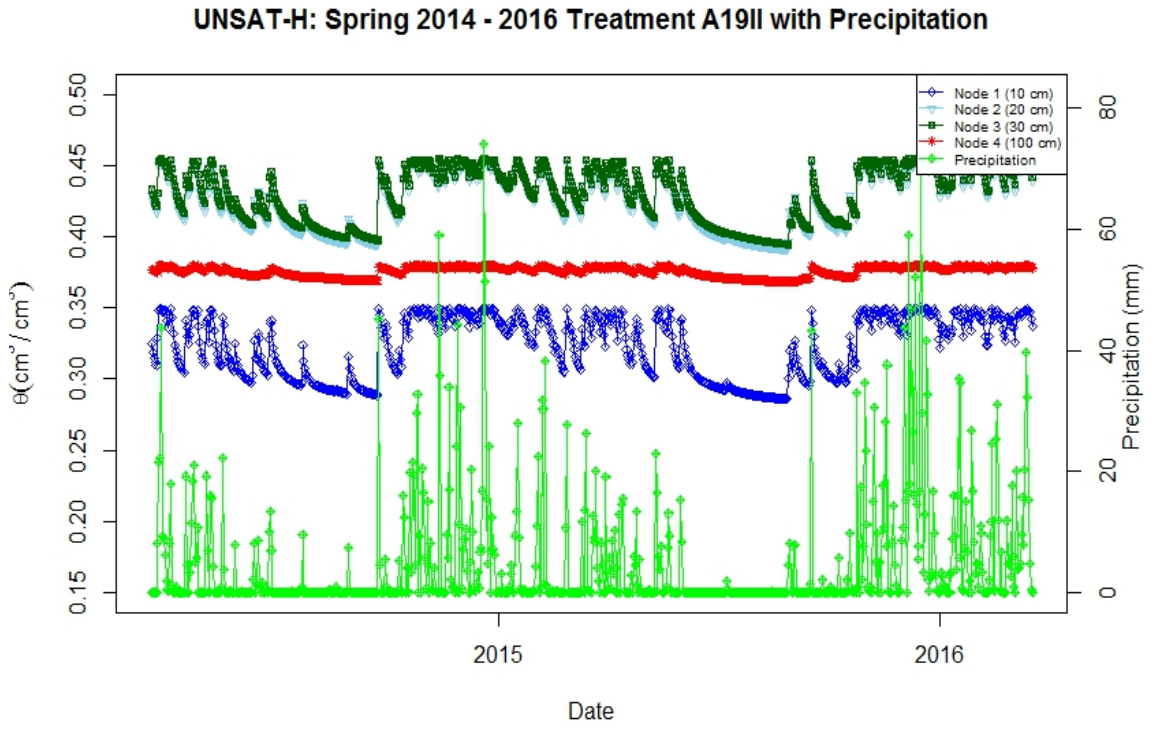

Figure D.4 Treatment Plot A19II Volumetric Water Content with Precipitation for 2-Year Simulation

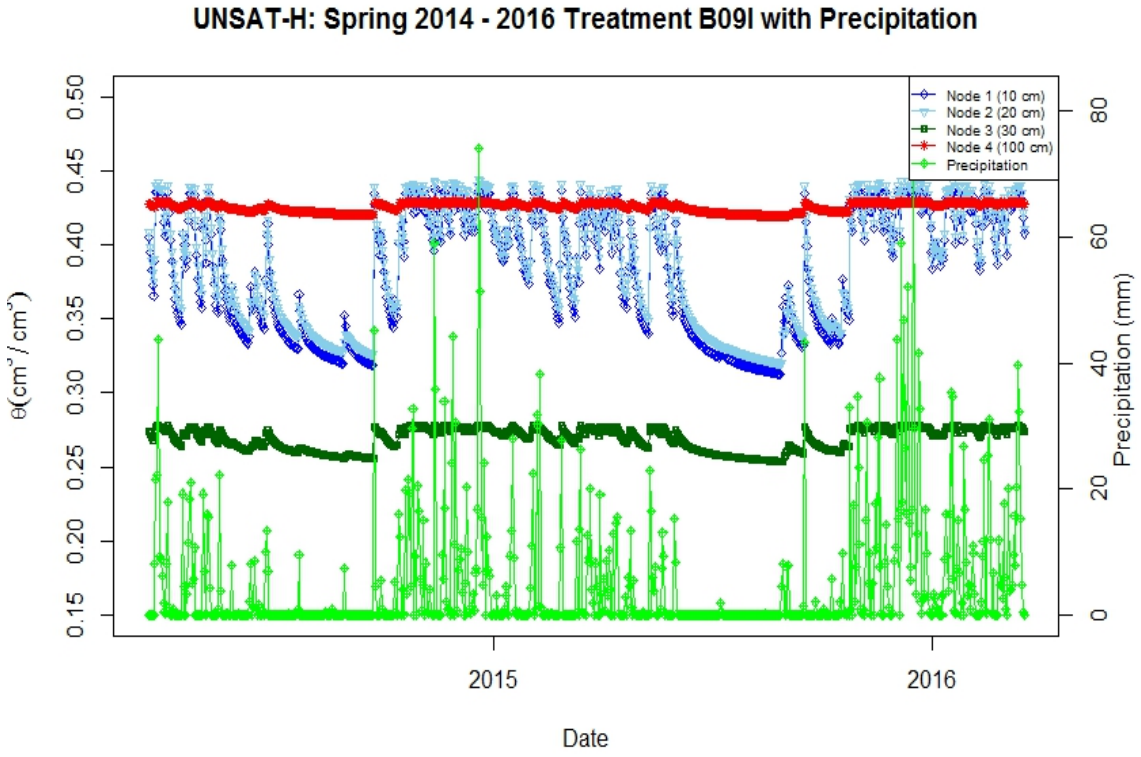

Figure D.5 Treatment Plot B09I Volumetric Water Content with Precipitation for 2-Year Simulation

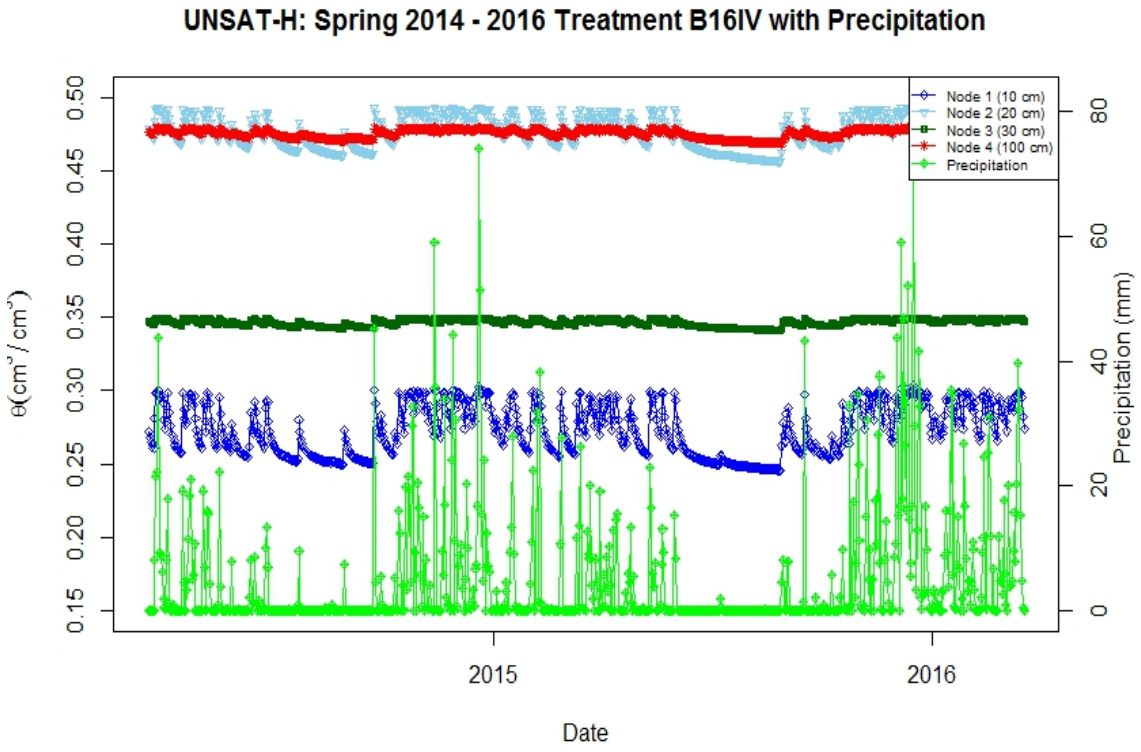

Figure D.6 Treatment Plot B16IV Volumetric Water Content with Precipitation for 2-Year Simulation

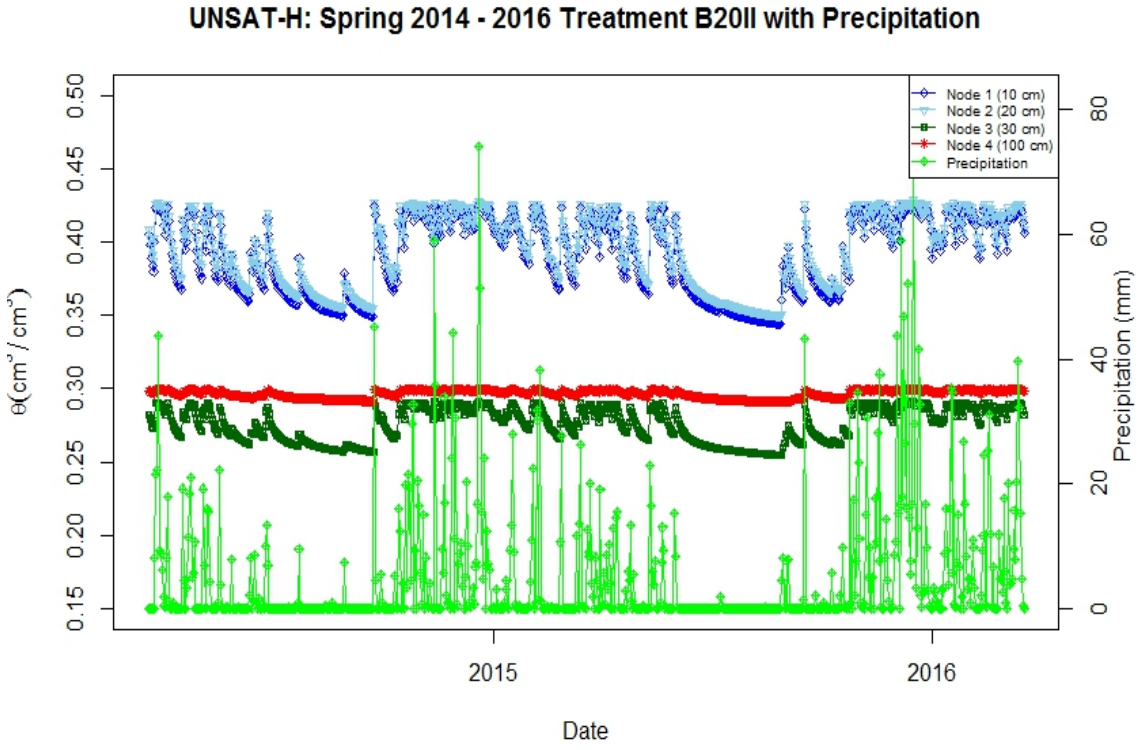

Figure D.7 Treatment Plot B20II Volumetric Water Content with Precipitation for 2-Year Simulation

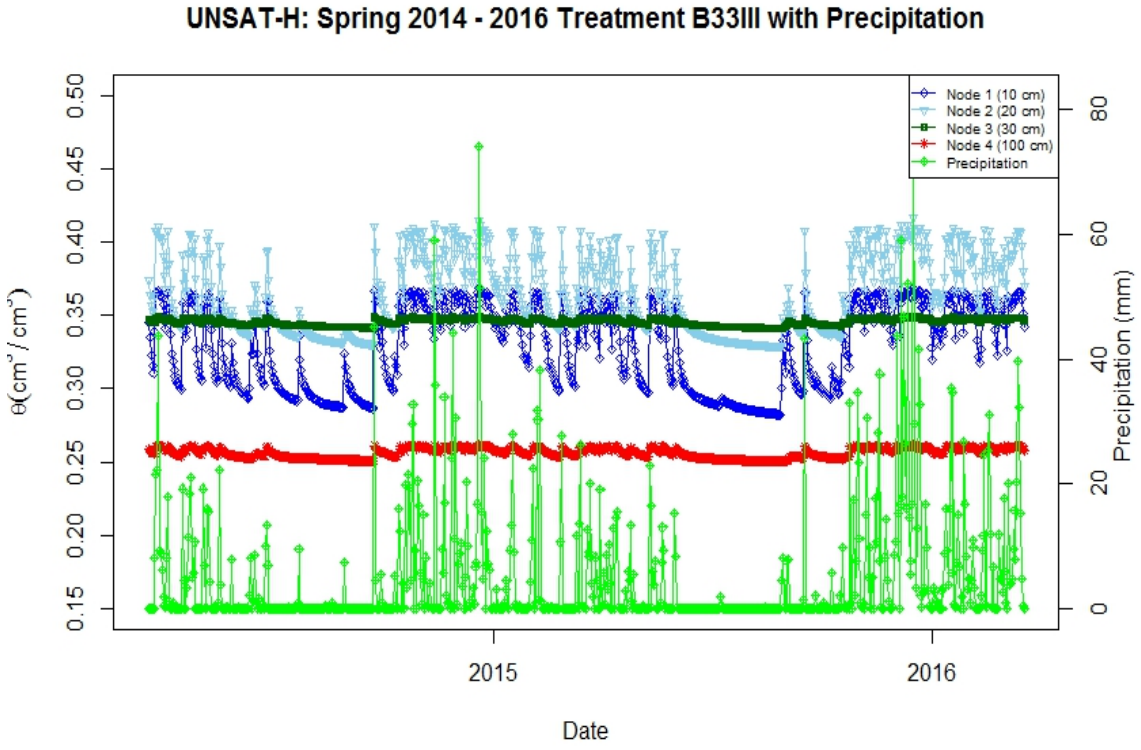

Figure D.8 Treatment Plot B33III Volumetric Water Content with Precipitation for 2-Year Simulation

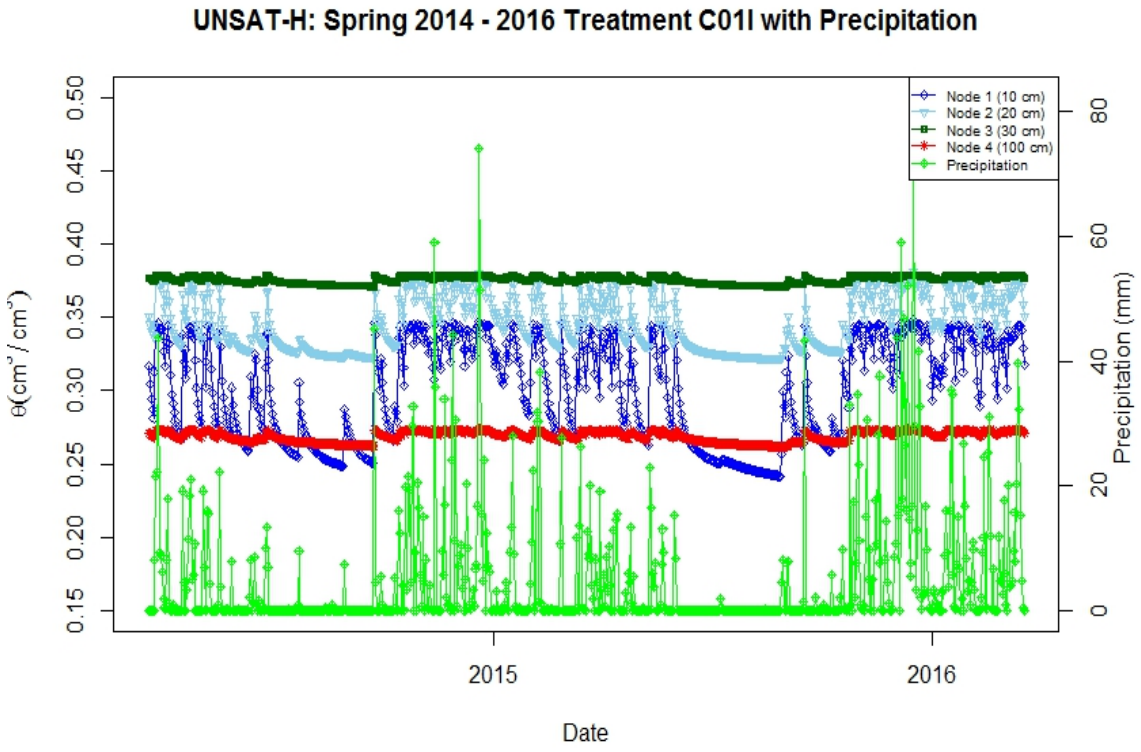

Figure D.9 Treatment Plot C01I Volumetric Water Content with Precipitation for 2-Year Simulation

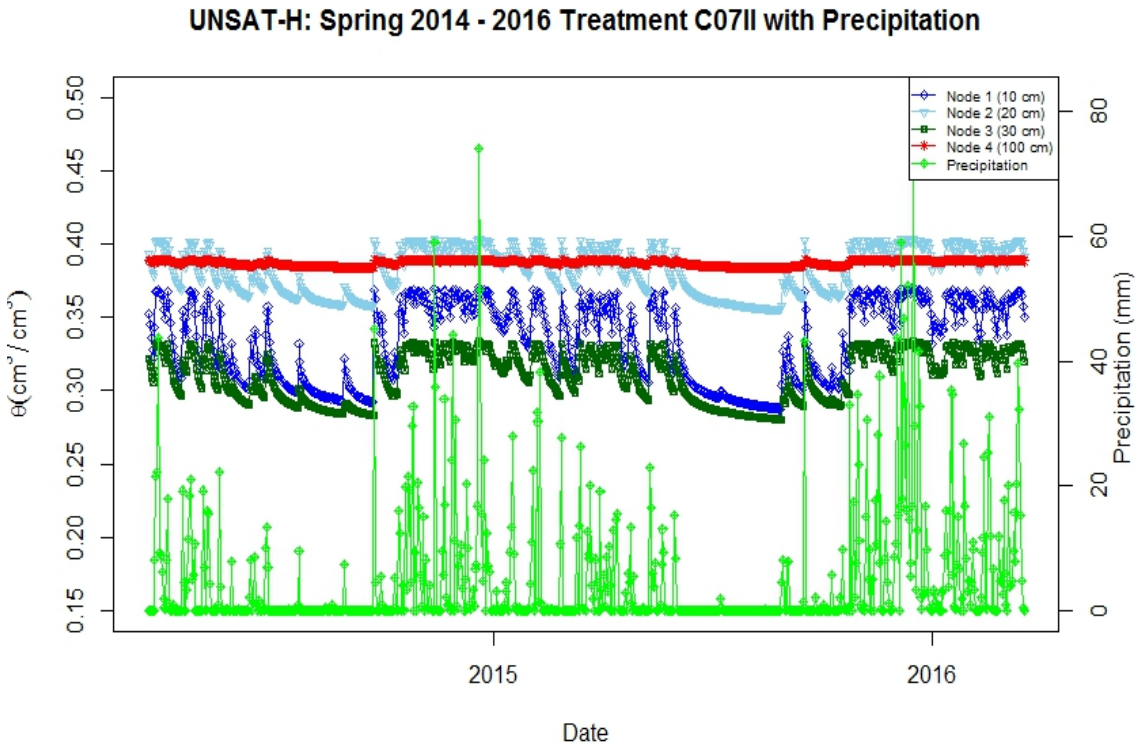

Figure D.10 Treatment Plot C07II Volumetric Water Content with Precipitation for 2-Year Simulation

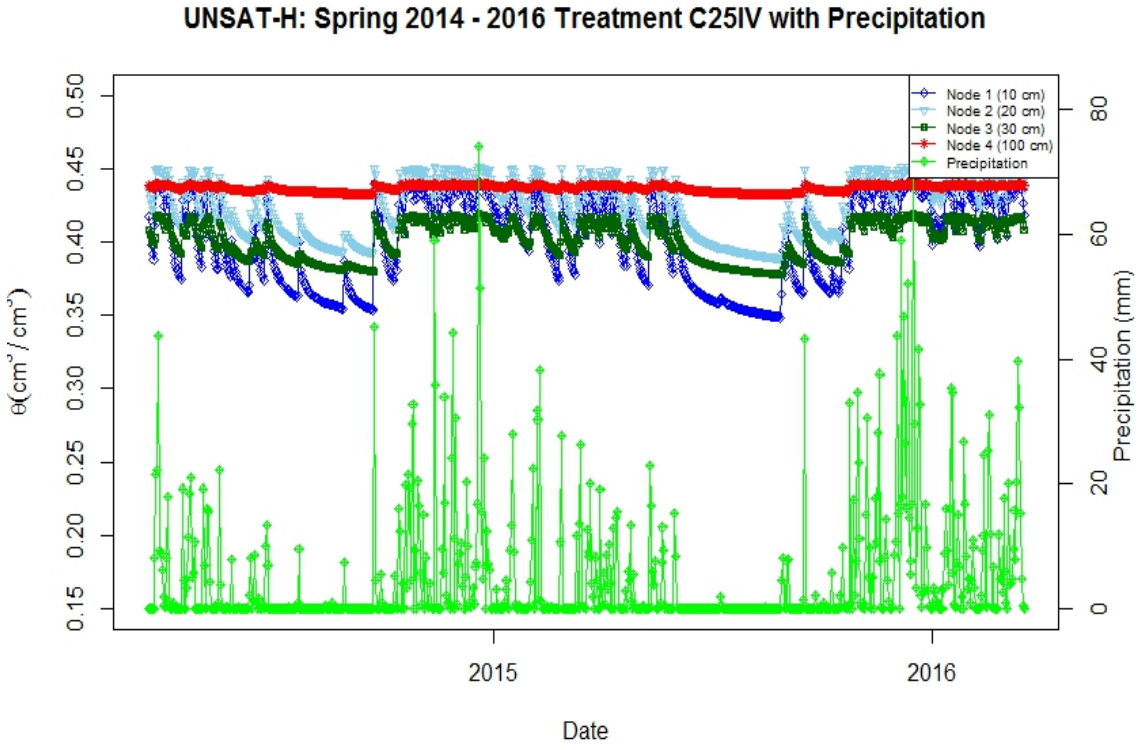

Figure D.11 Treatment Plot C25IV Volumetric Water Content with Precipitation for 2-Year Simulation

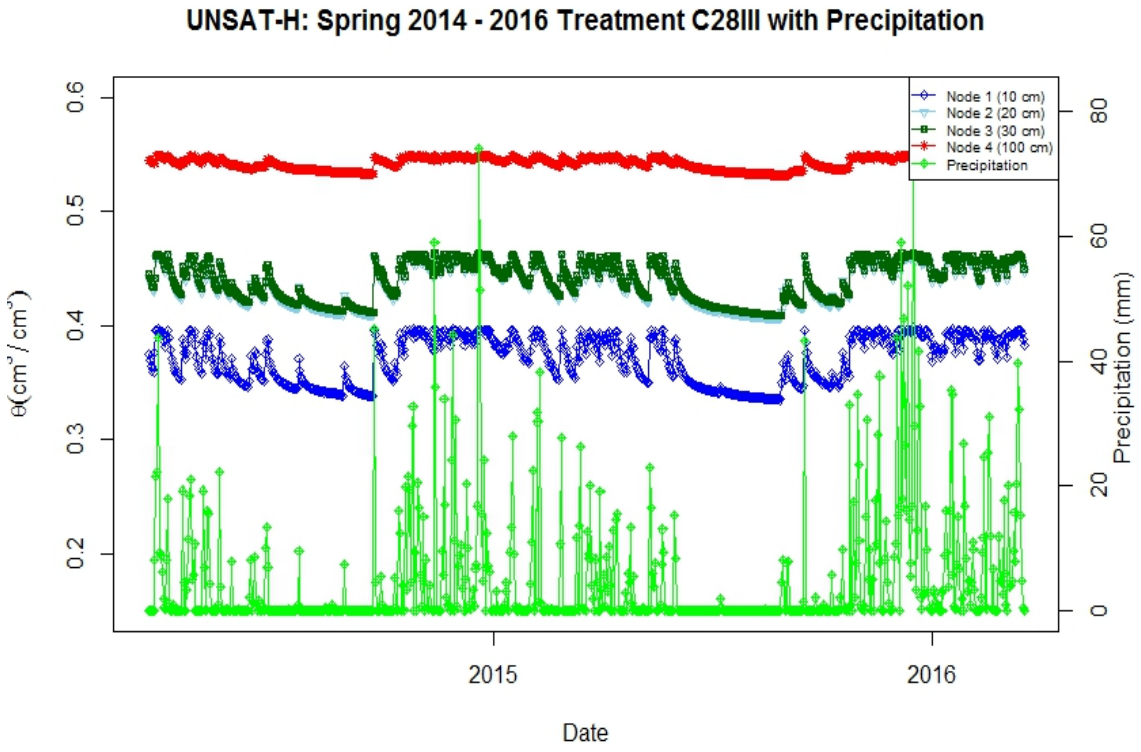

Figure D.12 Treatment Plot C28III Volumetric Water Content with Precipitation for 2-Year Simulation

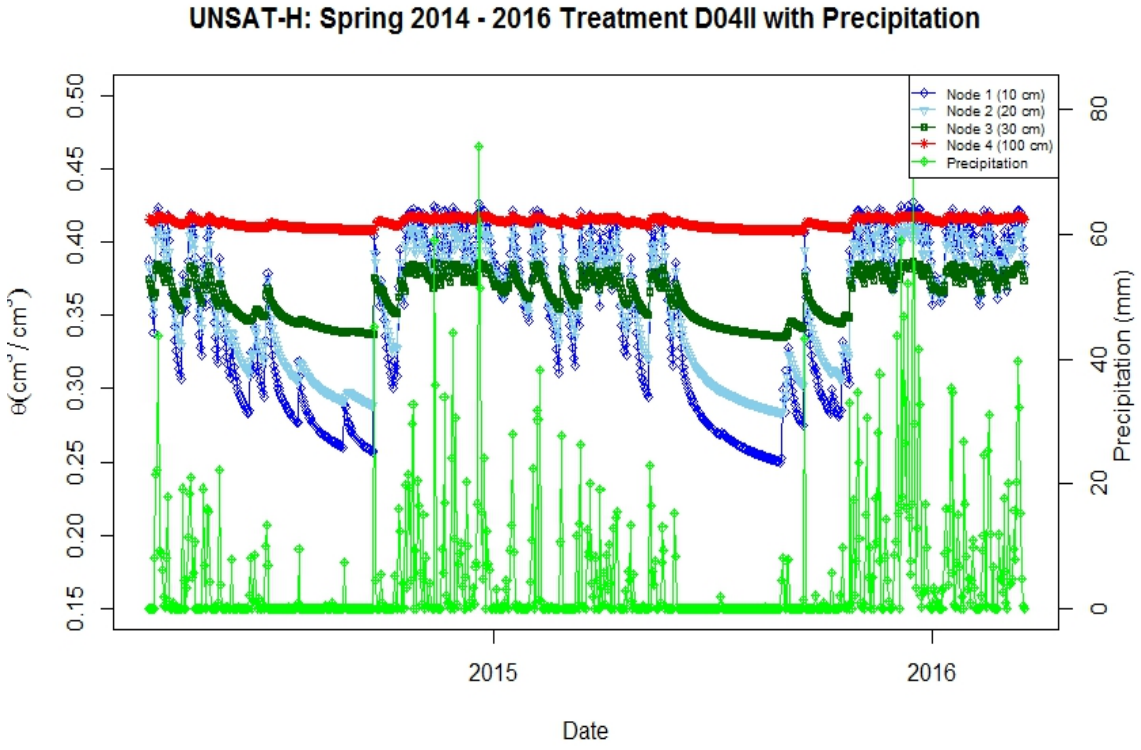

Figure D.13 Treatment Plot D04II Volumetric Water Content with Precipitation for 2-Year Simulation

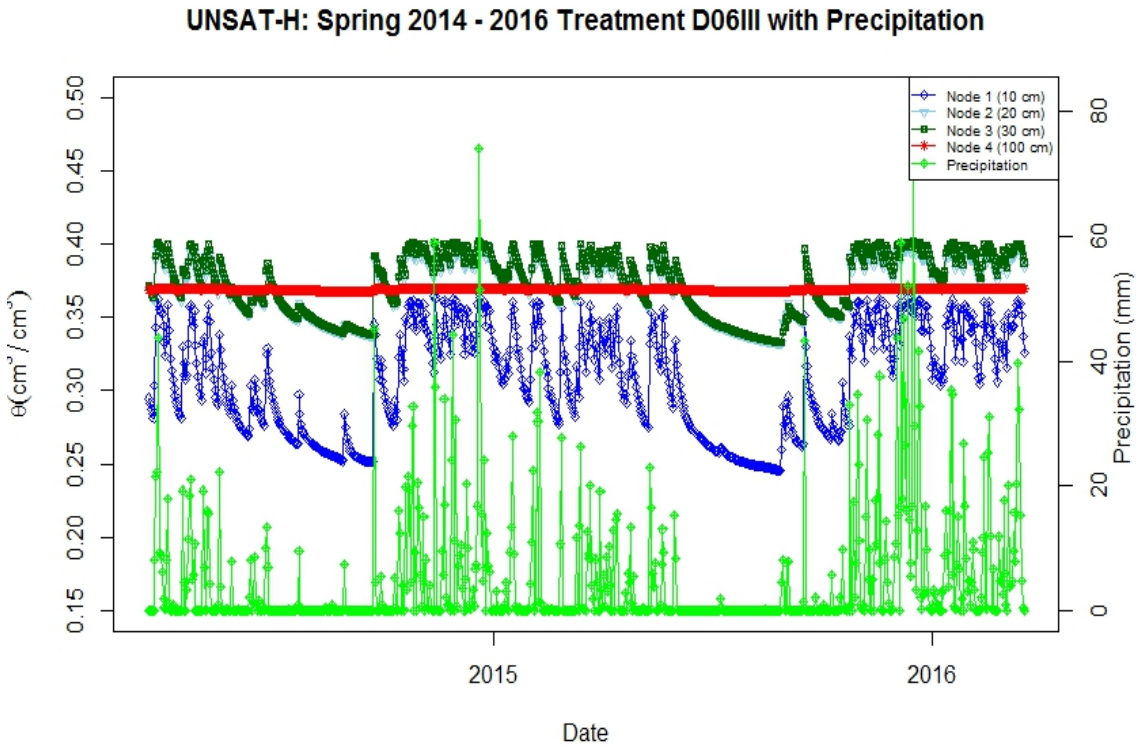

Figure D.14 Treatment Plot D06III Volumetric Water Content with Precipitation for 2-Year Simulation

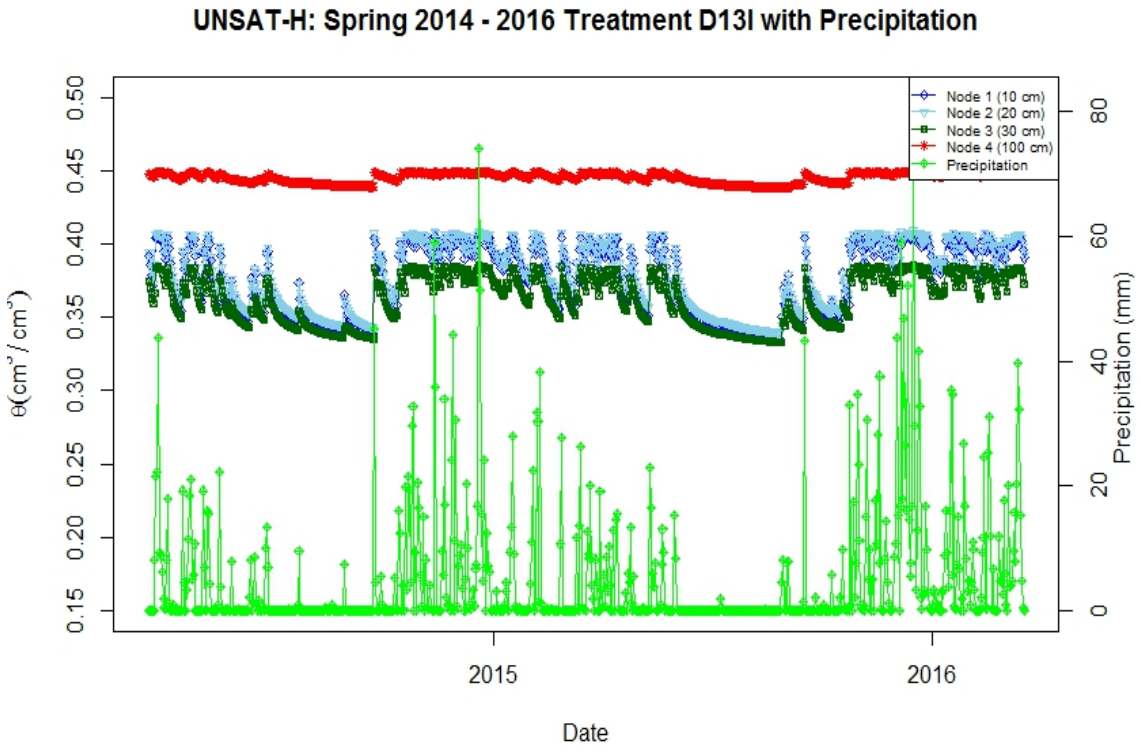

Figure D.15 Treatment Plot D13I Volumetric Water Content with Precipitation for 2-Year Simulation

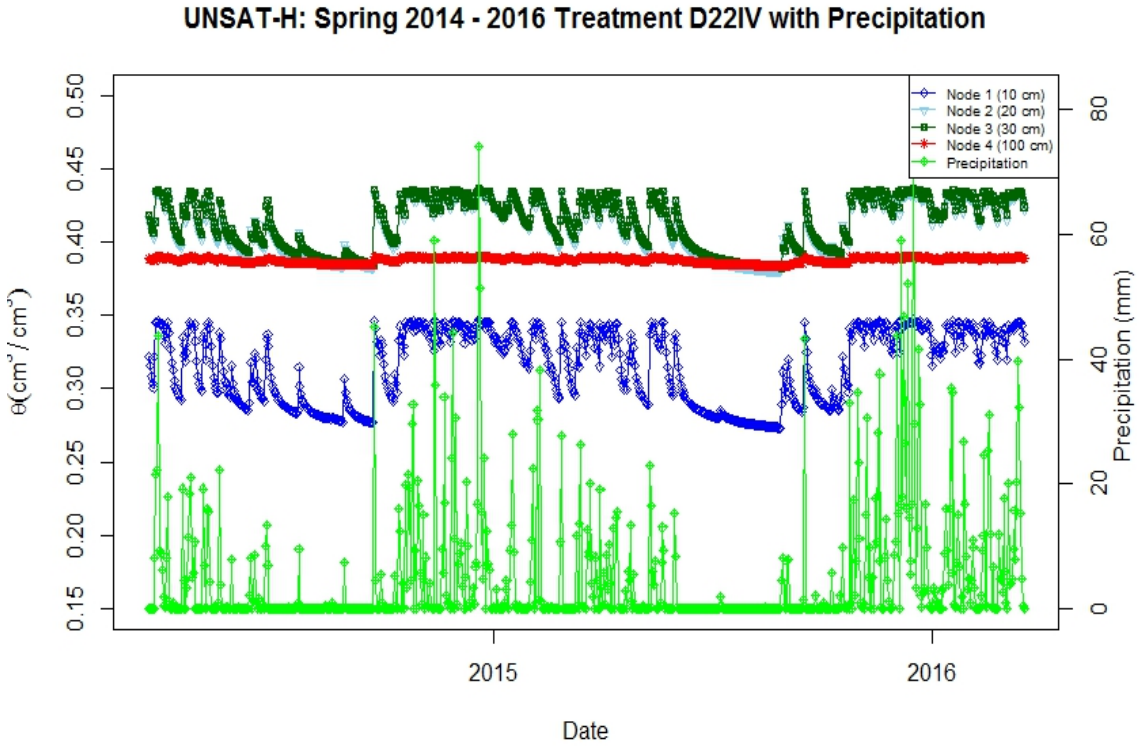

Figure D.16 Treatment Plot D22IV Volumetric Water Content with Precipitation for 2-Year Simulation

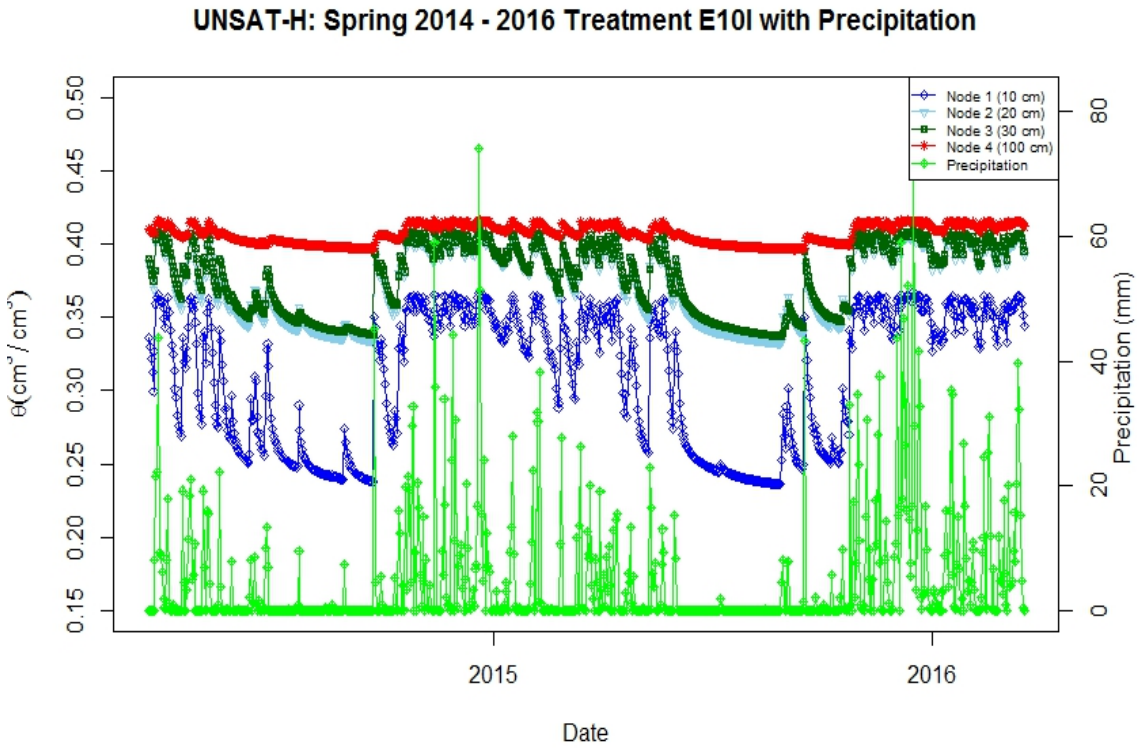

Figure D.17 Treatment Plot E10I Volumetric Water Content with Precipitation for 2-Year Simulation

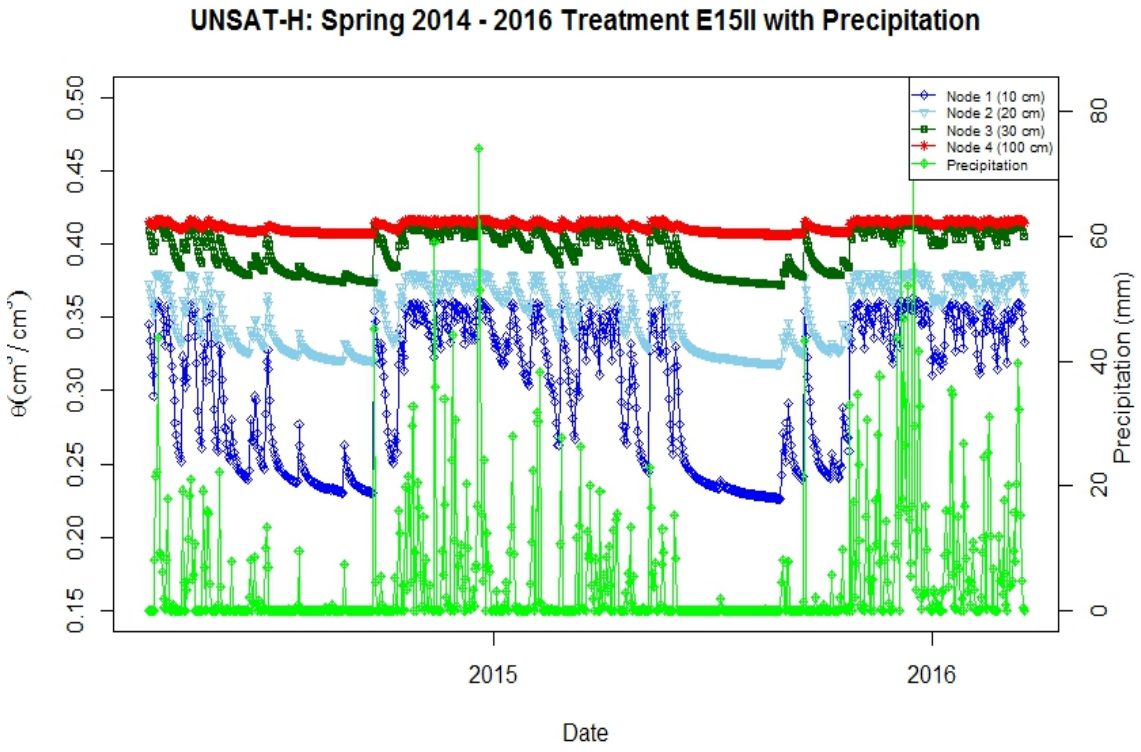

Figure D.18 Treatment Plot E15II Volumetric Water Content with Precipitation for 2-Year Simulation

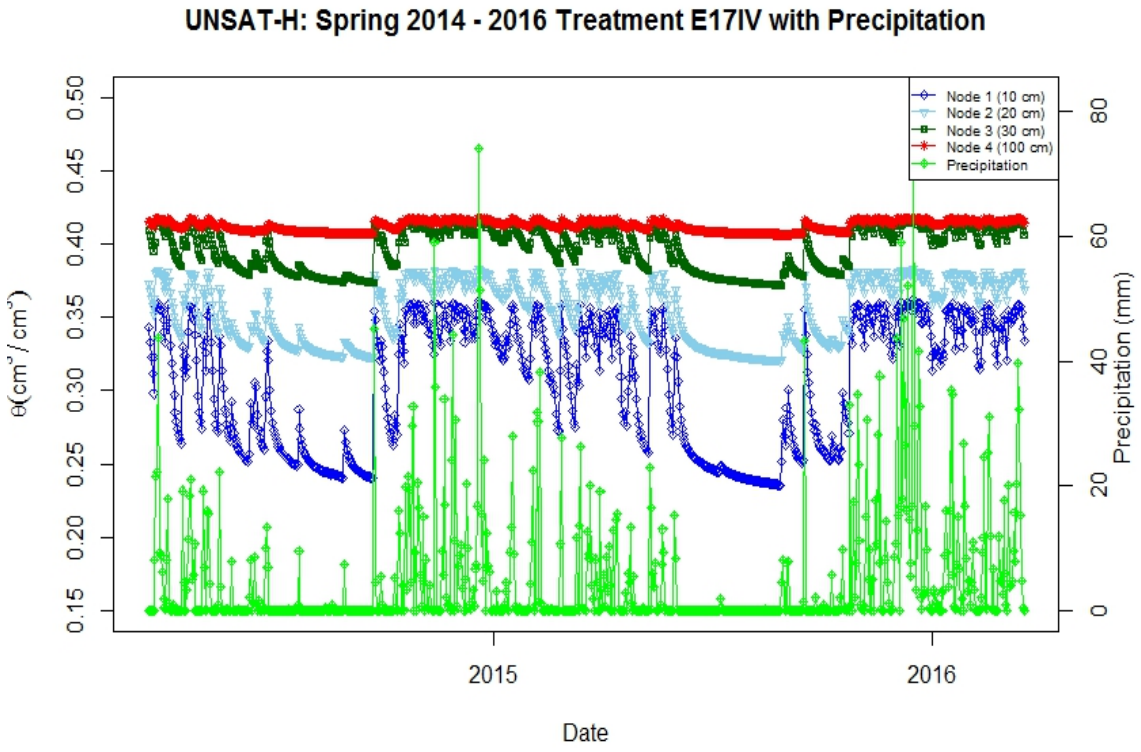

Figure D.19 Treatment Plot E17IV Volumetric Water Content with Precipitation for 2-Year Simulation

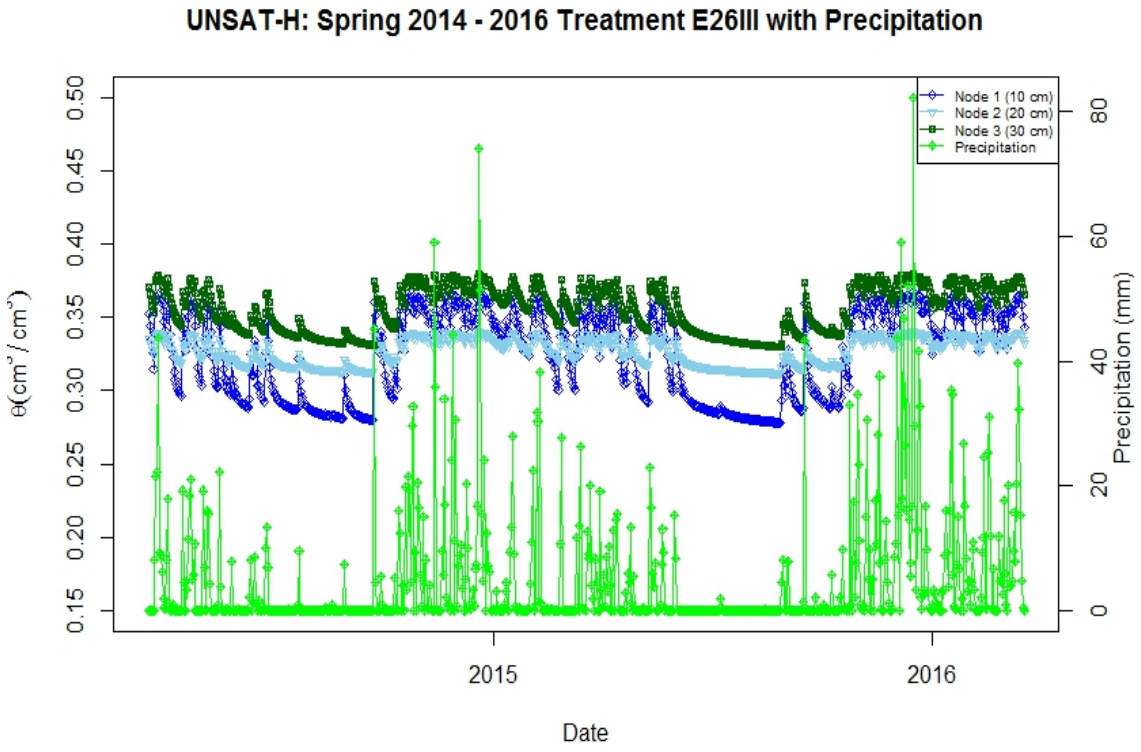

Figure D.20 Treatment Plot E26III Volumetric Water Content with Precipitation for 2-Year Simulation

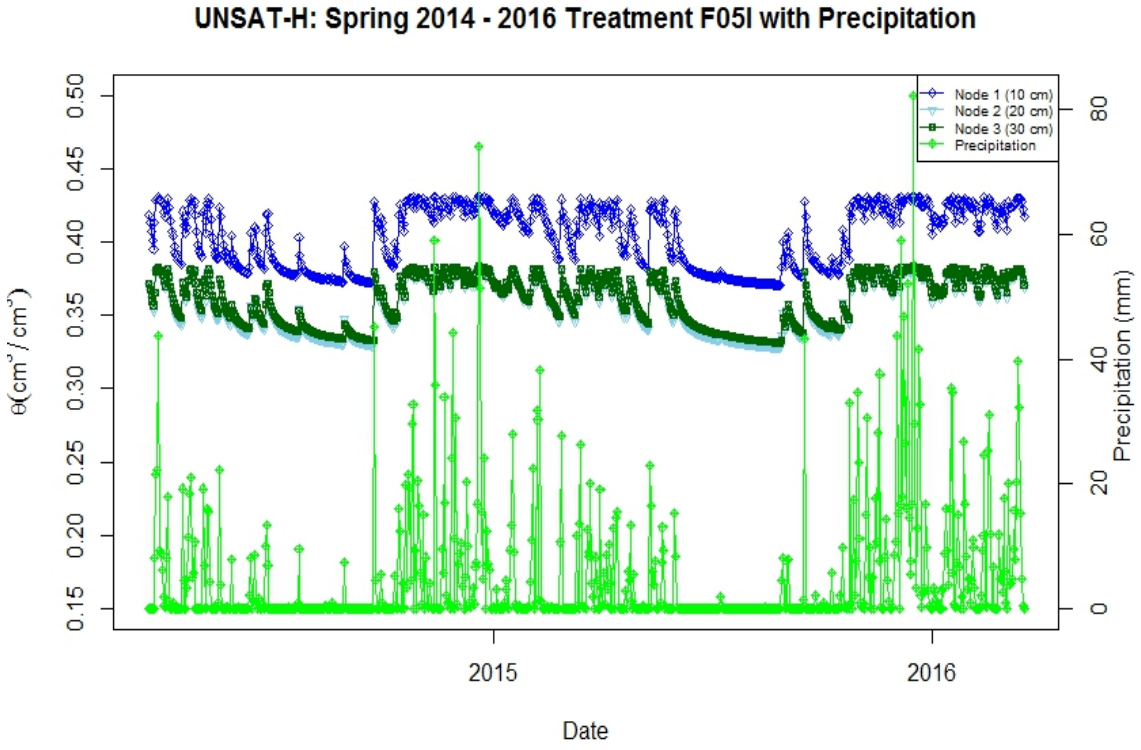

Figure D.21 Treatment Plot F05I Volumetric Water Content with Precipitation for 2-Year Simulation

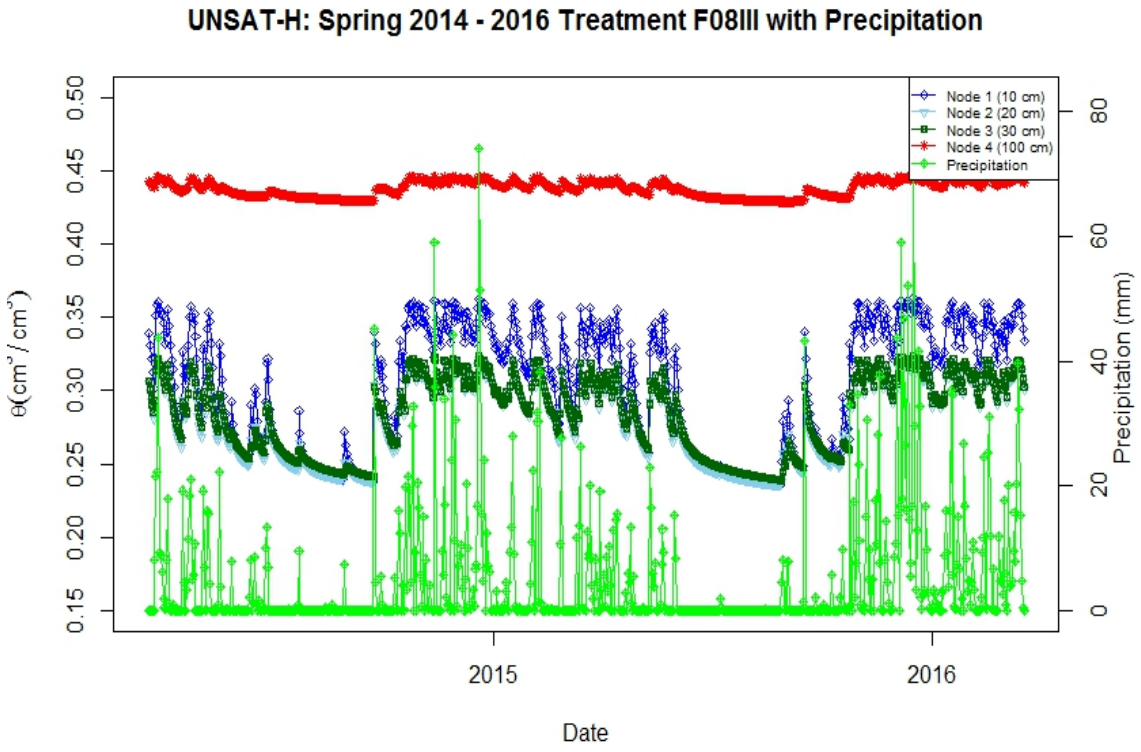

Figure D.22 Treatment Plot F08III Volumetric Water Content with Precipitation for 2-Year Simulation

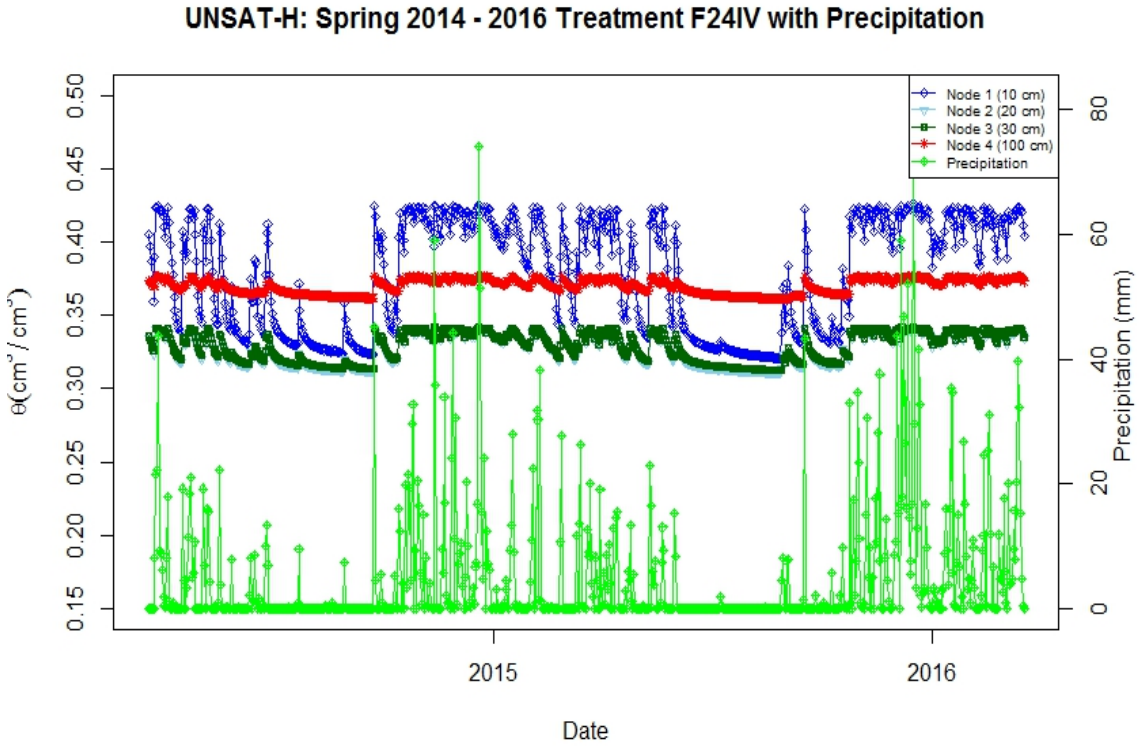

Figure D.23 Treatment Plot F24IV Volumetric Water Content with Precipitation for 2-Year Simulation

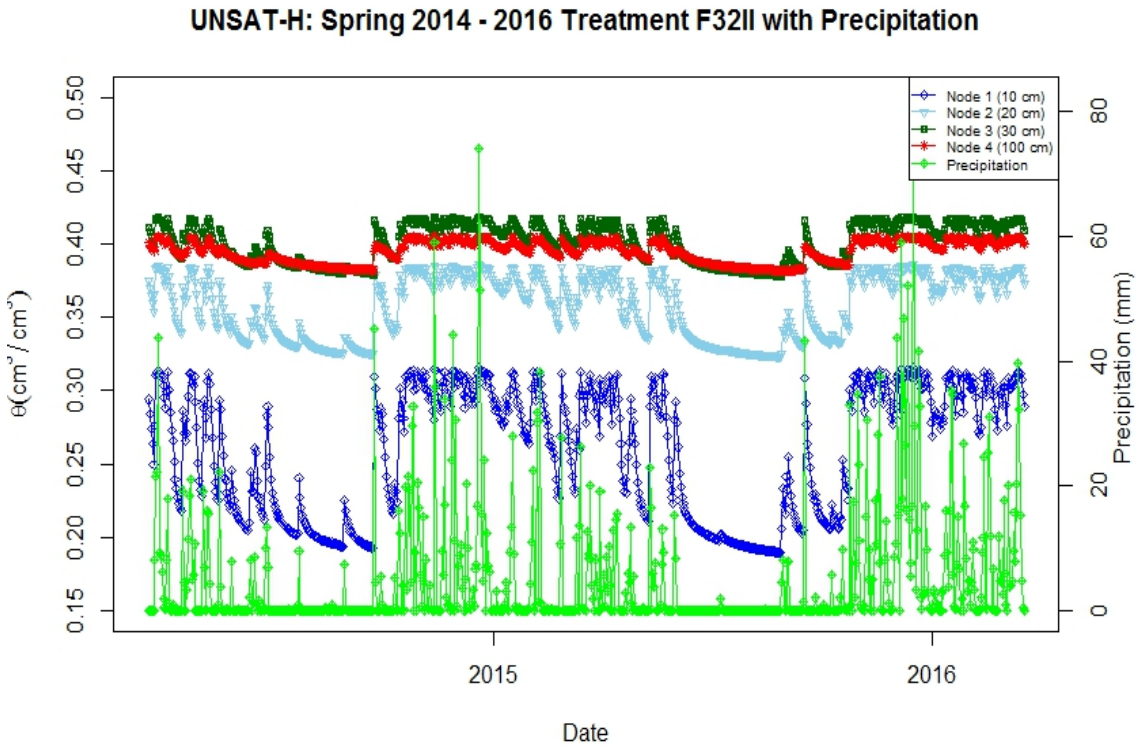

Figure D.24 Treatment Plot F32II Volumetric Water Content with Precipitation for 2-Year Simulation

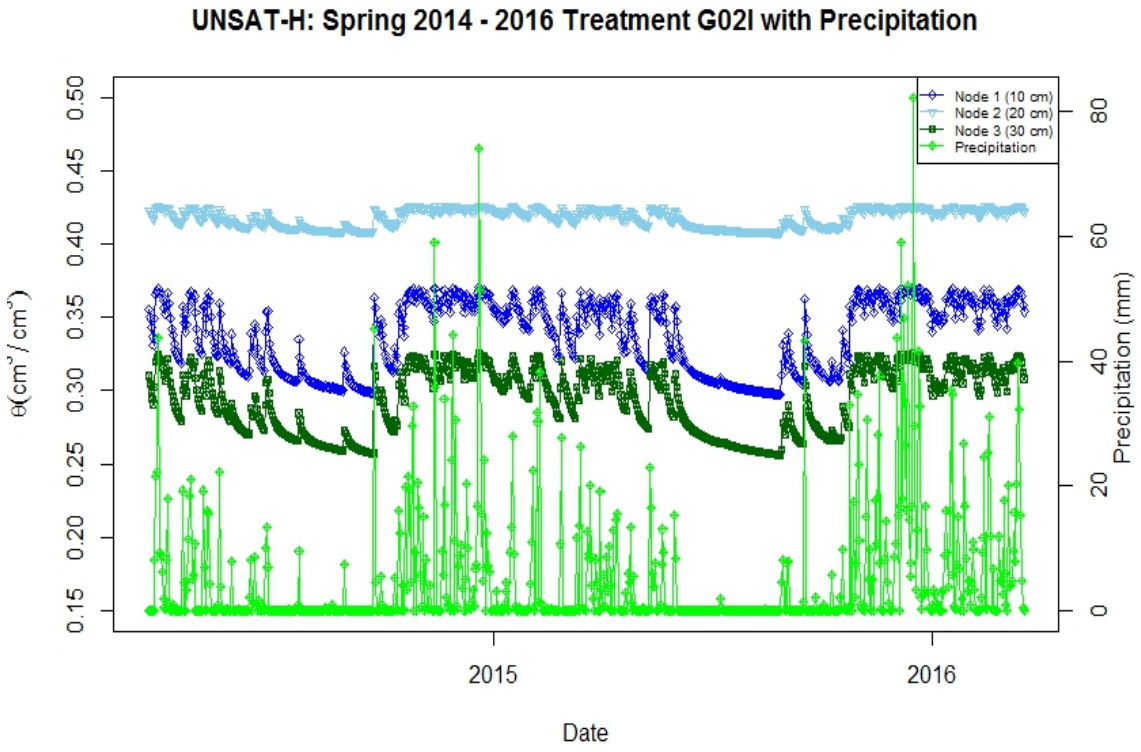

Figure D.25 Treatment Plot G02I Volumetric Water Content with Precipitation for 2-Year Simulation

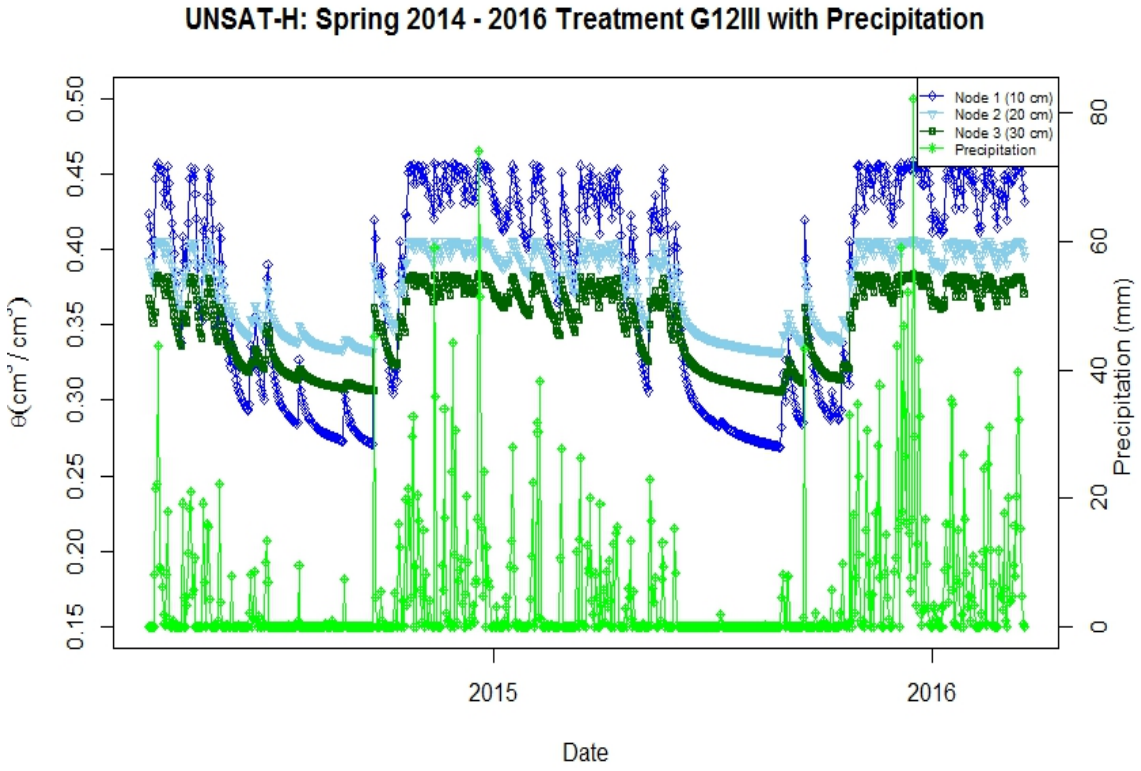

Figure D.26 Treatment Plot G12III Volumetric Water Content with Precipitation for 2-Year Simulation

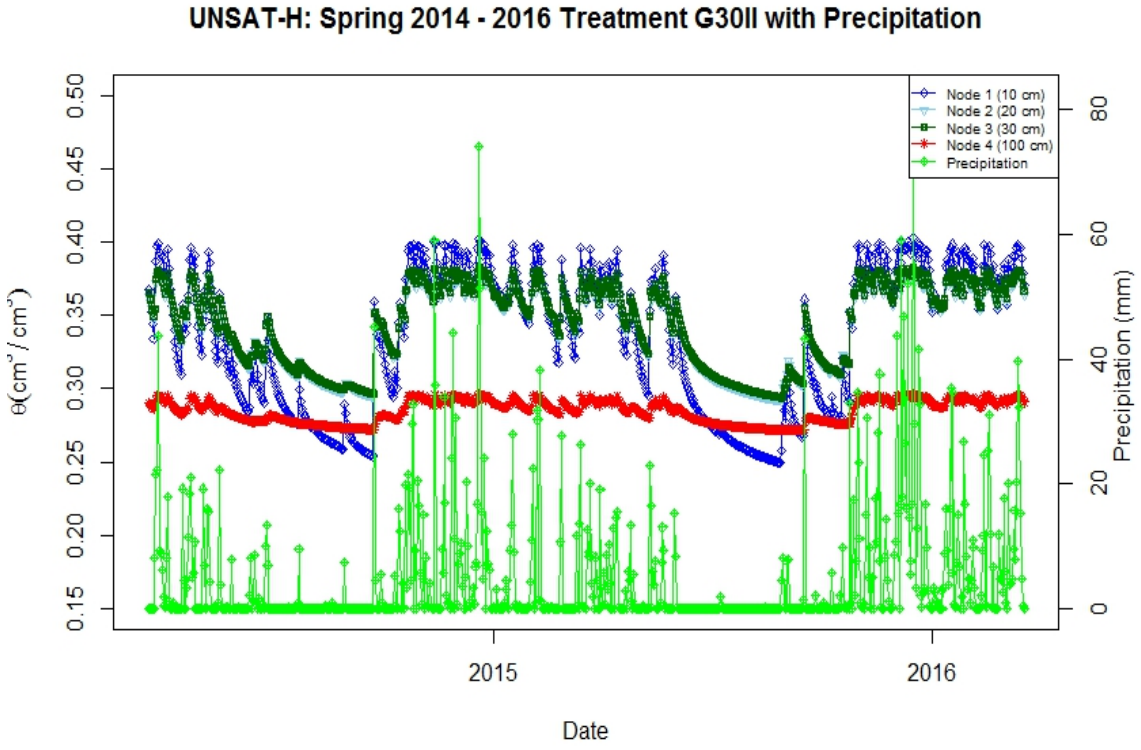

Figure D.27 Treatment Plot G30II Volumetric Water Content with Precipitation for 2-Year Simulation

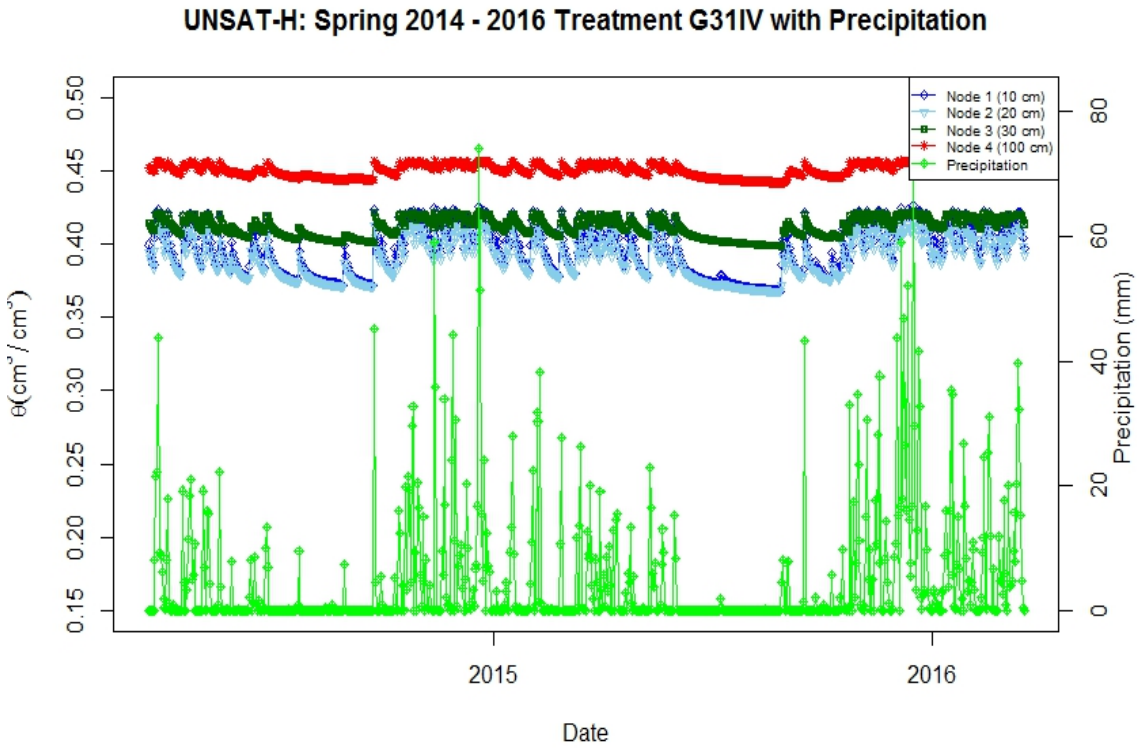

Figure D.28 Treatment Plot G31IV Volumetric Water Content with Precipitation for 2-Year Simulation

APPENDIX E

GRAPHICAL SUMMARIES OF DATATRAC WATER CONTENT MEASUREMENTS FOR TWO YEARS

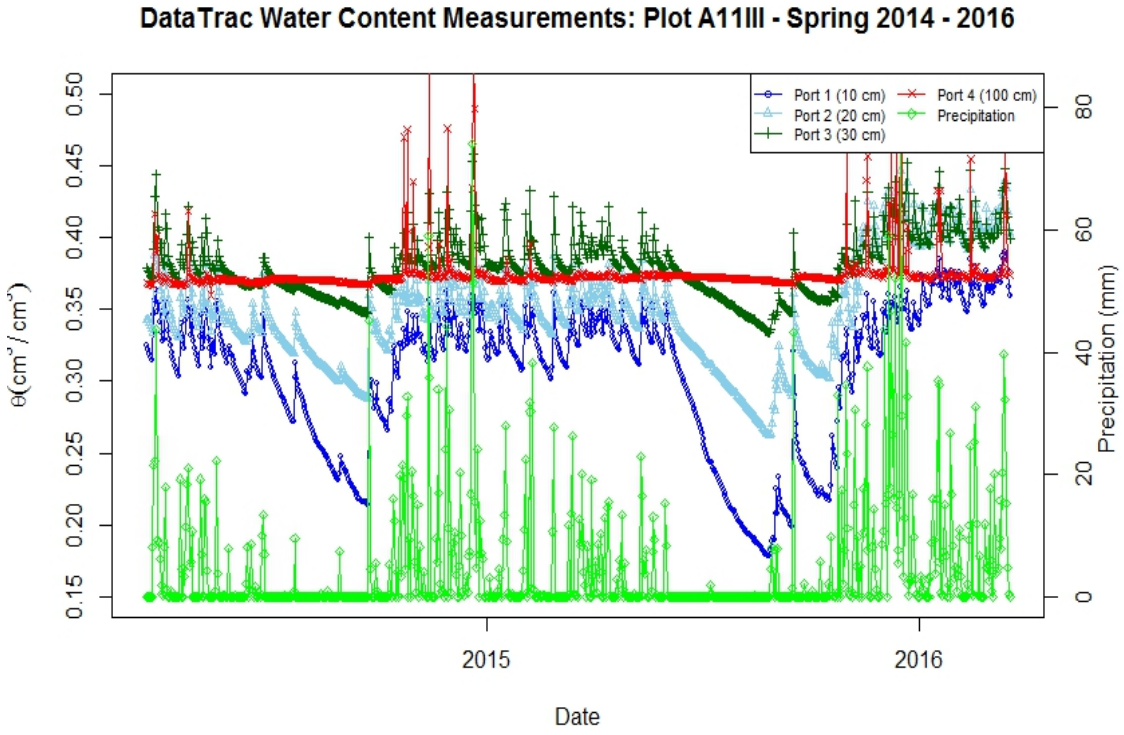

Figure E.1 DataTrac Plot A11III Volumetric Water Content with Precipitation for 2-Year Simulation

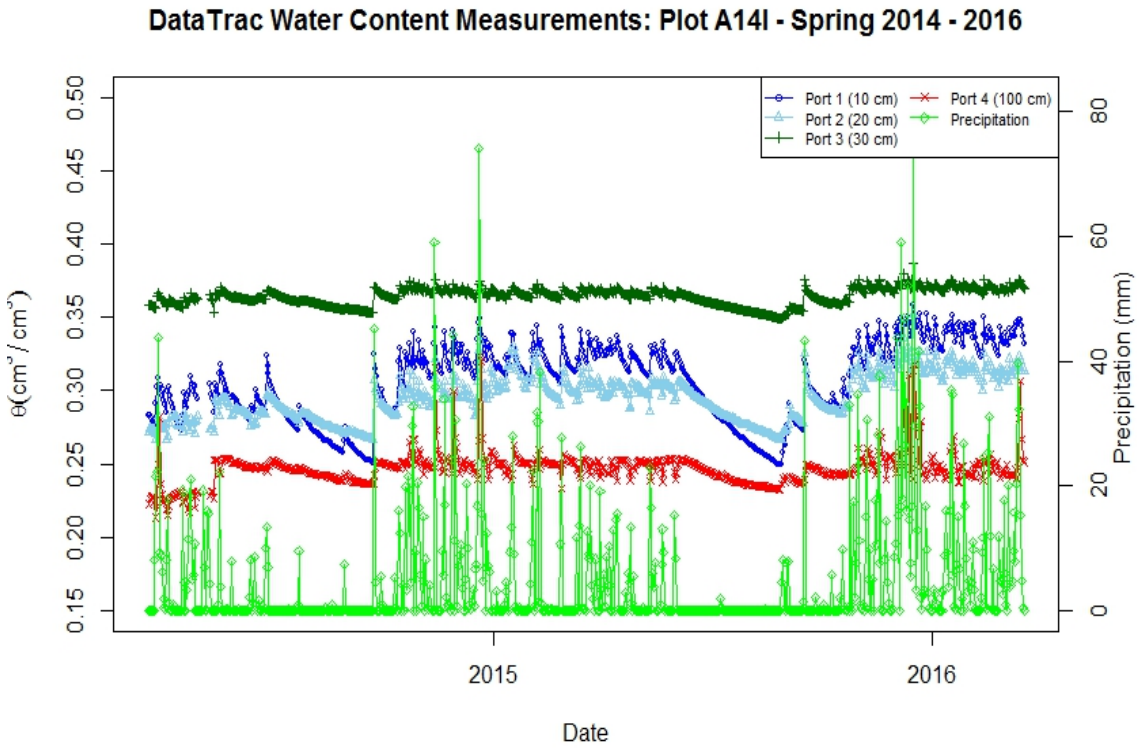

Figure E.2 DataTrac Plot A14I Volumetric Water Content with Precipitation for 2-Year Simulation

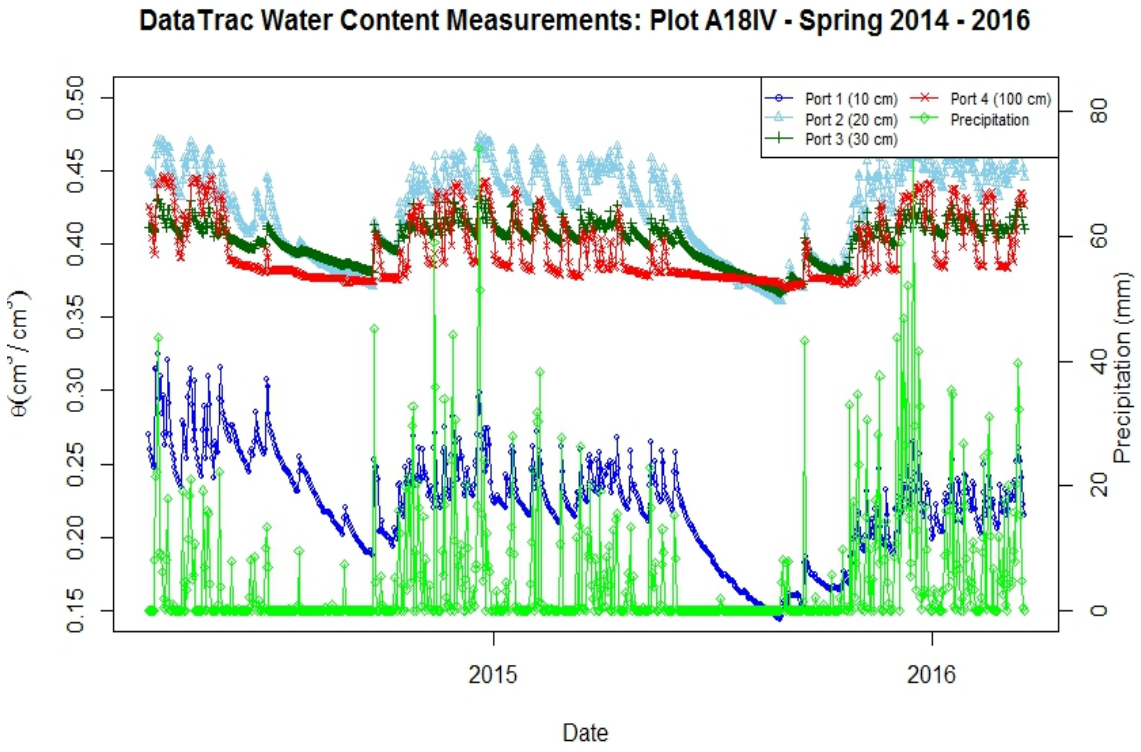

Figure E.3 DataTrac Plot A18IV Volumetric Water Content with Precipitation for 2-Year Simulation

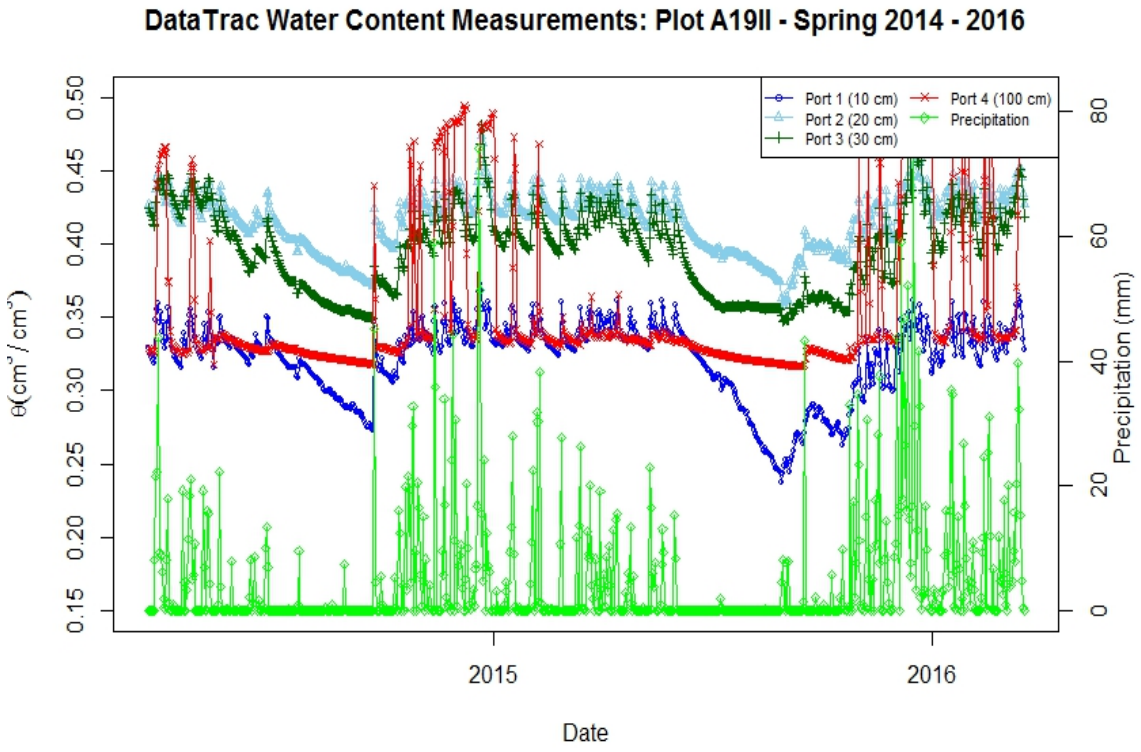

Figure E.4 DataTrac Plot A19II Volumetric Water Content with Precipitation for 2-Year Simulation

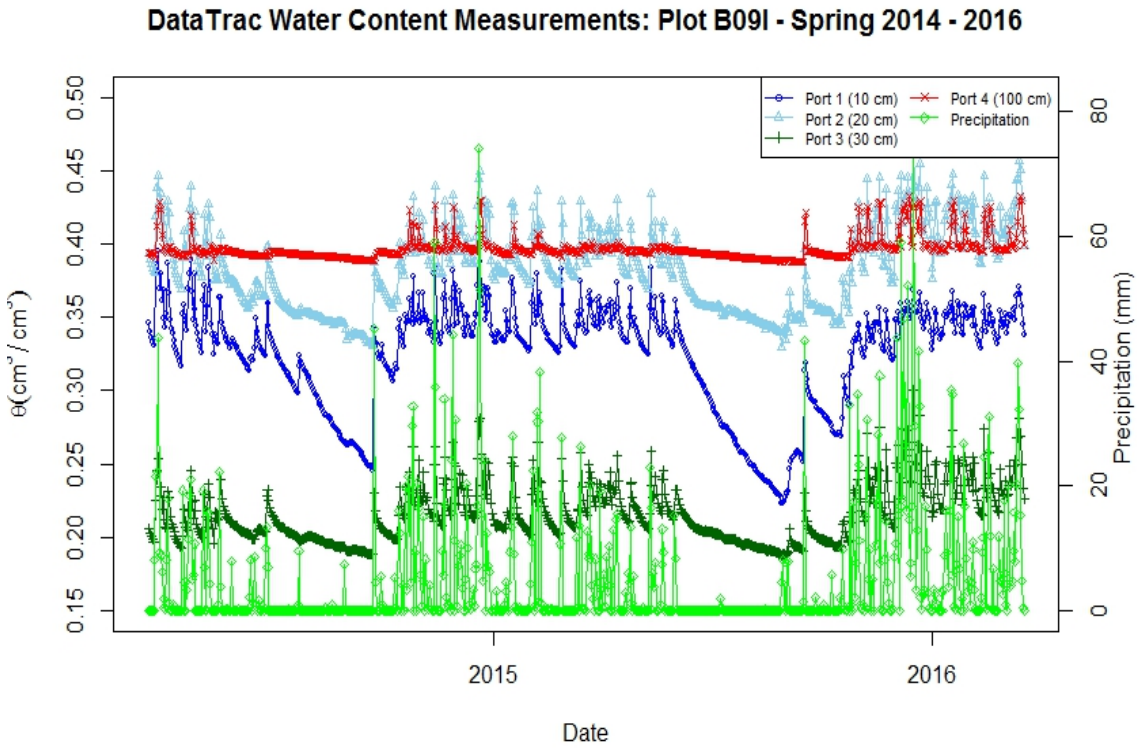

Figure E.5 DataTrac Plot B09I Volumetric Water Content with Precipitation for 2-Year Simulation

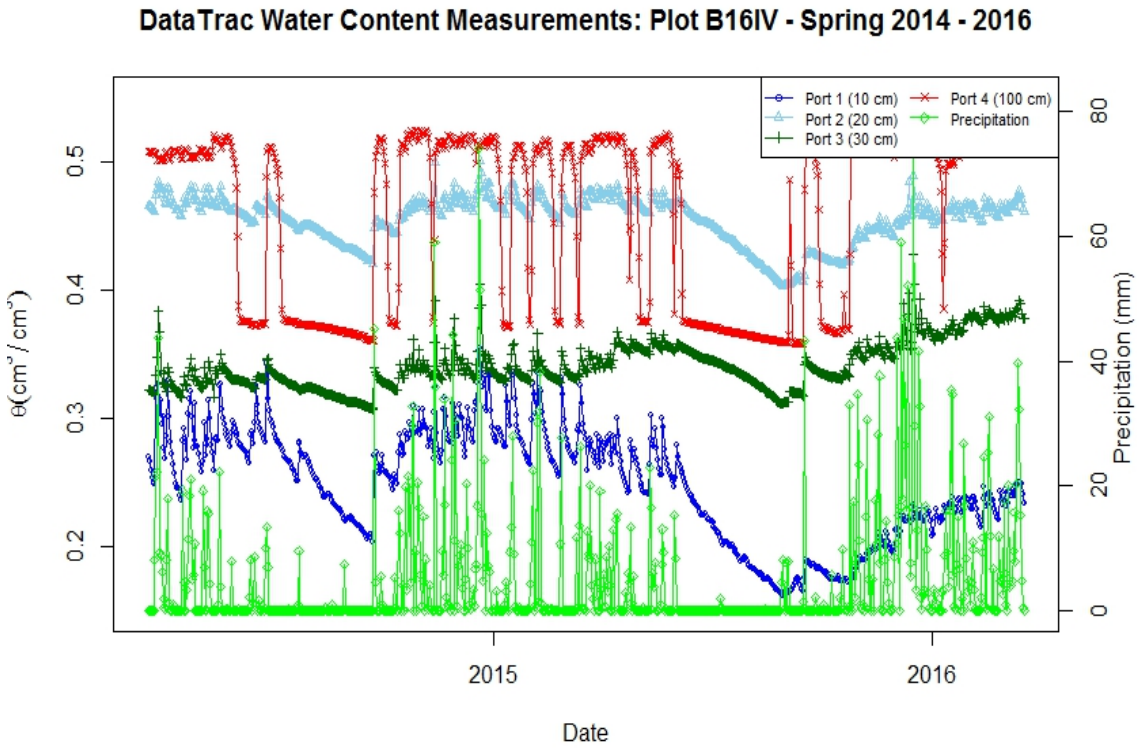

Figure E.6 DataTrac Plot B16IV Volumetric Water Content with Precipitation for 2-Year Simulation

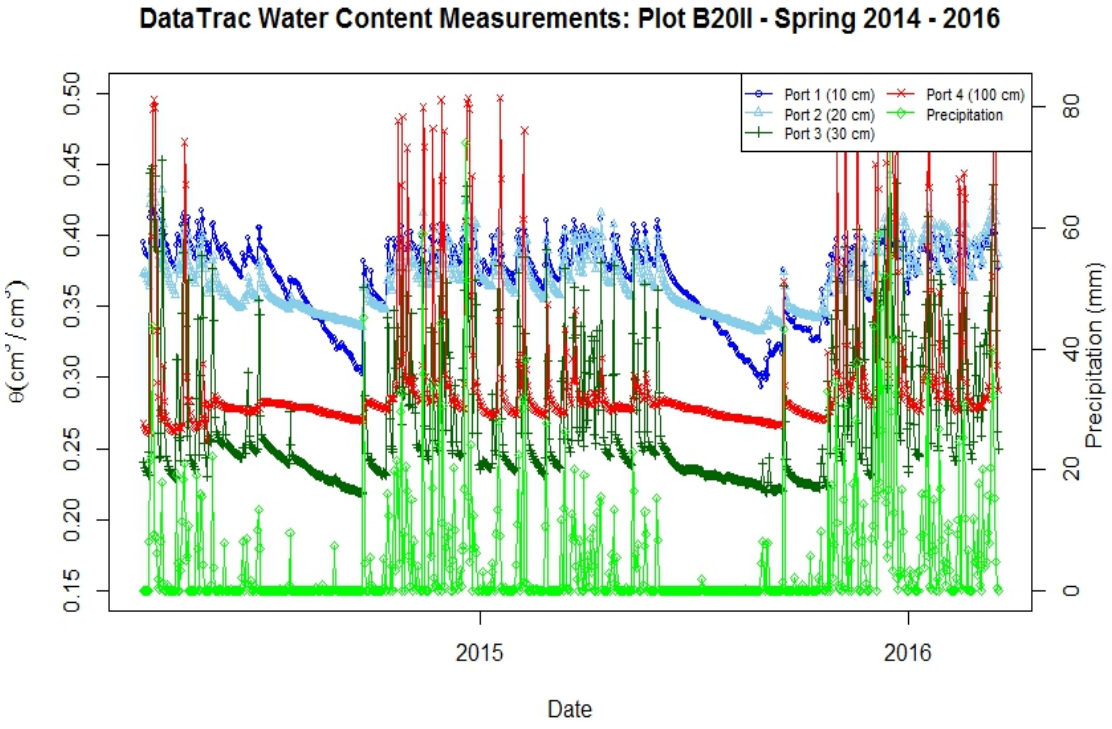

Figure E.7 DataTrac Plot B20II Volumetric Water Content with Precipitation for 2-Year Simulation

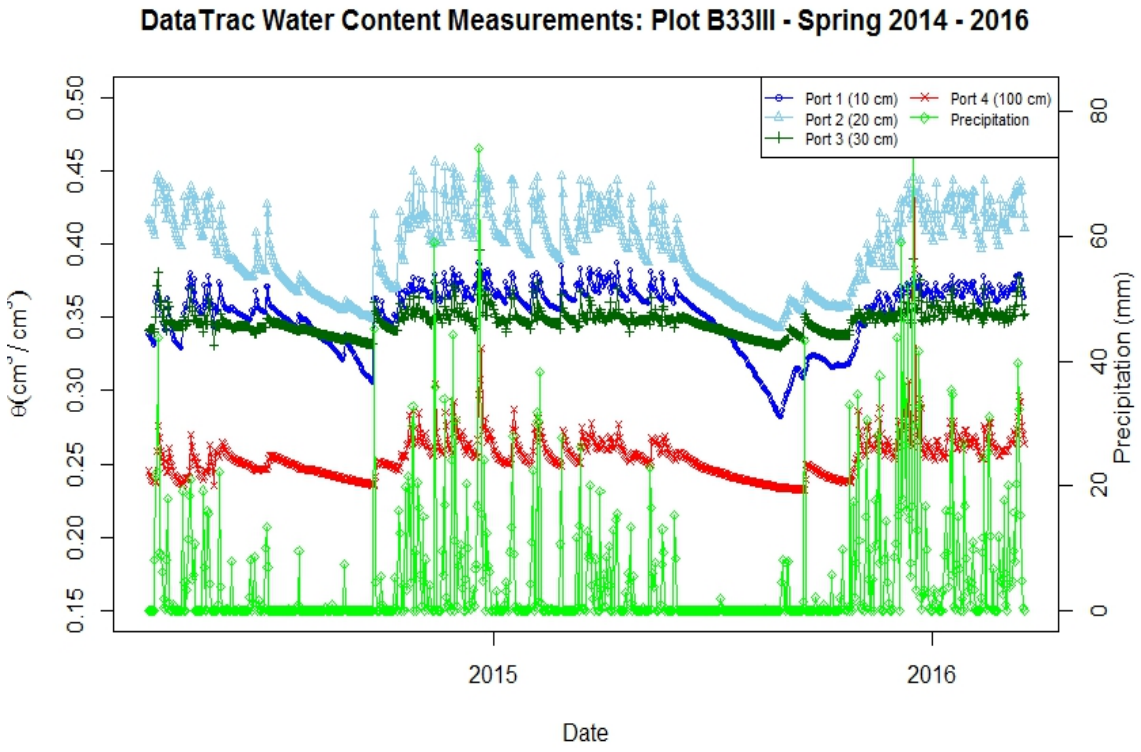

Figure E.8 DataTrac Plot B33III Volumetric Water Content with Precipitation for 2-Year Simulation

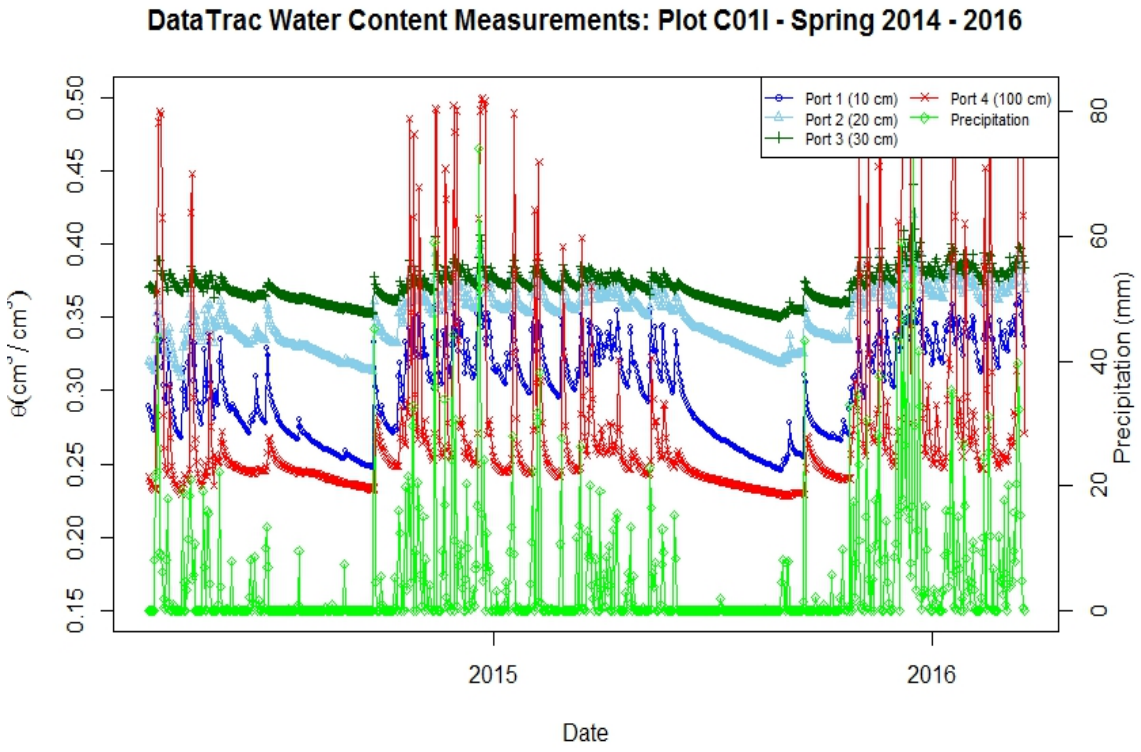

Figure E.9 DataTrac Plot C01I Volumetric Water Content with Precipitation for 2-Year Simulation

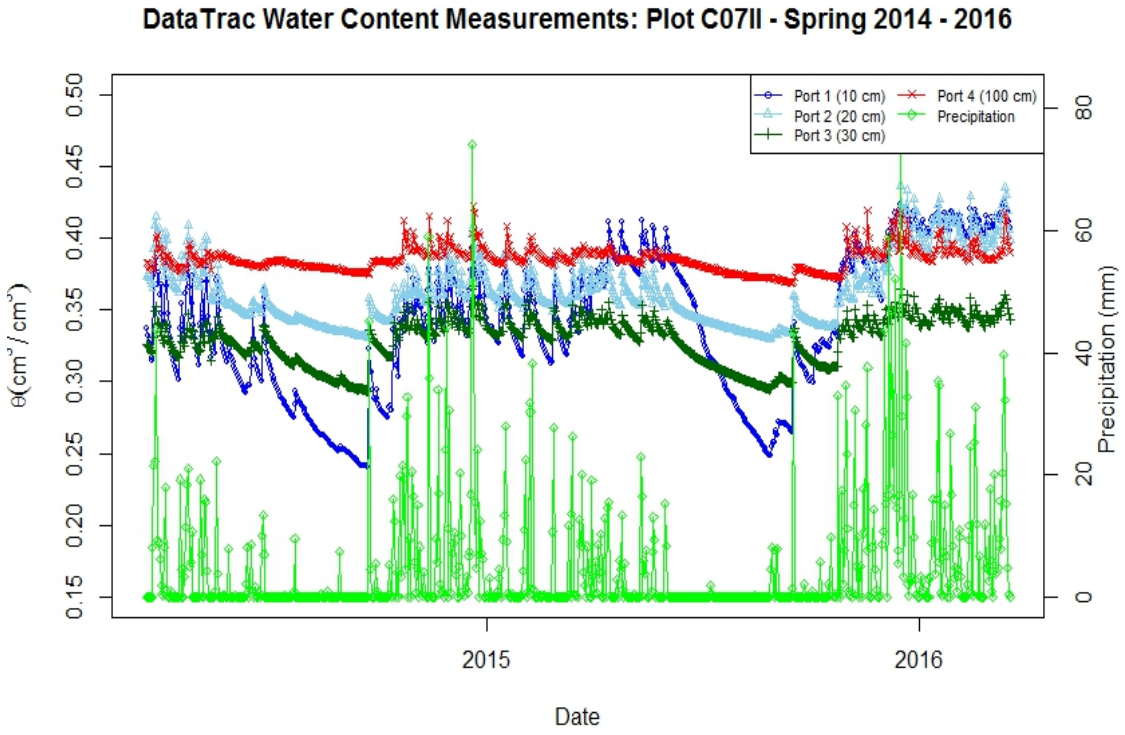

Figure E.10 DataTrac Plot C07II Volumetric Water Content with Precipitation for 2-Year Simulation

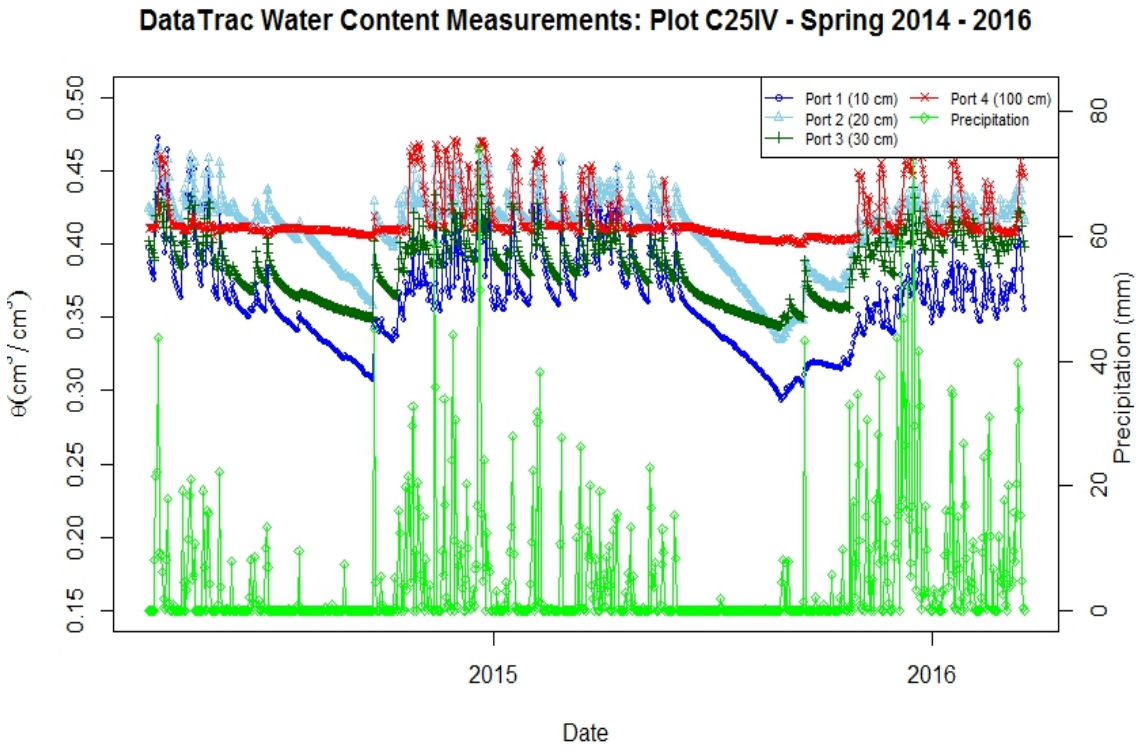

Figure E.11 DataTrac Plot C25IV Volumetric Water Content with Precipitation for 2-Year Simulation

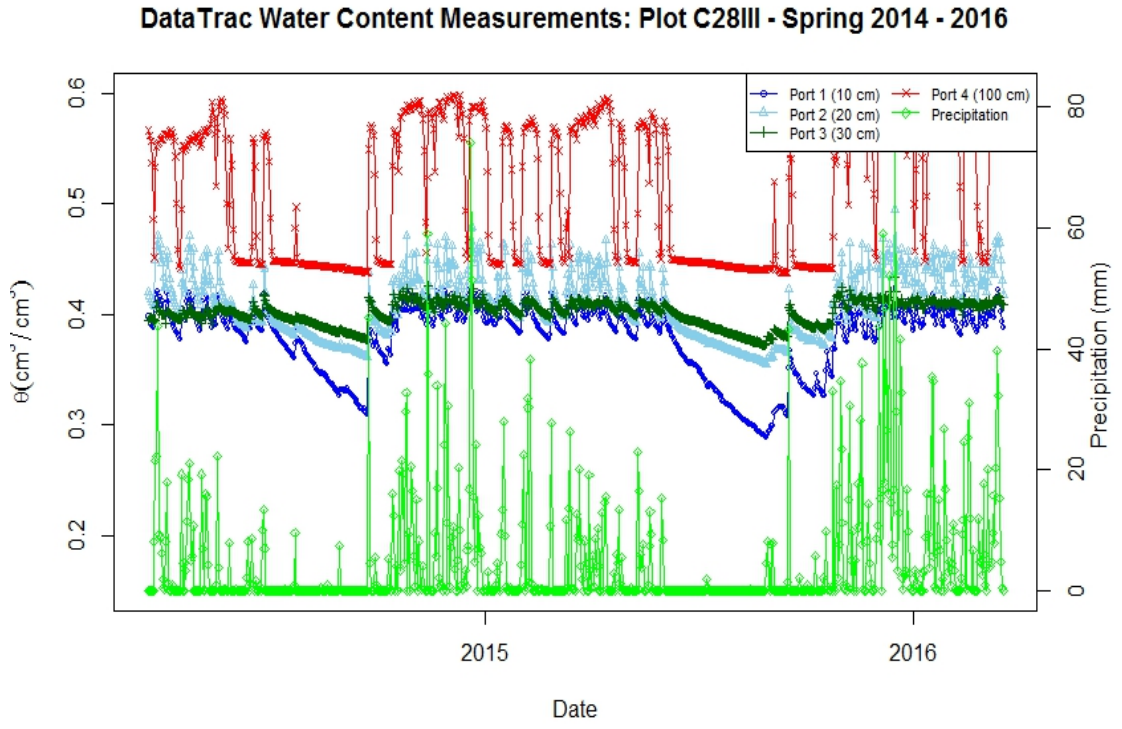

Figure E.12 DataTrac Plot C28III Volumetric Water Content with Precipitation for 2-Year Simulation

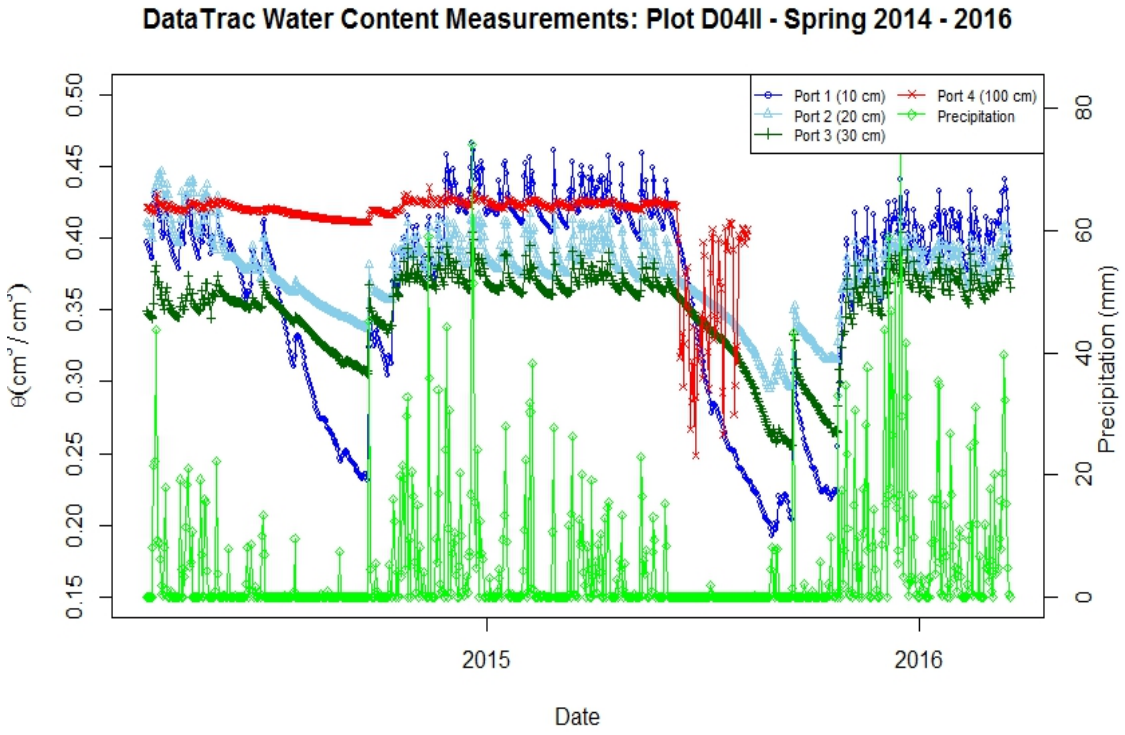

Figure E.13 DataTrac Plot D04II Volumetric Water Content with Precipitation for 2-Year Simulation

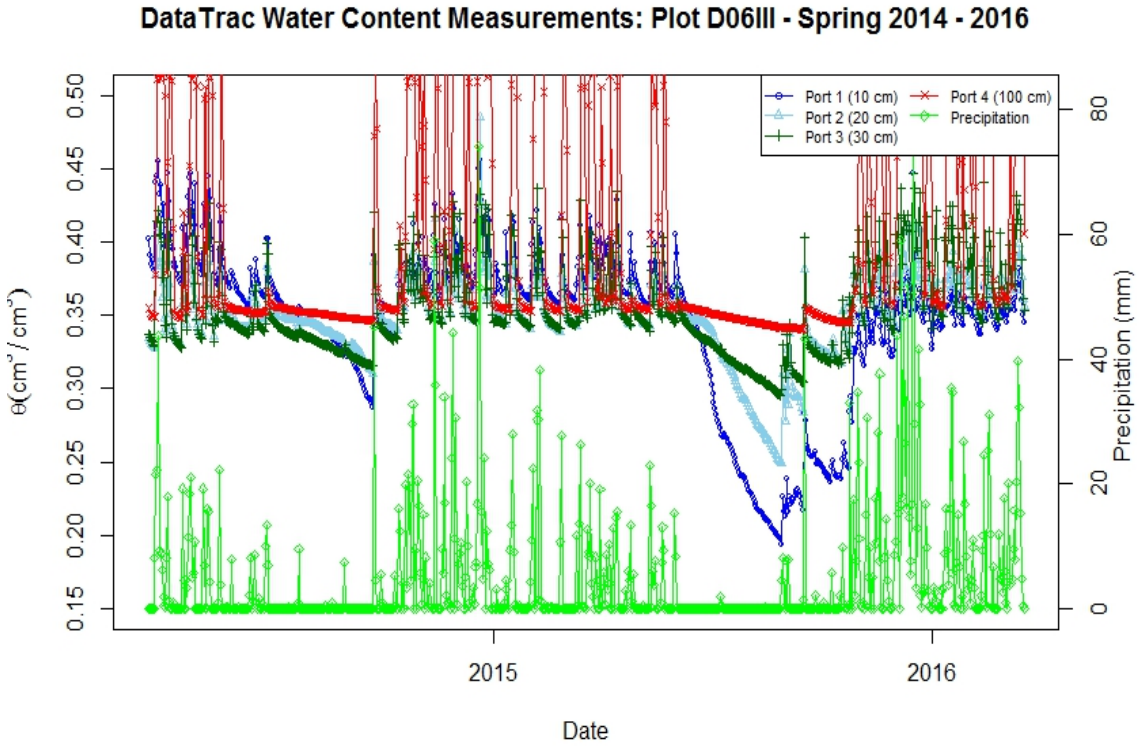

Figure E.14 DataTrac Plot D06III Volumetric Water Content with Precipitation for 2-Year Simulation

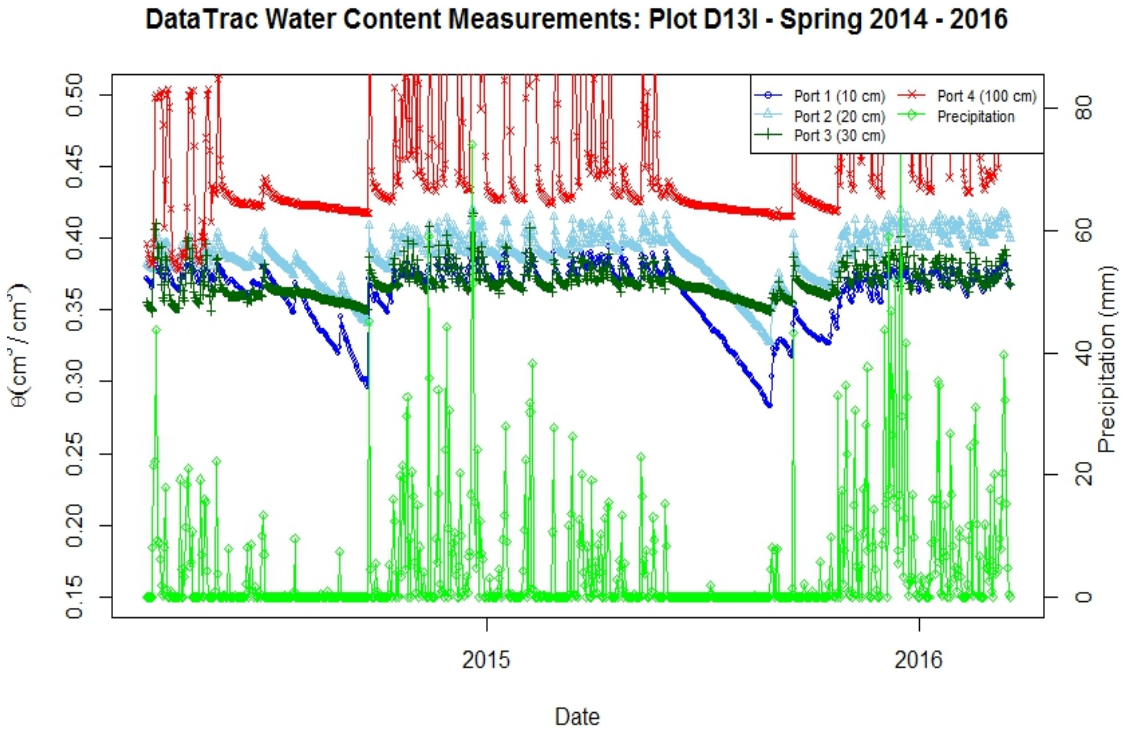

Figure E.15 DataTrac Plot D13I Volumetric Water Content with Precipitation for 2-Year Simulation

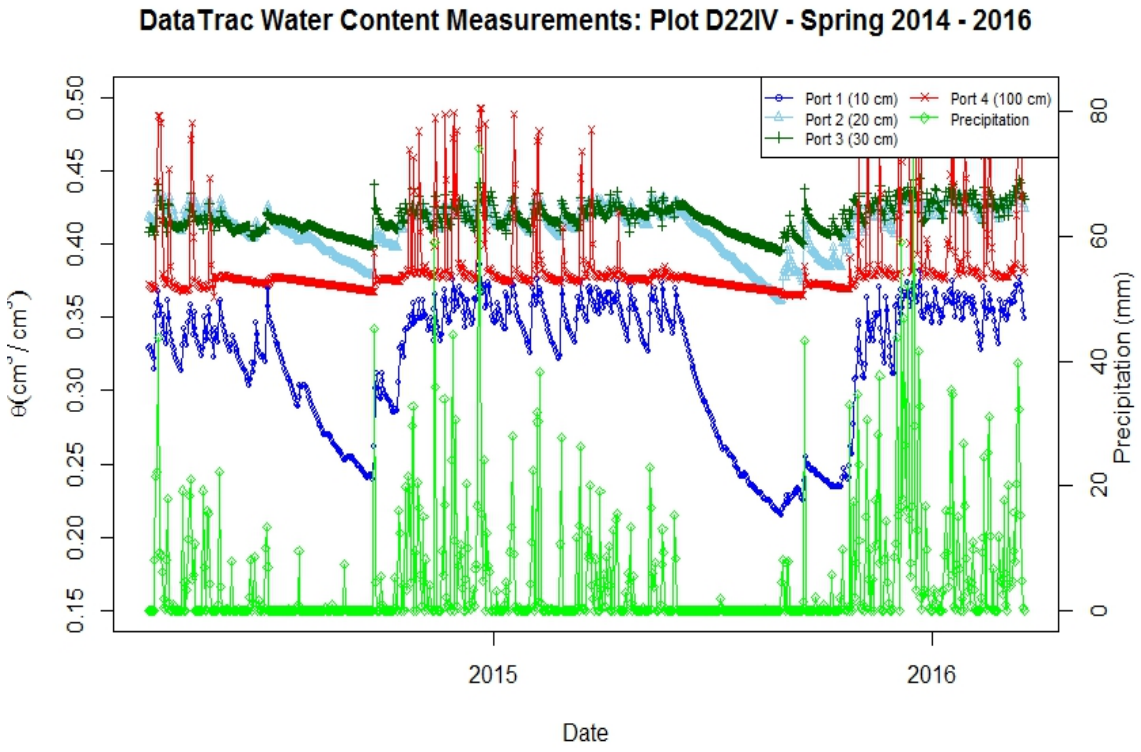

Figure E.16 DataTrac Plot D22IV Volumetric Water Content with Precipitation for 2-Year Simulation

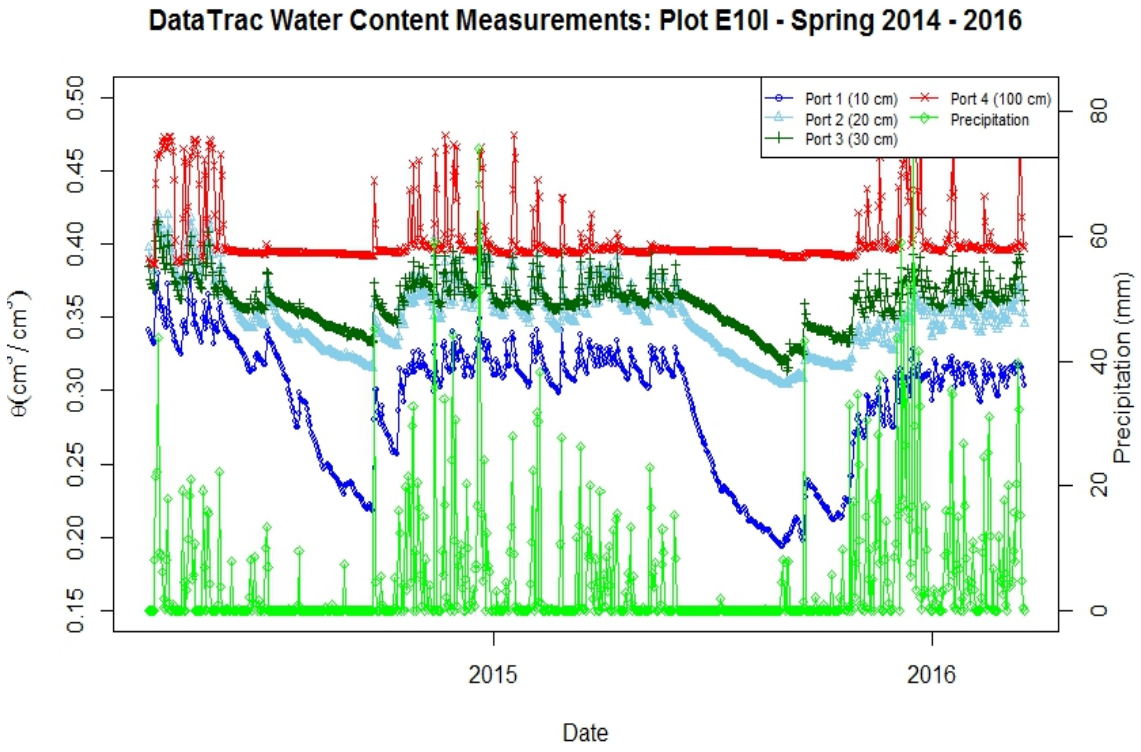

Figure E.17 DataTrac Plot E10I Volumetric Water Content with Precipitation for 2-Year Simulation

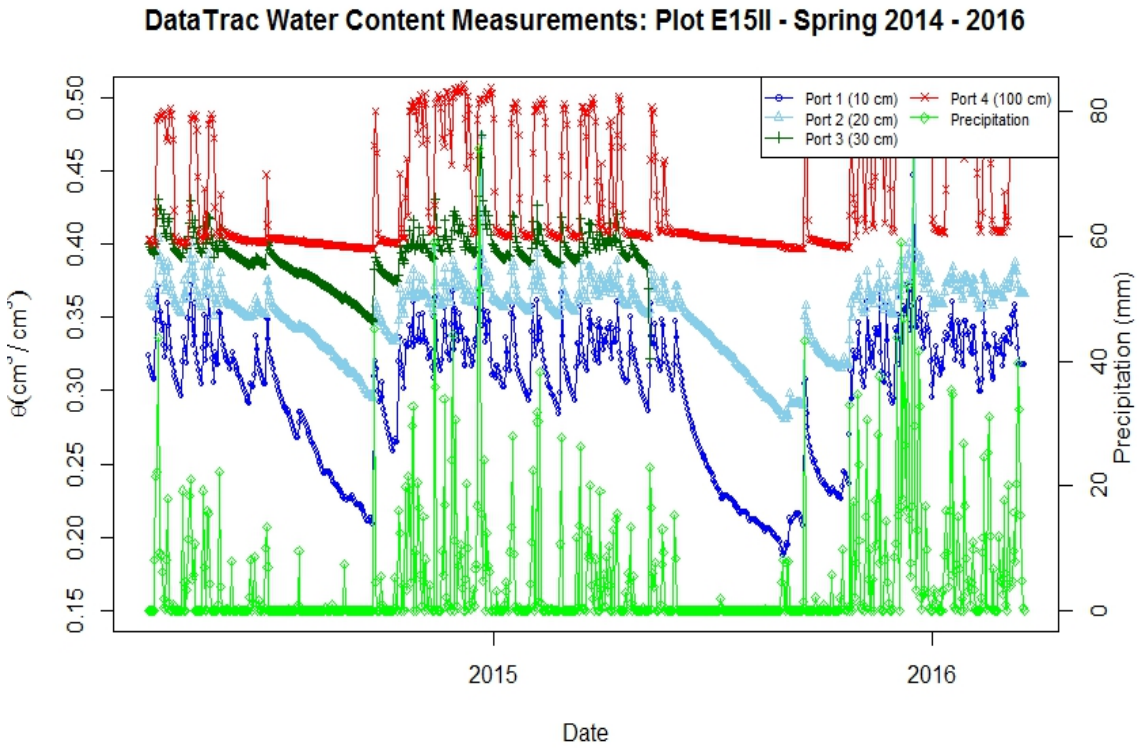

Figure E.18 DataTrac Plot E15II Volumetric Water Content with Precipitation for 2-Year Simulation

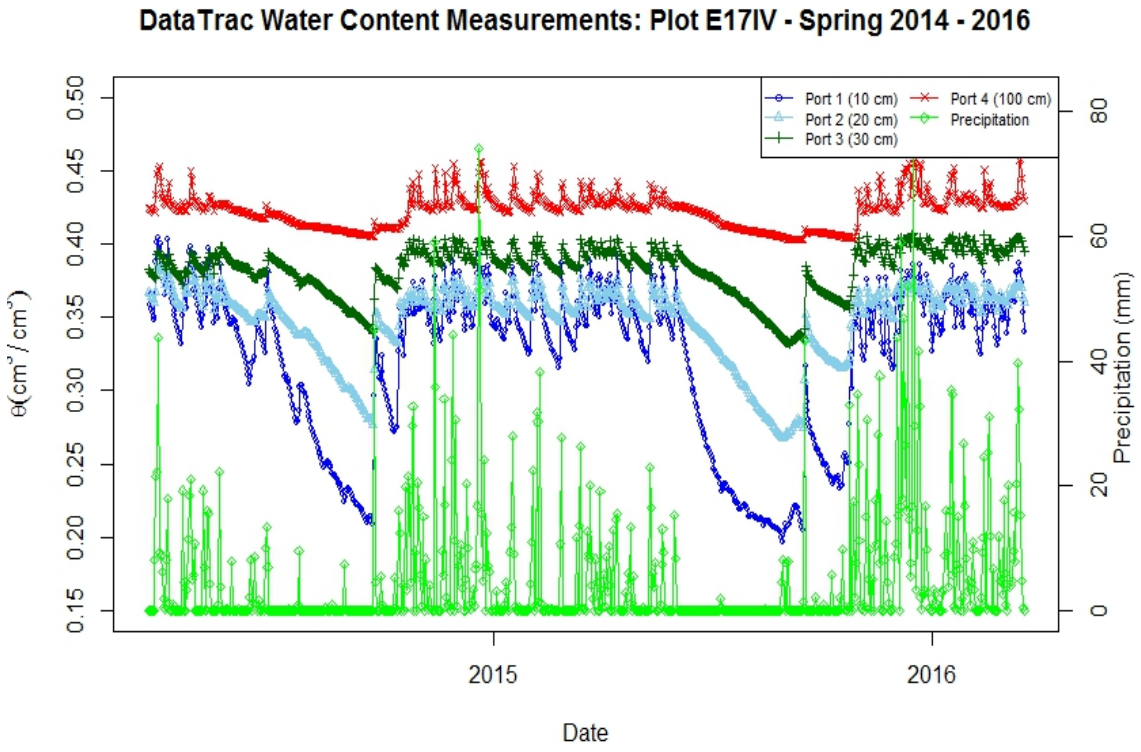

Figure E.19 DataTrac Plot E17IV Volumetric Water Content with Precipitation for 2-Year Simulation

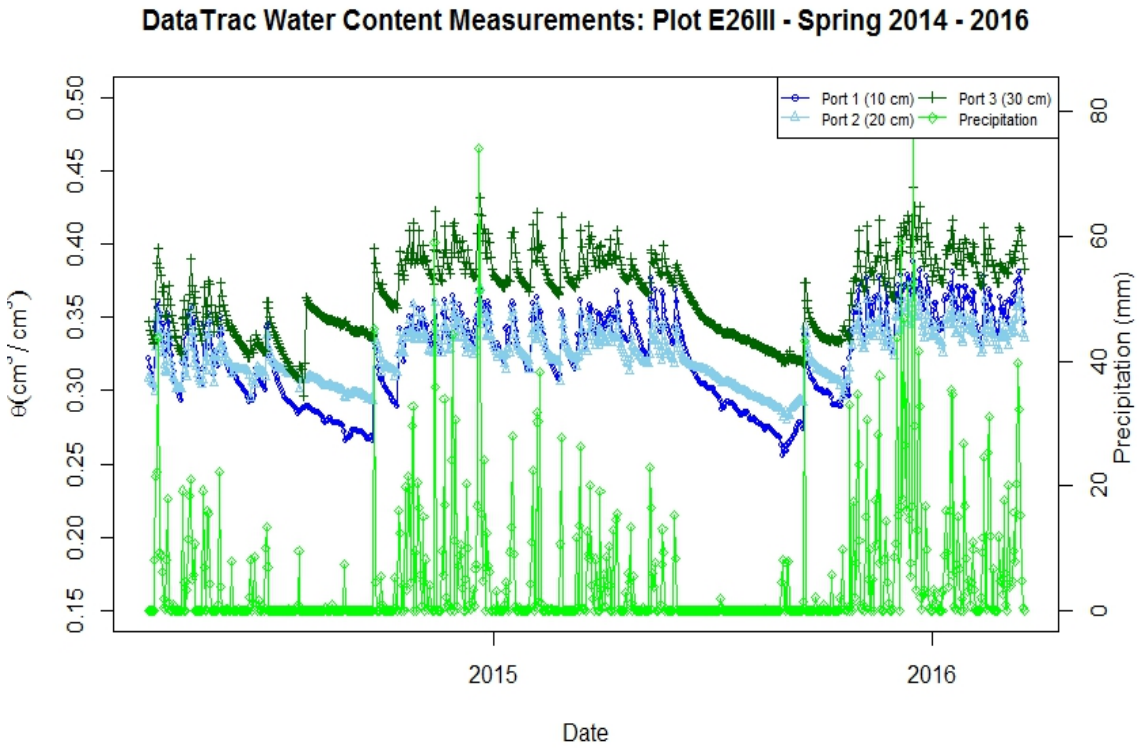

Figure E.20 DataTrac Plot E26III Volumetric Water Content with Precipitation for 2-Year Simulation

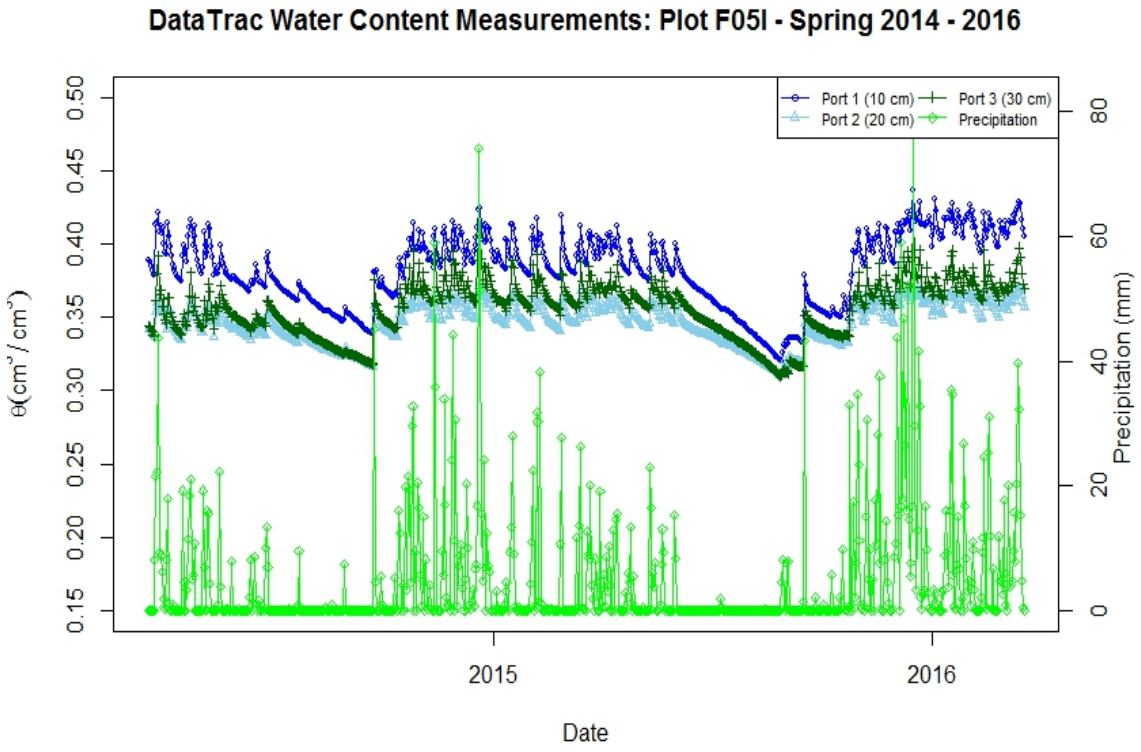

Figure E.21 DataTrac Plot F05I Volumetric Water Content with Precipitation for 2-Year Simulation

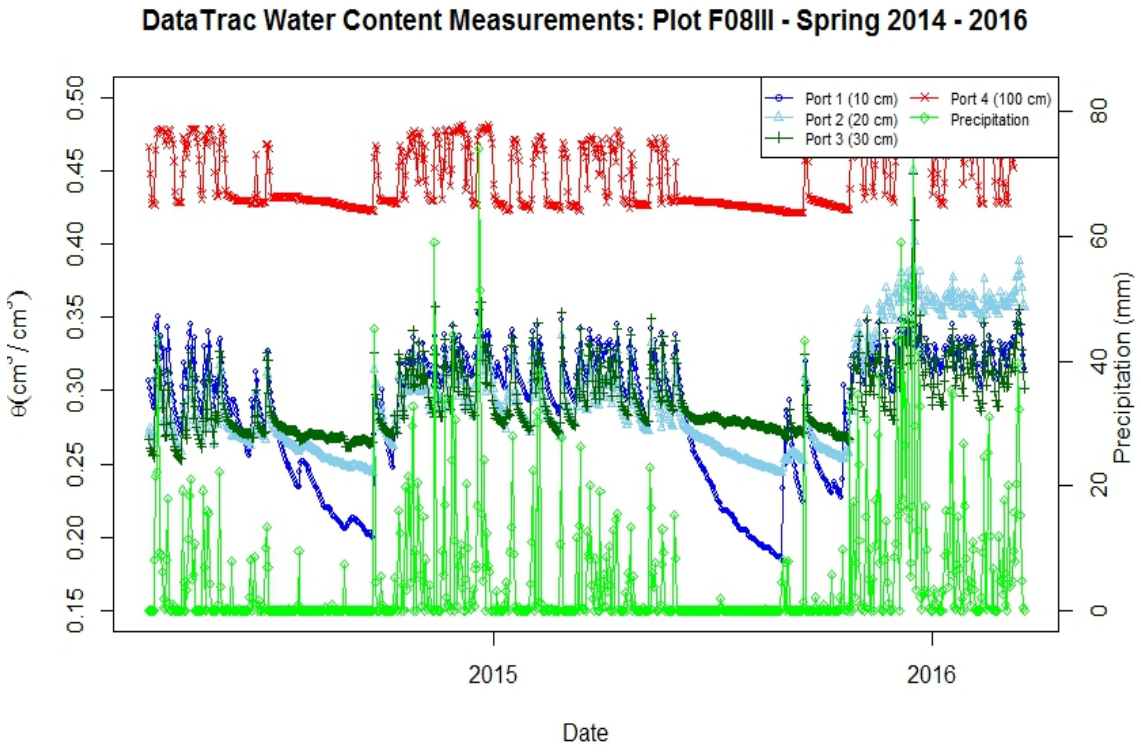

Figure E.22 DataTrac Plot F08III Volumetric Water Content with Precipitation for 2-Year Simulation

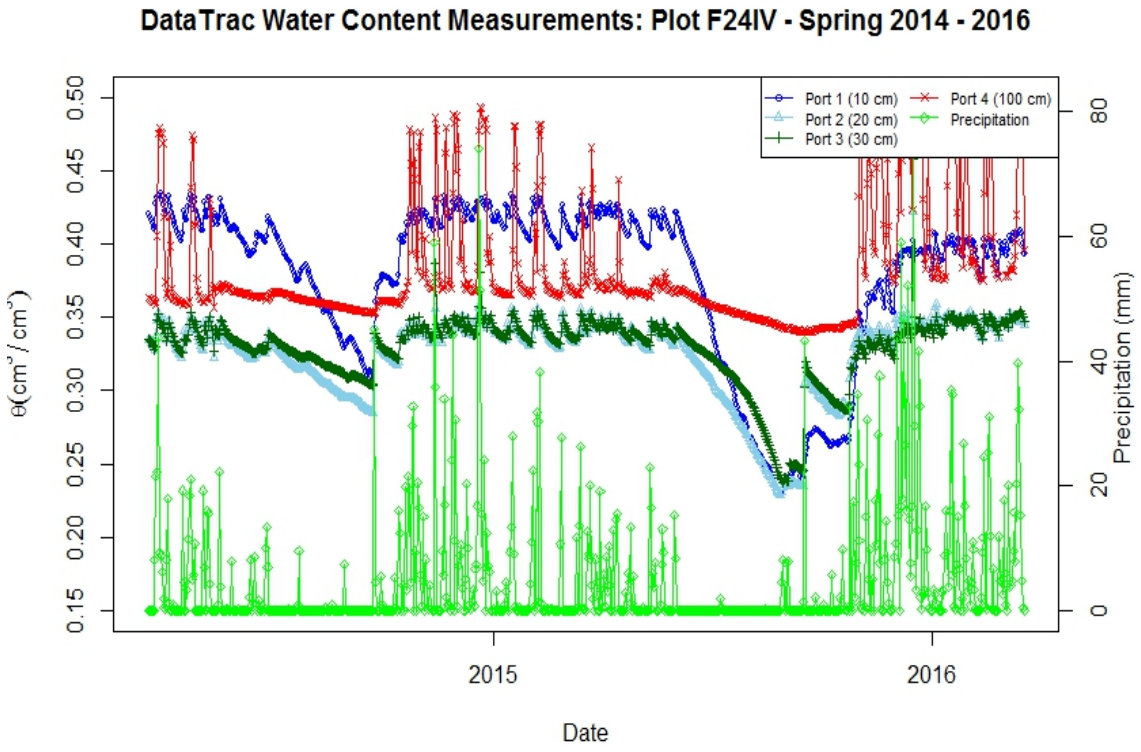

Figure E.23 DataTrac Plot F24IV Volumetric Water Content with Precipitation for 2-Year Simulation

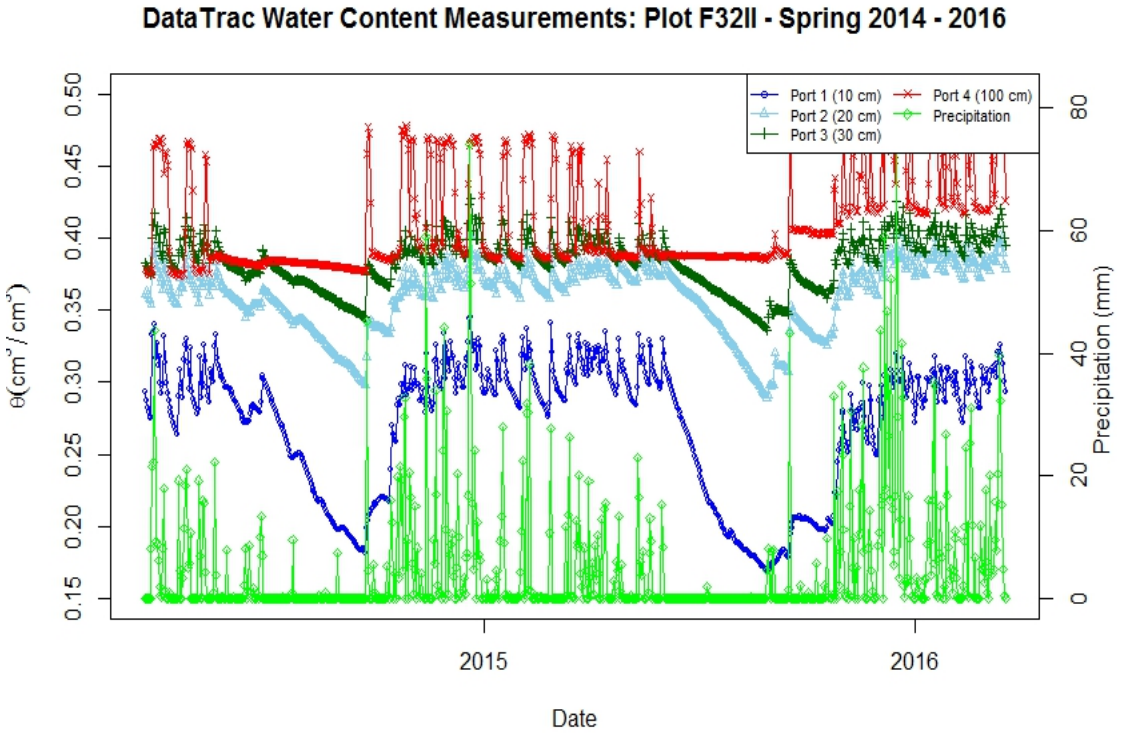

Figure E.24 DataTrac Plot F32II Volumetric Water Content with Precipitation for 2-Year Simulation

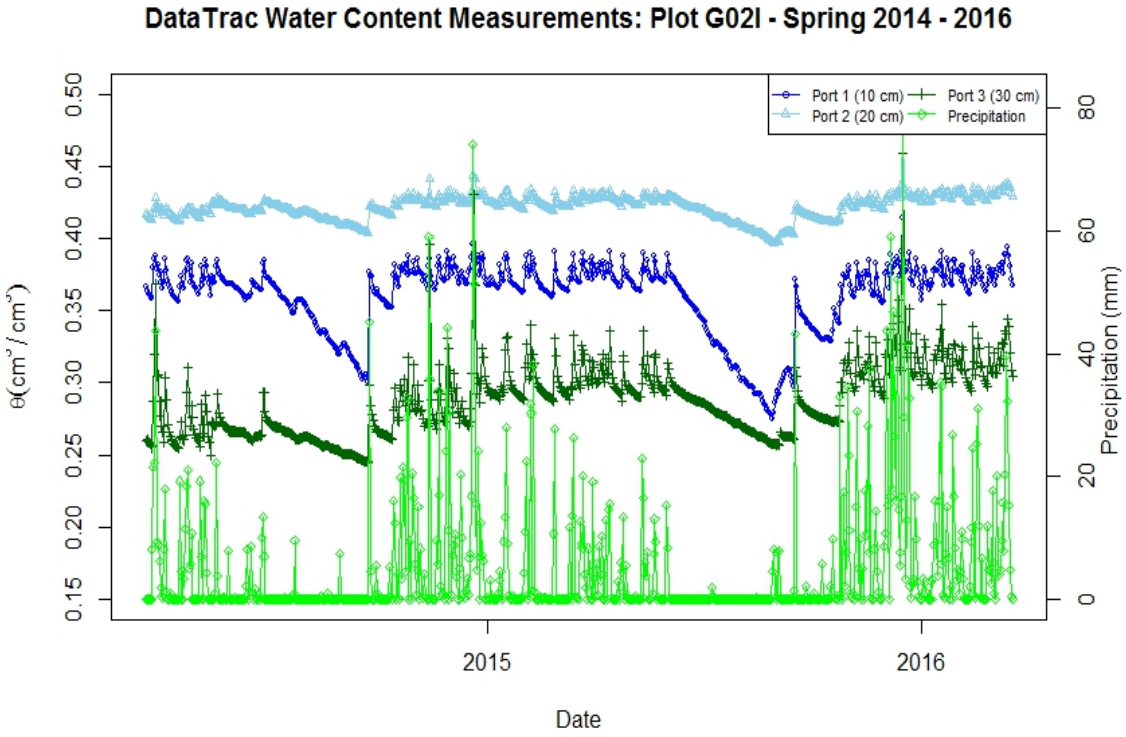

Figure E.25 DataTrac Plot G02I Volumetric Water Content with Precipitation for 2-Year Simulation

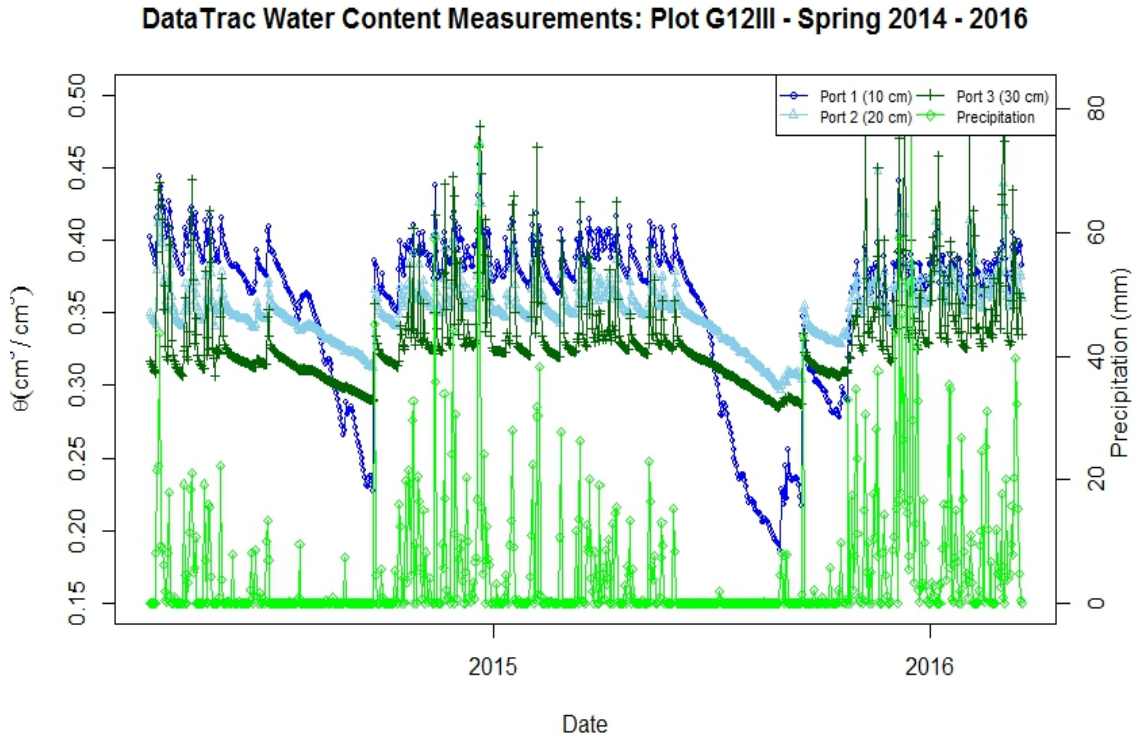

Figure E.26 DataTrac Plot G12III Volumetric Water Content with Precipitation for 2-Year Simulation

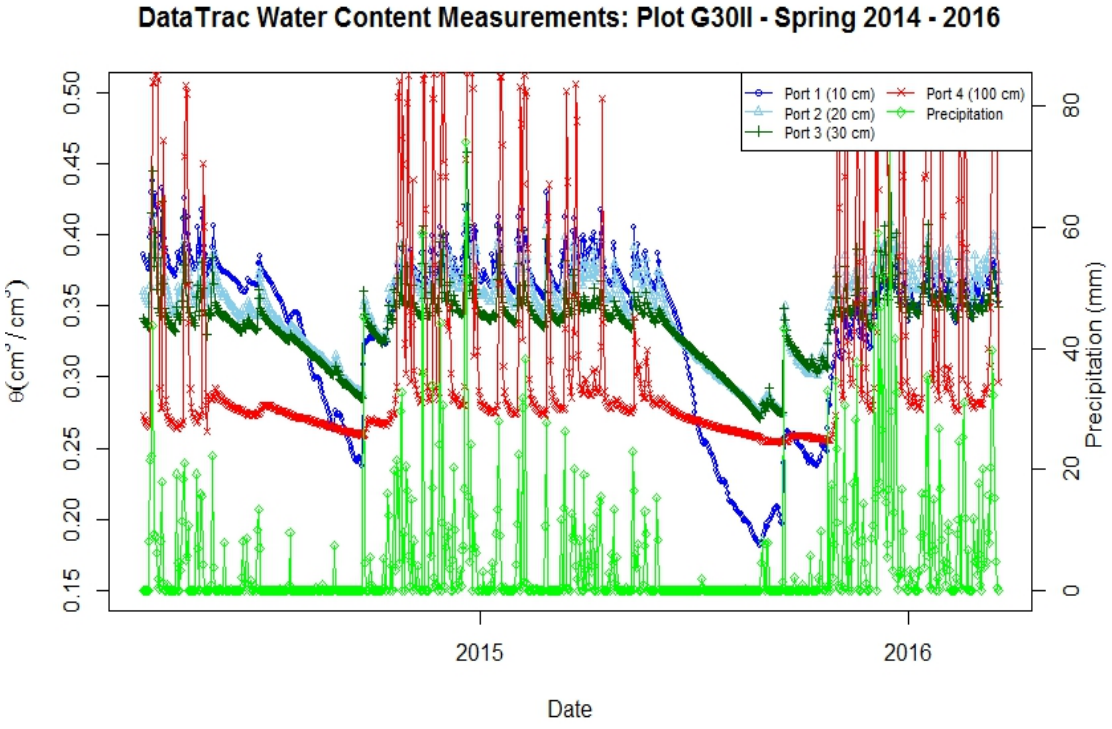

Figure E.27 DataTrac Plot G30II Volumetric Water Content with Precipitation for 2-Year Simulation

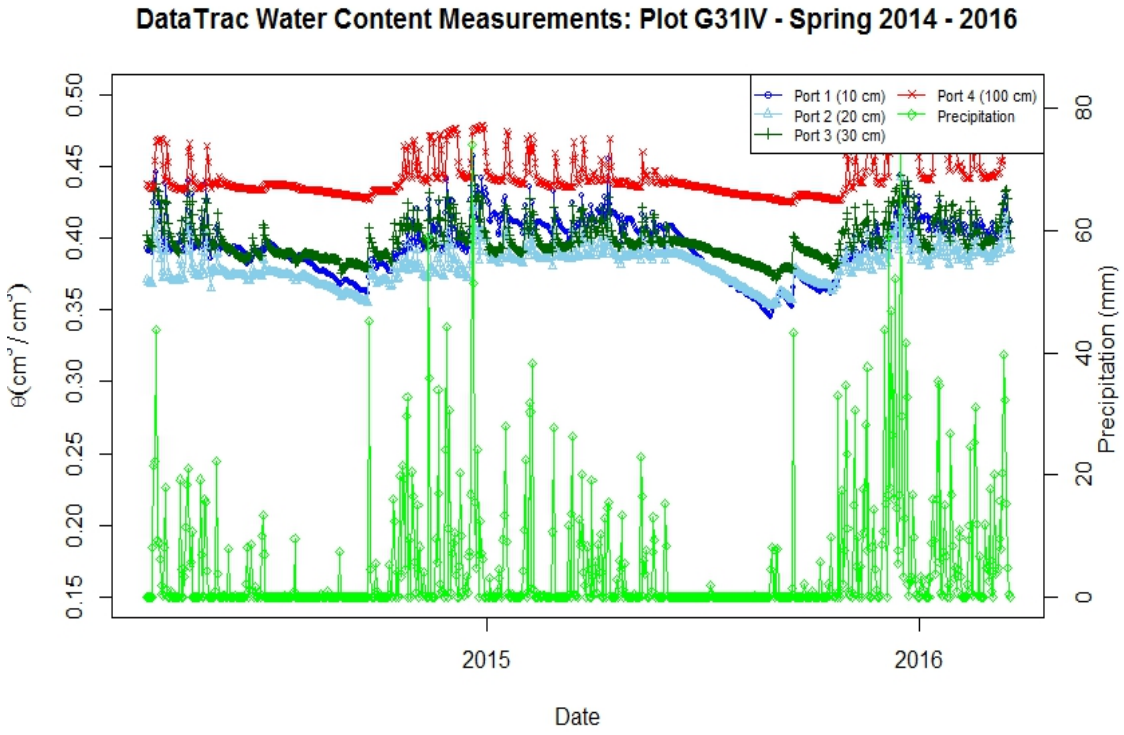

Figure E.28 DataTrac Plot G31IV Volumetric Water Content with Precipitation for 2-Year Simulation

APPENDIX F

SOIL COMPOSITION OF EACH TREATMENT

TYPE BY SUBSURFACE DEPTH

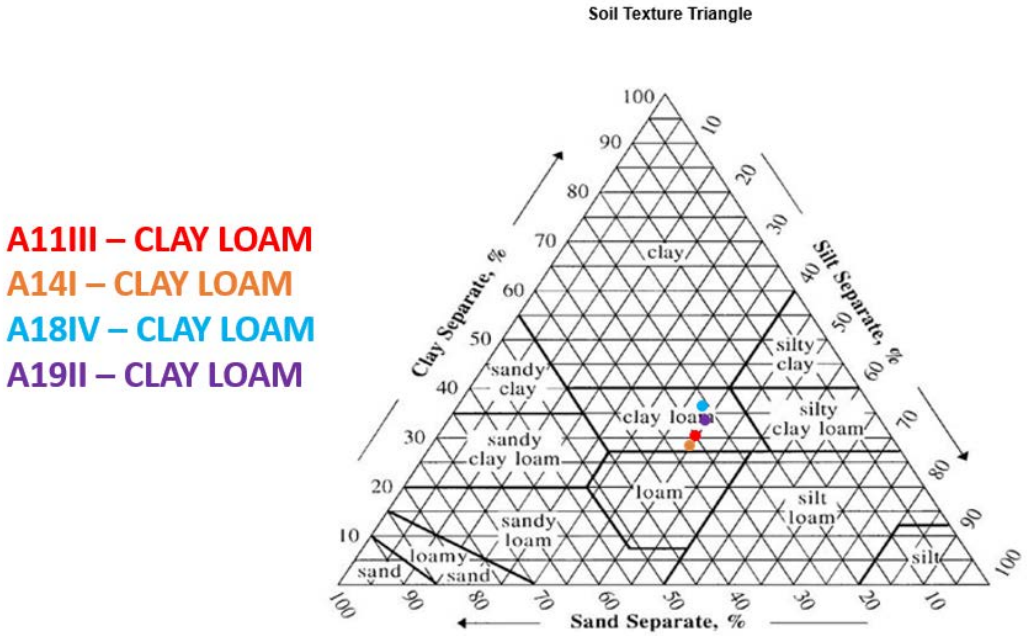

Figure F.1 Soil Composition for Treatment Type A, 0-30 cm Depth

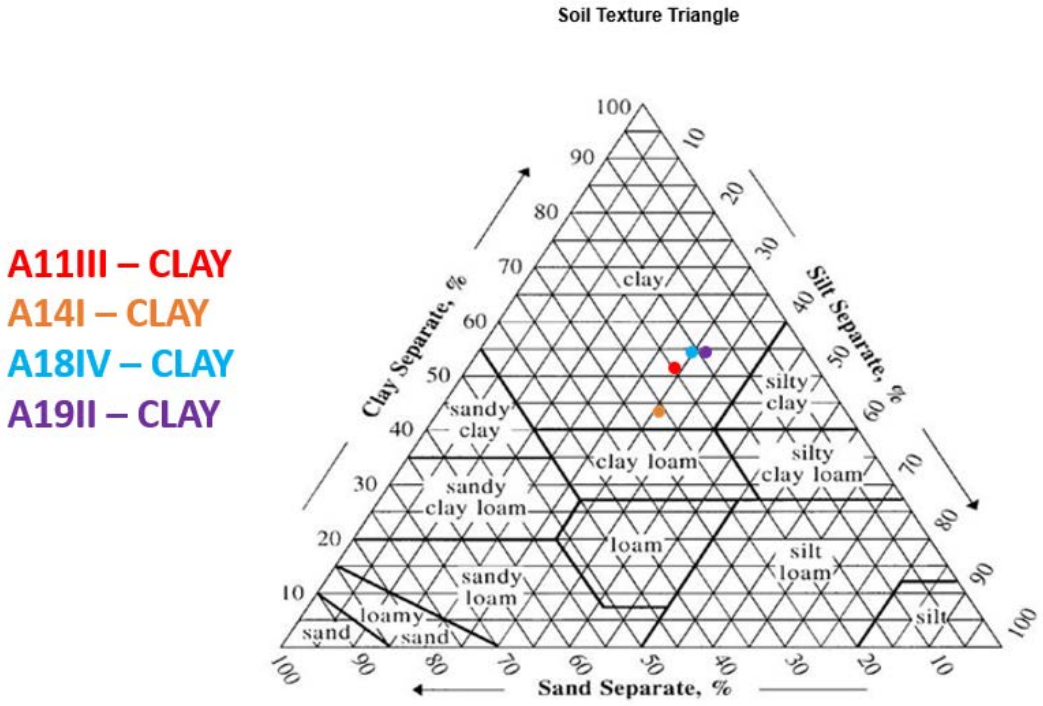

Figure F.2 Soil Composition for Treatment Type A, 30-100 cm Depth

B09I – CLAY LOAM
B16IV – LOAM
B20II – CLAY LOAM
B33III – CLAY LOAM

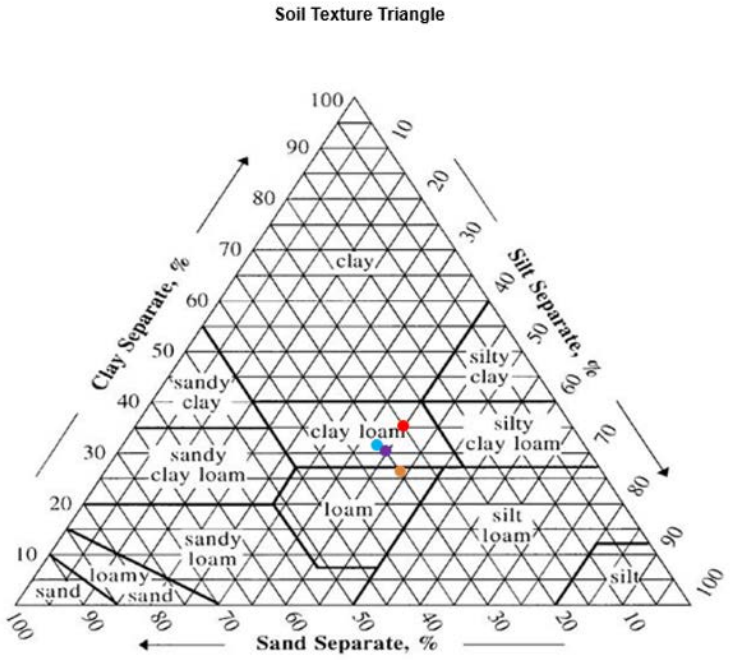

Figure F.3 Soil Composition for Treatment Type B, 0-30 cm Depth

B09I – CLAY
B16IV – CLAY
B20II – CLAY
B33III – CLAY

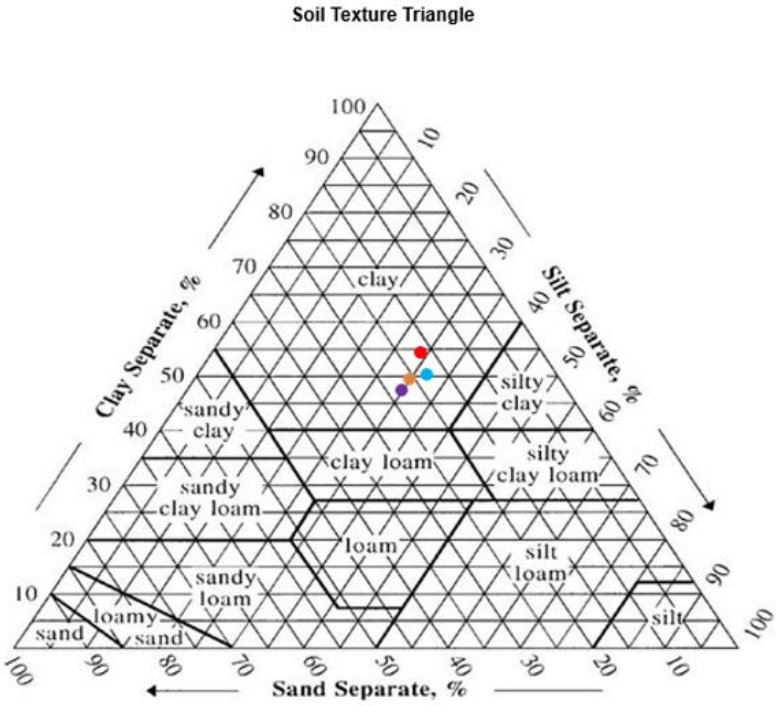

Figure F.4 Soil Composition for Treatment Type B, 30-100 cm Depth

C01I – CLAY LOAM
C07II – CLAY LOAM
C25IV – CLAY LOAM
C28III – CLAY LOAM

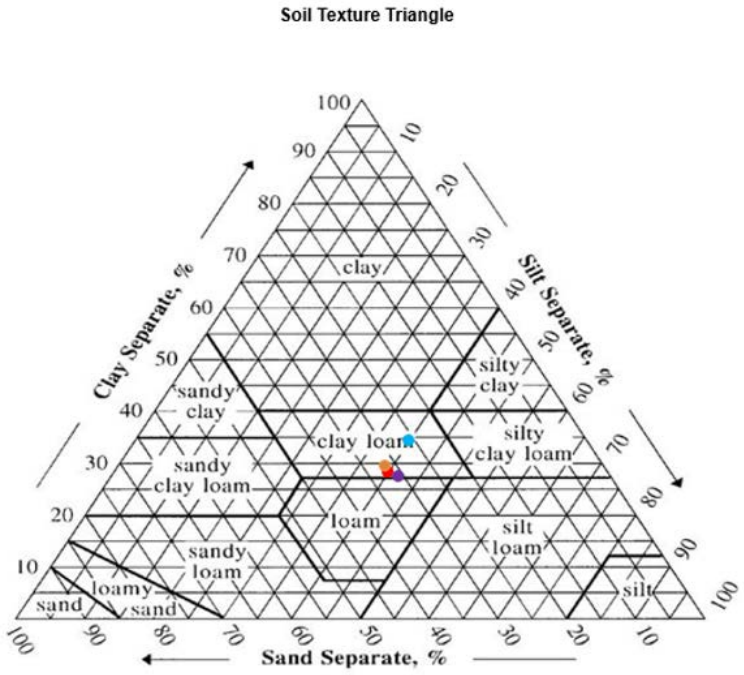

Figure F.5 Soil Composition for Treatment Type C, 0-30 cm Depth

C01I – CLAY
C07II – CLAY
C25IV – CLAY
C28III – CLAY

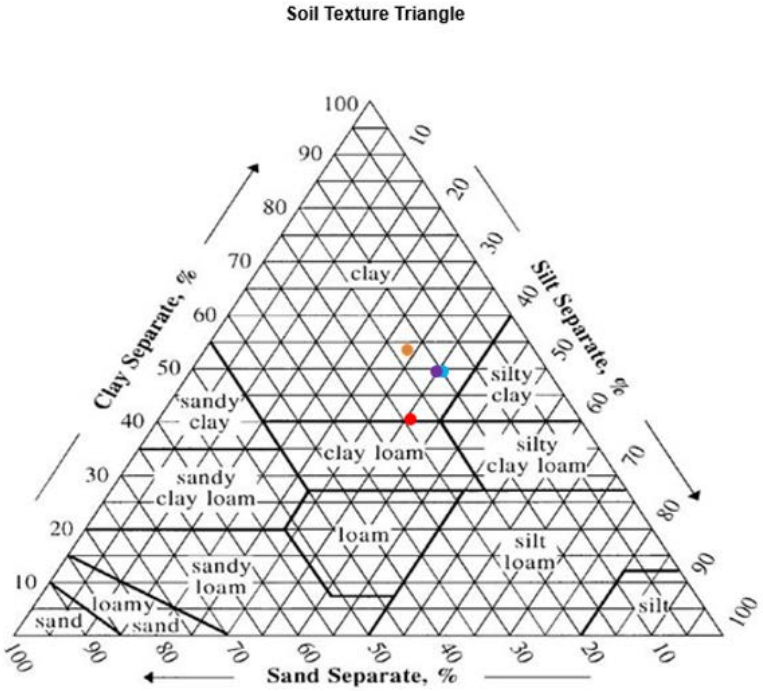

Figure F.6 Soil Composition for Treatment Type C, 30-100 cm Depth

D04II – CLAY LOAM
D06III – CLAY LOAM
D13I – CLAY LOAM
D22IV – CLAY LOAM

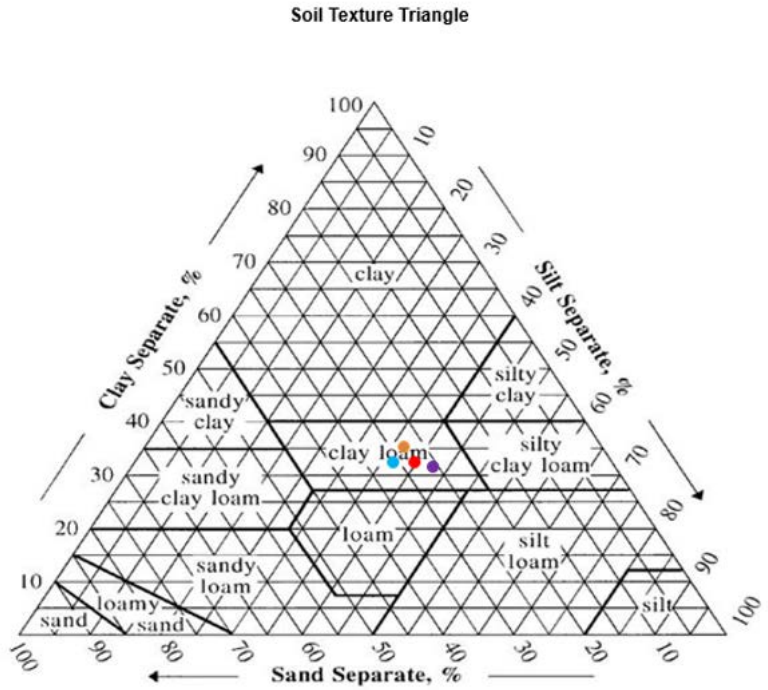

Figure F.7 Soil Composition for Treatment Type D, 0-30 cm Depth

D04II – CLAY
D06III – CLAY
D13I – CLAY
D22IV – CLAY

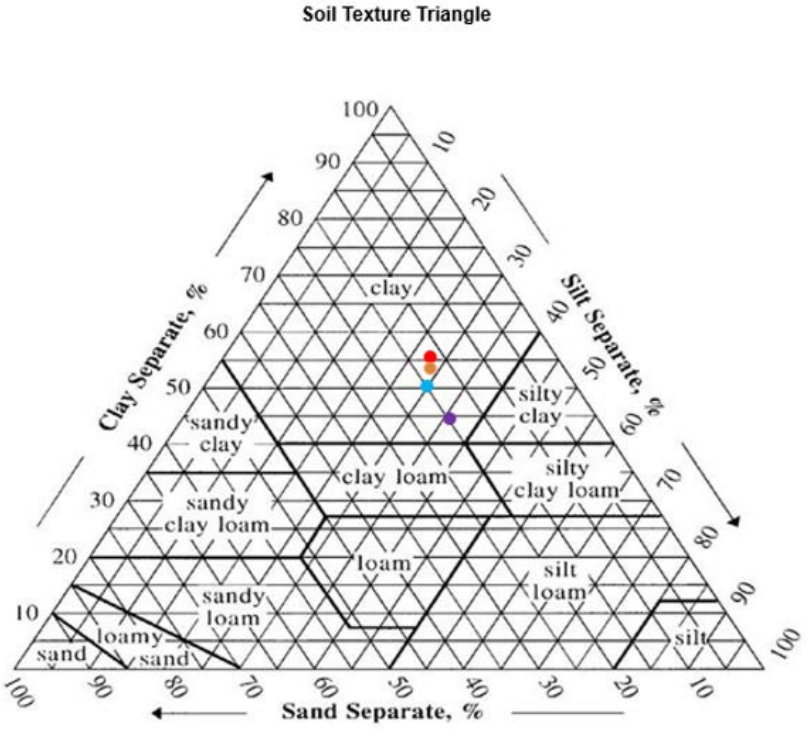

Figure F.8 Soil Composition for Treatment Type D, 30-100 cm Depth

E10I – CLAY LOAM
E15II – CLAY LOAM
E17IV – CLAY LOAM
E26III – LOAM

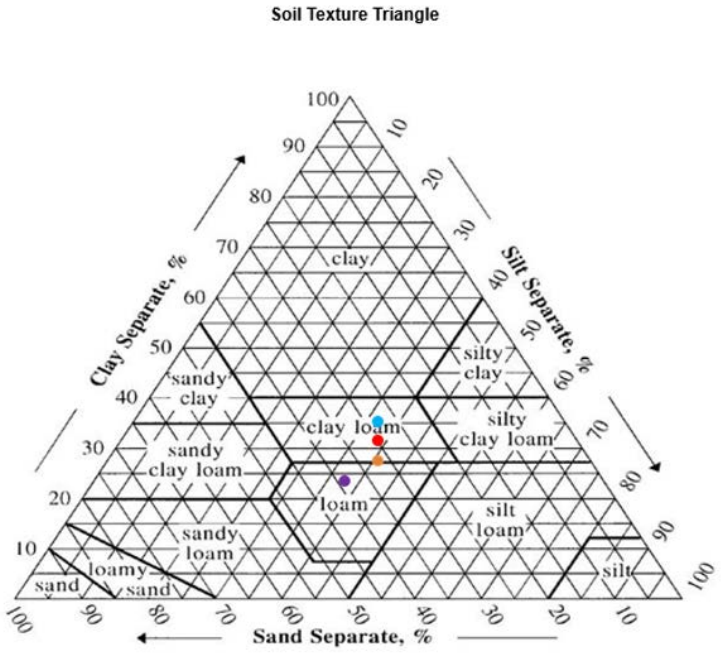

Figure F.9 Soil Composition for Treatment Type E, 0-30 cm Depth

E10I – CLAY
E15II – CLAY
E17IV – CLAY
E26III – CLAY LOAM

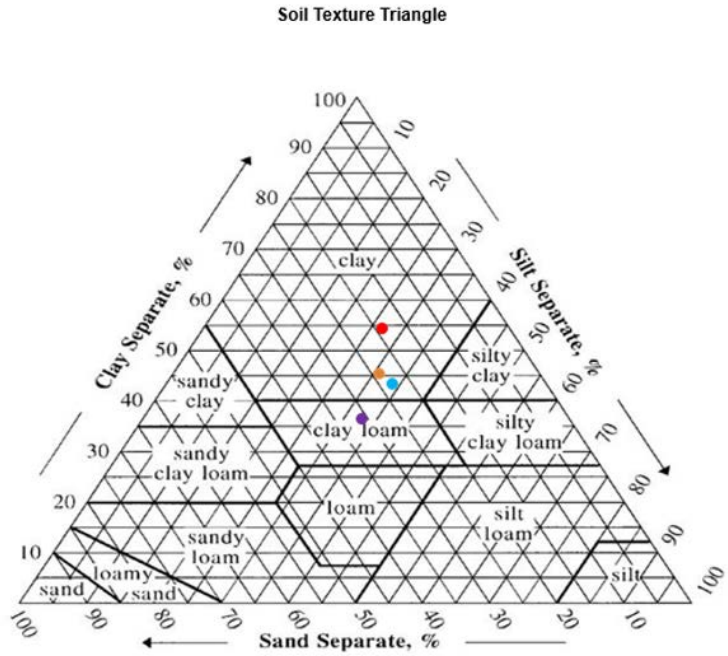

Figure F.10 Soil Composition for Treatment Type E, 30-100 cm Depth

F05I – CLAY LOAM
F08III – LOAM
F24IV – CLAY LOAM
F32III – CLAY LOAM

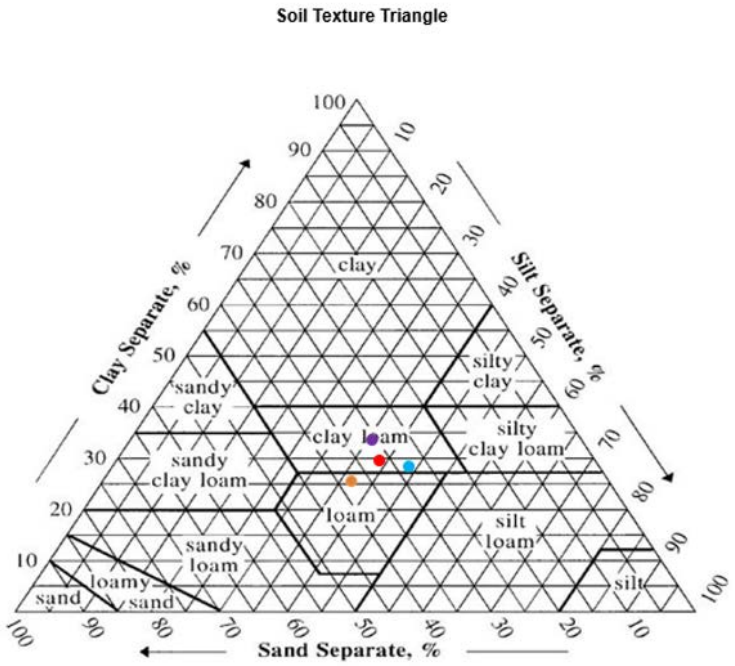

Figure F.11 Soil Composition for Treatment Type F, 0-30 cm Depth

F05I – CLAY
F08III – CLAY LOAM
F24IV – CLAY
F32III – CLAY

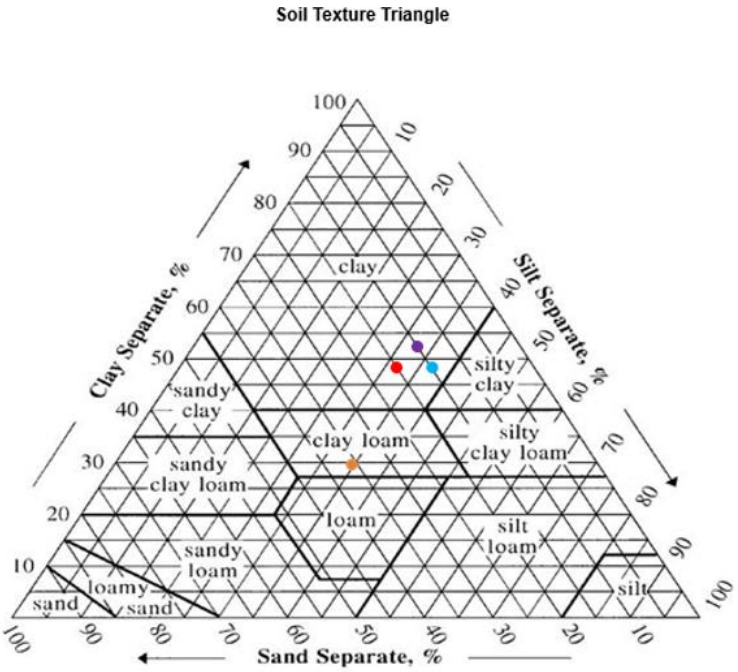

Figure F.12 Soil Composition for Treatment Type F, 30-100 cm Depth

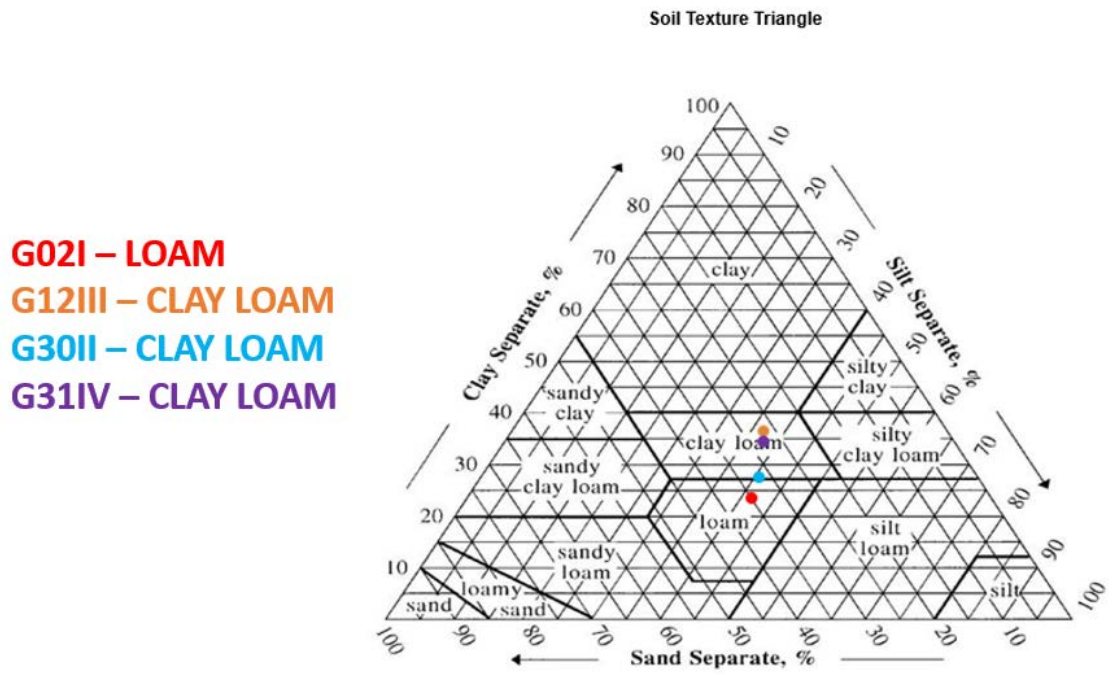

Figure F.13 Soil Composition for Treatment Type G, 0-30 cm Depth

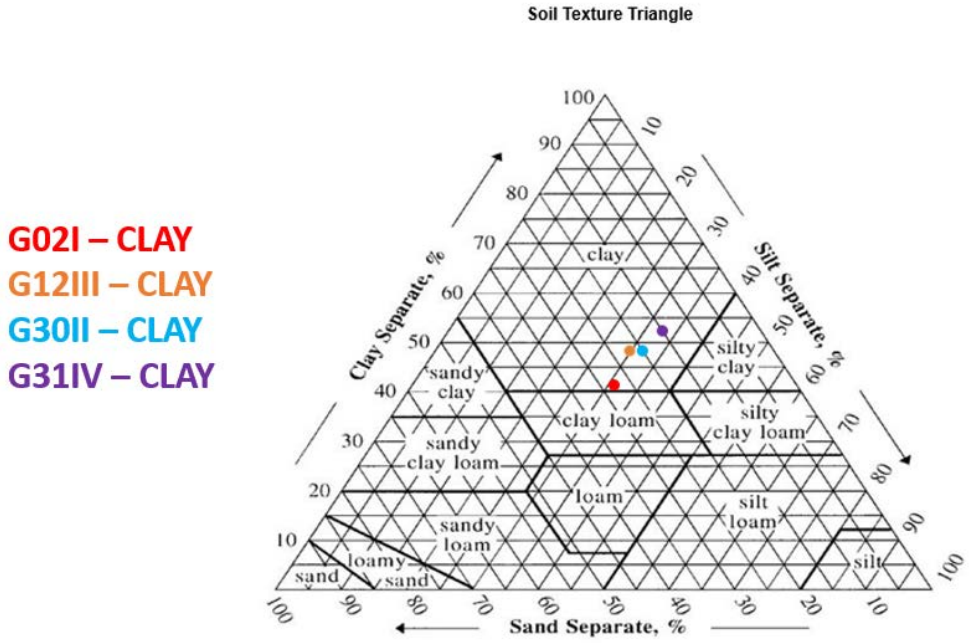

Figure F.14 Soil Composition for Treatment Type G, 30-100 cm Depth

REFERENCES

Alavalapati, J.; Lal, P.; Susaeta, S.; Abt R. C.; Wear, D. N. *Forest Biomass-Based Energy;* Technical Report for The Southern Forest Futures Project on GTR-SRS-178; USDA-Forest Service: Asheville, NC, August 2013.

Aransiola, E.F.; Ojumu, T.V.; Oyekola, O.O.; Madzimbamuto, T.F.; Ikhu-Omoregbe, D.I.O. A Review of Current Technology for Biodiesel Production: State of The Art. *Biomass Bioenergy*. **2014**, *61*, 276-297.

Assouline, S. A Model for Soil Relative Hydraulic Conductivity Based on the Water Retention Characteristic Curve. *Water. Resour. Res.* **2001**, *37*, 265-271.

Bellot, J.; Chirino, E. Hydrobal: An Eco-Hydrological Modelling Approach for Assessing Water Balances in Different Vegetation Types in Semi-Arid Areas. *Ecol. Model.* **2013**, *266*, 30-41.

Ben-Hur, M.; Wakindiki, I. I. C. Soil Mineralogy and Slope Effects on Infiltration, Interrill Erosion, and Slope Factor. *Water Resour. Res.* **2004**, *40*, 34-38.

Benson, C. 2007. Modeling Unsaturated Flow and Atmospheric Interactions. In *Theoretical and Numerical Unsaturated Soil Mechanics* [Online]; Schanz, T., Ed.; Springer: Berlin, 2007; pp 187- 202. https://www.researchgate.net/profile/Tom_Schanz/publication/265656058_Theoretical_and_Numerical_Unsaturated_Soil_Mechanics/links/570fceca08ae68dc79096b04/Theoretical-and-Numerical-Unsaturated-Soil-Mechanics.pdf (accessed Nov 9, 2016).

Beringer, T.; Lucht, W.; Schaphoff, S. Bioenergy Production Potential of Global Biomass Plantations Under Environmental and Agricultural Constraints. *GCB Bioenergy.* **2011**, *3*, 299-312.

Berndes, G. Bioenergy and Water—the Implications of Large-Scale Bioenergy Production for Water Use and Supply. *Global Environ. Change*. **2002**, *12*, 253-271.

Bonan, G. B. Frost Followed the Plow: Impacts of Deforestation on the Climate of the United States. *Ecol. Appl.* **1999**, *9*, 1305-1315.

Brooks, R. H.; Corey, A. T. *Hydraulic Properties of Porous Media*; Hydrology Papers: Colorado, 1964, Vol. 3, pp 1-18.

Campbell G. S. *Soil Physics with BASIC*. Elsevier: New York, 1985, Vol. 14, pp 45-59.

Carsel, R. F.; Rudolph, S. P. Developing Joint Probability Distributions of Soil Water Retention Characteristics. *Water Resour. Res.* **1988**, *24*, 55-69.

Chai, T.; Draxler, D. D. Root Mean Square Error (RMSE) or Mean Absolute Error (MAE)? – Arguments against Avoiding RMSE in the Literature. *Geosci. Model Dev.* **2014**, *7*,247-250.

Chen, M.; Smith, P. M.; Wolcott, M. P. U.S. Biofuels Industry: A Critical Review of Opportunities and Challenges. *Society of Wood Sci. Tech.* **2016**, *4*, 42-59.

Croke, J.; Hairsine, P.; Fogarty, P. Soil Recovery from Track Construction and Harvesting Changes in Surface Infiltration, Erosion, and Delivery Rates with Time. *For. Ecol. Manage.* **2001**, *3*, 3-12.

Doorenbos, J.; Pruitt, W. O. Guidelines for Predicting Crop Water Requirements. *F. A. O*. **1977,** *24*, 1-107.

Fayer, M. J. *UNSAT-H Version 3.0: Unsaturated Soil Water and Heat Flow Model;* Pacific Northwest Laboratories: Washington, 2000, pp 1-184.

Fiedler, F R.; Ramirez, J. A. A Numerical Method for Simulating Discontinuous Shallow Flow over an Infiltrating Surface. *Int. J. Numer. Methods Fluids.* **2000**, *32*, 19-39.

Gupta, H. V.; Sorooshian, S.; Yapo, P. O. Status of Automatic Calibration for Hydrologic Models: Comparison with Multilevel Expert Calibration. *J. Hydrol. Eng*. **1999**, *4*, 35-43.

Johansson, D.J.A.; Azar, C. A Scenario Based Analysis of Land Competition Between Food and Bioenergy Production in the US. *Clim. Change*. **2007**, *82*, 267-291.

Keim, R. F.; Tromp-Van Meerveld, H. J.; McDonnell, J. J. A Virtual Experiment on the Effects of Evaporation and Intensity Smoothing by Canopy Interception on Subsurface Stormflow Generation. *J. Hydrol.* **2006**, *4*, 352-364.

Keppeler, E. T.; Ziemer, R. R. Logging Effects on Streamflow: Water Yield and Summer Low Flows at Caspar Creek in Northwestern California. *Water Resour. Res.* **1990**, *26*, 669-679.

Khire, M. V.; Benson, C. H.; Bosscher, P. J. Water Balance Modeling of Earthen Final Covers. *J. Geotech. Geoenviron. Eng.* **1997**, *123*, 44-54.

Kollet, S. J.; Maxwell, R. M. Integrated Surface Groundwater Flow Modeling: A Free-surface Overland Flow Boundary Condition in a Parallel Groundwater Flow Model. *Adv. Water Resour.* **2006**, *29*, 45-58.

Labedzki, L.; Kanecka-Geszke, E.; Bak, B.; Slowinsk, S.; Estimation of Reference Evapotranspiration Using the FAO Penman-Monteith Method for Climatic Condition of Poland. In *Evapotranspiration* [Online]; Labedzki, L., Ed.; *InTech.*

Rijeka, Croatia, 2011; Chapter 12, pp 275-294. https://cdn.intechopen.com/pdfs-wm/14190.pdf (assessed Oct 17, 2016).

Lam, L.; Fredlund D. G.; Barbour, S. L. Transient Seepage Model for Saturated-Unsaturated Soil Systems: A Geotechnical Engineering Approach. *Can. Geotech. J.* **1987,** *24*, 565- 580.

Liew, M. W.; Van, T. L.; Veith, D. D.; Bosch, D.; Arnold, J. G. Suitability of SWAT for the Conservation Effects Assessment Project: Comparison on USDA Agricultural Research Service Watersheds. *J. Hydrol. Eng.* **2007**, *12*, 73-89.

Link, T. E.; Unsworth, M.; Marks, D. The Dynamics of Rainfall Interception by a Seasonal Temperate Rainforest. *Agric. For. Meteorol.* **2004**, *124*, 171-191.

Mann, L.; Tolbert, V. Soil Sustainability in Renewable Biomass Plantings. *AMBIO*. **2000**, *29*, 492-499.

Miller, J. R.; Turner, M. G.; Smithwish, E. H.; Dent, L. C.; Stanley, E. H. Spatial Extrapolation: The Science of Predicting Ecological Patterns and Processes. *BioScience.* **2004**, *54*, 310-321.

Moriasi, D. N.; Arnold, J. G.; Van Liew, M. W.; Bingner, R. L.; Harmel, R. D.; Veith, T. L. Model Evaluation Guidelines for Systematic Quantification of Accuracy in Watershed Simulations. *Trans. ASABE.* **2007**, *50*, 885-900.

Mualem, Y. A New Model for Predicting the Hydraulic Conductivity of Unsaturated Porous Media. *Water Resour.* **1978**, *12*, 513-522.

Ogorzalek, A. S.; Bohnhoff, G. L.; Shackelford, C. D.; Benson, C. H.; Apiwantragoon, P. Comparison of Field Data and Water-Balance Predictions for a Capillary Barrier Cover. *J. Geotech. Geoenviron. Eng*. **2008**, *134*, 470-486.

Penman, H. L.; Keen, B. A. Meteorological and Soil Factors Affecting Evaporation from Fallow Soil. *Q. J. R. Meteorol. Soc.* **2007**, *66*, 401-410.

Philip, J. R.; De Vries, D. A. Moisture Movement in Porous Materials under Temperature Gradients. *Trans., Am. Geophys. Union.* **2007**, *38*, 222-232.

Philip, J. R. Evaporation, and Moisture and Heat Fields in the Soil. J. Meteorol. 1957, 14, 354-366.

Ponder, F.; Fleming, R. L.; Berch, S.; Busse, M. D.; Elioff, J. D.; Hazlett P. W.; Kabzems, R. D.; Kranabetter, J. M.; Morris, D. M.; Page-Dumroese, D.; Palik, B. J.; Powers, R. F.; Sanchez, F. G.; Scott, D. A.; Stagg, R. H.; Stone, D. M.; Young, D. H.; Zhang, J.; Ludovici, K. H.; Mckenney, D. W.; Mossa, D. S.; Sanborn, P. T.; Voldseth, R. A. Effects of Organic Matter Removal, Soil Compaction and Vegetation Control on 10th Year Biomass and Foliar Nutrition: LTSP Continent-wide Comparisons. *For. Ecol. Manage.* **2012**, *278*, 35-54.

Raat K. J.; Draaijers, G. P. J.; Shaap, M. G.; Tietema, A.; Verstraten, J. M. Spatial Variability of Throughfall Water and Chemistry and Forest Floor Water Content in a Douglas Fir Forest Stand. *Hydrol. Earth Syst. Sci.* **2002**, *6*, 363-374.

Rawls, W. J.; Brakensiek, D. L.; Saxtonn, K. E. Estimation of Soil Water Properties. *Trans. ASAE.* **1982**, *25*, 1316-1320.

Ren, D. A. Modified Richard's Equation, It's Adjoint, and a New Perspective on Land Data Assimilation. *Meteorol. Atmos. Phys.* **2005**, *92*, 25-32.

Schaap, M. G.; Leij, F. J. Improved Prediction of Unsaturated Hydraulic Conductivity with the Mualem-van Genuchten Model. *Soil Sci. Soc. Am. J.* **2000**, *64*, 843-851.

Shi, L.; Song, X.; Tong J.; Zhu, Y.; Zhang, Q. Impacts of Different Types of Measurements on Estimating Unsaturated Flow Parameters. *J. Hydrol.* **2015**, *524*, 549-561.

Soane, B. D.; Ouwerkerk, C. V. *Soil Compaction in Crop Production*, 1st ed.; Elsevier: Amsterdam, 1994; pp 452-485.

Van Genuchten, M. T. A Closed-Form Equation For Predicting the Hydraulic Conductivity of Unsaturated Soils. *Soil Sci. Soc. Am. J.* **1980**, *44*, 892-898.

Warren, J. M.; Meinzer, F. C.; Brooks, J. R.; Domec, J. C. Vertical Stratification of Soil Water Storage and Release Dynamics in Pacific Northwest Coniferous Forests. *Agric. For. Meteorol*. **2005**, *130*, 39-58.

Yanful, E. K.; Mousavi, S. M.; Yang, M. Modeling and Measurement of Evaporation in Moisture-retaining Soil Covers. *Adv. Environ. Res.* **2003**, *7*, 783-801.